Modeling Impact of Changing Hydroclimatic Regime on Dissolved Organic Carbon Export from Baker Creek Catchment

A Thesis Submitted to the College of
Graduate and Postdoctoral Studies
In Partial Fulfillment of the Requirements
For the Degree of Master of Environment and Sustainability
With the School of Environment and Sustainability &
Global Institute for Water Security
University of Saskatchewan
Saskatoon, Canada

By

Shanta Sharma

Permission to use

In presenting this thesis in partial fulfillment of the requirements for a Postgraduate degree from the University of Saskatchewan, I agree that the Libraries of this University may make it freely available for inspection. I further agree that permission for copying of this thesis in any manner, in whole or in part, for scholarly purposes may be granted by the professor who supervised my thesis work or, in their absence, by the Head of the Department or the Dean of the College in which my thesis work was done. It is understood that any copying or publication or use of this thesis or parts thereof for financial gain shall not be allowed without my written permission. It is also understood that due recognition shall be given to me and to the University of Saskatchewan in any scholarly use which may be made of any material in my thesis.

Disclaimer

Reference in this thesis to any specific commercial products, process, or service by trade name, trademark, manufacturer, or otherwise, does not constitute or imply its endorsement, recommendation, or favoring by the University of Saskatchewan. The views and opinions of the author expressed herein do not state or reflect those of the University of Saskatchewan, and shall not be used for advertising or product endorsement purposes.

Requests for permission to copy or to make other uses of materials in this thesis/dissertation in whole or part should be addressed to:

Director
School of Environment and Sustainability
University of Saskatchewan
117 Science Place, Kirk Hall
Saskatoon, Saskatchewan, S7N 5C8, Canada

OR

Dean
College of Graduate and Postdoctoral Studies
University of Saskatchewan
116 Thorvaldson Building, 110 Science Place
Saskatoon, Saskatchewan, S7N 5C9, Canada

Abstract

The subarctic is anticipated to undergo hydroclimatic regime change, which can impact hydrological processes and water yield. Explaining landscape-scale carbon (C) budgets and pollutant transfer is necessary for understanding the impact of changing hydroclimatic regimes. This research investigates dissolved organic carbon (DOC) fluxes in a hydrologically complex watershed (Baker Creek) in the Northwest Territories. Discharge, DOC concentration, and DOC export were simulated using a rainfall-runoff model (PERSiST), and a catchment biogeochemical model (INCA-C). Model calibration (2012–2016) was done using available discharge and DOC concentration data in sub-catchments of Baker Creek. The model successfully reproduced hydrological flow in the catchment (R^2: 0.87–0.94; NS: 0.82–0.91) and reasonably captured DOC concentration (R^2: 0.19–0.31). Future conditions were simulated using two climate scenarios (elevated temperature, elevated temperature and precipitation), and compared against a scenario with baseline conditions. Average discharge over 30 years is predicted to decrease under elevated temperature scenario (22–27% of baseline) and increase (116–175% of baseline) under elevated temperature and precipitation scenario. For this scenario, discharge increases in early winter indicate a change in hydroclimatic regime from nival to combined nival and pluvial. Average DOC flux over 30 years is predicted to decrease (24–27% of baseline) under elevated temperature scenario and increase (64–81% of baseline) under elevated temperature and precipitation scenario where a large increase in DOC export will occur in early winter. DOC flux in Baker Creek is controlled by runoff in the catchment. Under future climate scenario, increased DOC export from Baker Creek catchment with increased discharge can increase the mobility of previously deposited airborne metal contaminants such as arsenic from Giant Mine.

Acknowledgments

Firstly, I would really like to acknowledge my supervisor, Dr. Colin Whitfield, for providing invaluable knowledge, guidance, and support throughout the entire process. Colin, I feel so lucky to have received that email back to start an MSc with you. I am forever grateful for the opportunity and experience gained working under you. Secondly, I would like to acknowledge my committee members, Dr. Christopher Spence, Dr. Jason Venkiteswaran and Dr. Martyn N. Futter for your precious time, advice, and constructive criticisms throughout. Martyn, I am not sure if you know it but your support was significantly greater than anything I could ever put in writing here. Chris, thank you so much for your suggestions that always helped me to get better picture of catchment and its behavior. Jason, discussion with you always helped me to focus on my rational and create a solid work of science. I would also like to thank Dr. Kerry McPhedran for being on my examining committee and providing suggestions to make this thesis a better piece of science. Special thanks to following individuals of Bigfoot and SaskWatChe lab group for your support throughout: Anthony Baron, Lauren Dyck, Laura McFarlan, Emily Cavaliere and Amy Hergott. I would like to acknowledge Sub-Arctic Metal Mobility Studies (SAMMS) for funding, Global Institute for Water Security and the School of Environment and Sustainability for providing the space and platform to perform. I would like to thank my dad, mom, and brothers for your emotional support throughout this work. Dipak, you have always believed in what I could do and helped me through the times when it felt so very far away. You were always there and I feel incredibly lucky to have someone who just gets it, and is excited for where it will all take us.

Dedication

I would like to dedicate this thesis to my parents, Tilak Ghimire and Hemanta Ghimire. Although they were unknown about the scientific aspects of changing climate and environment, they were always concerned about the negative changes they experienced in their surrounding mountains, forests, and rivers. They were grown and cultured in male dominated society but they never discriminated me and had done their best to educate me in this area. They instilled in me the pride that can arise from hard work and dedication. They largely fueled my passion and determination for shaping my life towards environmental and sustainability sciences. Words cannot describe how much I miss them. I would also like to dedicate this thesis to my close family and friends for their continual support, encouragement, and emotional strength throughout. Completion of this project would not have been possible without you all.

Table of contents

List of tables

List of figures

List of abbreviations

AD	Absolute proportional difference
$^{\circ}C$	degrees Celsius
C	Carbon
CO_2	carbon dioxide
DIC	Dissolved Inorganic Carbon
DOC	Dissolved Organic Carbon
ESM	Earth System Models
GHGs	greenhouse gases
$g\ m^{-2}\ yr^{-1}$	gram per square meter per year
HER	Hydrologically effective rainfall
INCA	INtegrated CAtchment
INCA-C	Integrated Catchment Model for Carbon
km	kilometer
km^2	square kilometer
m	meter
MC	Monte Carlo
mm	millimeter
$mg\ L^{-1}$	milligram per liter
$m^3\ s^{-1}$	cubic meter per second
NS	Nash-Sutcliffe
NWT	Northwest Territories
PDC	Potential Dissolved Carbon
PERSiST	Precipitation, evapotranspiration and runoff simulator for solute transport
Pg C	Petagram of carbon
Q5	5th percentile
Q95	95th percentile

R^2	Pearson Correlation coefficient
SMD	Soil moisture deficit
SOC	Solid Organic Carbon
SWE	Snow Water Equivalent
Var	Ratio of variances
VT	Vital Tower
WMO	World Meteorological Organization
WSC	Water Survey of Canada
YKA	Yellowknife Meteorological Station A

Chapter 1: Introduction

1.1 Introduction

Many studies have highlighted the impact of climate change on hydroclimatic regimes (e.g., ACIA, 2004; Furgal et al., 2008; Lemmen et al., 2008). Understanding the impact of changing hydroclimatic regimes on dissolved organic carbon (DOC) is crucial in explaining the landscape-scale carbon (C) budget and pollutant transfer in catchment areas (Hudson et al., 2003; Oni et al., 2012), and DOC flux is known to change with hydroclimatic regimes (Evans et al., 2005; Futter et al., 2009; Noacco et al., 2019; Spence et al., 2015; Striegl et al., 2005; Walvoord & Striegl, 2007). Various driving factors are affecting DOC export in catchments, but these factors vary with the local landscape and regional hydroclimate. Thus, understanding the process of DOC export in the past can help determine how it will likely respond under future climate.

Within Canada, the Northwest Territories (NWT) are projected to undergo significant climatic change during the remainder of this century (ACIA, 2004, 2005; GNWT, 2008). Climate induced changes in runoff in catchments of NWT such as Baker Creek can affect seasonal DOC loads in surface water (Spence et al., 2015). The Baker Creek catchment has been polluted by metal deposition from nearby mines (Baldwin, 2006; Falk et al.,1973; Golder, 2013; Golder 2018). As DOC plays a significant role in metal mobility (Al-Reasi et al., 2013; Baken et al., 2011), it is crucial to understand the process of DOC export in these catchments and predict changing concentrations in the future under changing hydroclimatic regimes. Process-based catchment models can help achieve these aims. This study uses a catchment-scale water quality model to simulate DOC concentration and predict DOC export under different climate scenarios for Baker Creek. The research both develops knowledge about the sensitive parameters for DOC dynamics in subarctic catchments and can assist policymakers more generally in thinking through adaptation measures for potential water contamination.

1.2. Literature review

This literature review discusses the potential impact of changing hydroclimatic regimes on DOC. The review first summarizes the current understanding of changing hydroclimatic regimes and discusses the source, behavior, and pattern of DOC in catchments. Then, the export of DOC with changing hydroclimatic regimes is reviewed. The last part of the literature review discusses water quality models for C, which helps in selecting a suitable water quality model for understanding DOC dynamics in changing hydroclimatic regimes on a catchment scale. The review ends with the identification of critical gaps in knowledge, the purpose of the proposed research, and its significance.

1.2.1 Changing subarctic hydroclimatic regimes

Climate change is the pressing challenge of the 21st century. Almost all regions of the world have experienced warmer conditions during the last four decades (IPCC, 2021). The global surface temperature (2001–2020) has increased by 0.99 (0.84 to 1.10) $^{\circ}$C and increased by 1.09 (0.95 to 1.2) $^{\circ}$C from 2011 to 2020 compared to 1850–1900 (IPCC, 2021). Similarly, climate change has

increased the frequency and intensity of precipitation events since the 1950s and has changed seasonal precipitation patterns from the tropics to higher latitudes (IPCC, 2021; Lemmen et al., 2008; Song et al., 2018). In preindustrial times the primary cause of the increase in atmospheric carbon dioxide (CO_2) was due to deforestation and land-use change (Ciais et al., 2013); however, the rise in global temperature since the industrial revolution (after 1750) is unequivocally caused by anthropogenic greenhouse gas (GHG) emission via fossil fuel combustion and other industrial processes (IPCC, 2021). According to the World Meteorological Organization's (WMO) annual Greenhouse Gas Bulletin, the atmospheric CO_2 concentration in 2017 reached 146% of the preindustrial (pre−1750) level (WMO, 2017). Of C emitted by humans since 1959, 45% has been absorbed by the atmosphere, 24% by the oceans, and 30% by land (Quéré et al., 2018).

There is evidence of the unprecedented impacts of climate change, such as the increasing frequency of climate-related hazards, extreme weather events, change in precipitation phases, decreases in snow cover, changes in the groundwater table, permafrost thaw, and sea-level rise (Bauwens et al., 2013; IPCC, 2014; IPCC, 2021; Stagl et al., 2014; Huang et al., 2019). Last four decades were the warmest ones since 1850 (IPCC, 2021). Warming and acidification of global upper ocean (0–700 m) and decrease in oxygen levels in many upper ocean regions have observed (IPCC, 2021). Indeed, the atmospheric moisture-holding capacity has also increased due to the warmer atmosphere (Stagl et al., 2014). Many regions, such as the Middle East and the Mediterranean basin are experiencing prolonged and robust drought events (Hoegh-Guldberg et al., 2018). Hence, substantial and varying evidence of global climate change and its impacts are seen in different regions.

Climate change impacts are particularly severe in arctic and subarctic regions (typically between 50°N and 70°N latitude: Figure 1.1). The average temperature increase for this region (1.9°C over the past three decades) is almost double that of the rise in global average temperature (Warren & Lemmen, 2014). The average annual precipitation in the form of rain has increased by 8% over the past century (Furgal & Prowse, 2007), while the snow cover (1974−2003) has declined by 10% (ACIA, 2004). Similarly, permafrost has warmed by 2 to 3°C in recent decades and the southern extent of continuous permafrost is projected to shift northward by several hundred kilometers (ACIA, 2004). These changes in precipitation and temperature, and shifts in permafrost can affect infiltration, flow pathways, primary productivity, and microbial activities, all of which, in turn, affect river flows and nutrient export (Santín & Doerr, 2016; Walvoord & Striegl, 2007). Additionally, other consequences such as decreasing lake and sea ice, melting glaciers, rising sea levels, melting ice sheets, and various other impacts on the biophysical environment have been observed due to changing climate in subarctic regions (ACIA, 2004; Foy et al., 2011; Nistor, 2017; Nistor & Petcu, 2015).

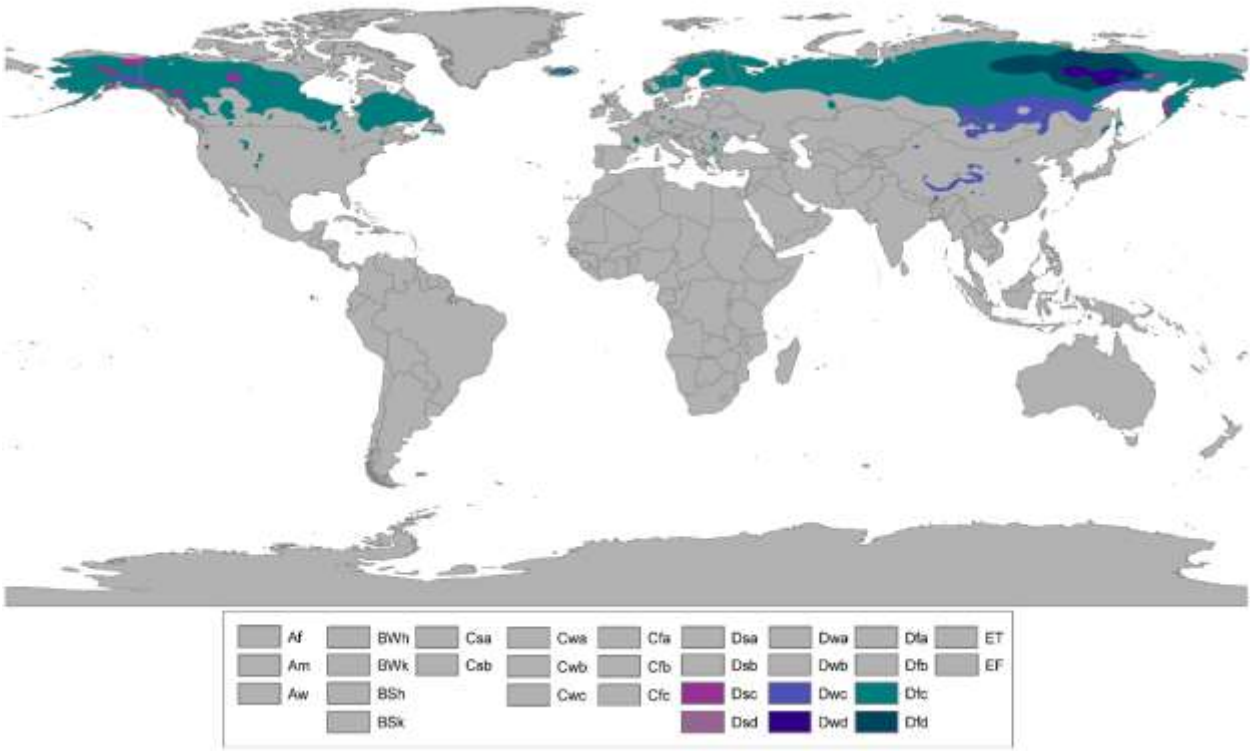

Figure 1.1: Map of regions with sub-arctic climate classified by Köppen-Geiger climate classification (Source: https://commons.wikimedia.org/wiki/File:Koppen_World_Map_Hi-Res.png)

Climate projections of 36 Earth System Models (ESM) predict an average increase in subarctic mean annual temperature by 3.7˚C by 2050 in comparison to the 1981 to 2005 period (Overland et al., 2013). These models project that, by 2050, the mean summer temperature will increase by 2˚C and the mean winter temperature by 5.3˚C (Overland et al., 2013). The projected warming in summer is about 1.5–2 times and winter is 3 times the rate of global warming (IPCC, 2021). Furthermore, ESMs under an intermediate GHG emission scenario project a rise of 4.3˚C and those more extreme scenarios a rise of 8.7˚C in mean annual temperature by 2100 (Schuur, McGuire, Romanovsky, Schädel, & Mack, 2018). The increased warming in the subarctic is projected to increase evaporation and is also projected to increase total precipitation by 20% by the end of the century (ACIA, 2004, 2005). The Coupled Model Intercomparison Project Phase 5 projected loss of more than 75% of glaciers in some regions of the subarctic, such as Scandinavia and western Canada, by the end of the century (Shannon et al., 2019). Under mid and high GHG emission scenarios, the Arctic Ocean is projected to be ice-free at least once before 2050 (IPCC, 2021). The projected change in precipitation, temperature, snow, ice, and glacier cover can affect energy balance, decrease feedback on land-surface albedo, and can affect hydrological and nutrient cycles (Lemmen et al., 2008).

There are various indications of a changing subarctic hydroclimatic regime. Since the middle and late 1900s, winter streamflow in northern Canada has been increasing (Walvoord & Striegl, 2007).

Climate warming (1977−2007) has increased the glacial retreat of Kaskawulsh Glacier, Yukon, decreasing the total area of the glacier by 1.5% (Foy et al., 2011; Ge et al., 2013). Glacial retreat has increased the discharge of glacial-fed rivers, which has affected the hydrological regime of the Yukon River (Moore et al., 2009). Furthermore, climate change impacts are also severe in Scandinavia, with warming driving earlier ice melt and decline in summer sea-ice cover (ACIA, 2005). Likewise, in some areas of northern Sweden, frequently fluctuating warm and cold episodes affecting the freeze-thaw cycle have been observed (ACIA, 2004). Indeed, there is high uncertainty for the future subarctic hydroclimatic regime but understanding past and present climate scenarios can assist in the better projection of future hydroclimatic patterns.

1.2.2 Catchment controls on organic carbon

Biogeochemical cycles are tied to physical conditions, including temperature, water availability, and water movement; therefore, the impacts of climate warming can be seen in biogeochemical cycles. Warming in high latitude regions increases primary productivity and also stimulates permafrost thaw. Permafrost thaw can change the C budget by releasing stored methane and CO_2 to the atmosphere, and also mobilizing DOC (Ma et al., 2019). Understanding drivers and processes of catchment control on C (source, behavior, pattern, and export), including flow pathways is necessary to know DOC dynamics in the catchment.

1.2.2.1. Dissolved organic carbon

The DOC in an aquatic ecosystem is derived from either autochthonous or allochthonous sources. Autochthonous sources are produced inside the water bodies by algal and bacterial biomass. In the formation of autochthonous sources, nutrients present in water bodies play a major role (Kaplan & Bott, 1982), helping in the growth of algal and bacterial biomass. In contrast, allochthonous sources are produced outside the water bodies from the soil, vegetation, and microbes in the terrestrial ecosystem (Hood et al., 2003). The DOC from these sources have free radicals which can act as both electron donors, and acceptors depending upon the situation and are also active in oxidation-reduction reaction with transition metals (McKnight et al., 1992) which can alter water chemistry.

DOC is a complex substance that controls a large number of physicochemical and biological parameters in water bodies (Hudson et al., 2003). DOC complexes can affect bioavailability, toxicity, and mobility of metals in the environment (Koprivnjak & Moore, 2006; Ledesma et al., 2012; McKnight et al., 1992) such as copper (Ashworth & Alloway, 2007), mercury (Ravichandran, 2004), aluminum, iron (McKnight et al., 1992), and arsenic (Howell, 2014). DOC is composed of diverse functional groups having a strong metal binding capacity (Mostofa et al., 2013). DOC undergoes oxidation-reduction reactions with metal pollutants and binds protons, affecting the redox property of organic ligands (Koprivnjak & Moore, 2006; Ledesma et al., 2012; McKnight et al., 1992).

Additionally, DOC makes organic complexes with nutrients such as nitrogen and phosphorus, increasing their solubility and mobility (Yang et al., 2013), and those nutrients act as fuel for

microbial production (Biddanda & Cotner, 2002). DOC can absorb ultraviolet radiation, which reduces the biological activities of aquatic organisms (Rautio & Korhola, 2002). Furthermore, DOC in the source of drinking water is harmful to human health. Drinking water treatment involves the chlorination process which prevents microbial growth during water distribution; however, this chlorine can react with available DOC in water (Chow et al., 2003) to form carcinogenic and mutagenic by-products such as trihalomethanes and haloacetic acids (WHO, 2011). Thus, DOC is an important consideration in drinking water treatment processes.

1.2.2.2. Dissolved organic carbon behavior at catchment scales

Multiple catchment-scale drivers such as landcover, hydrology, connectivity, temperature, sea salt deposition, and acid deposition can influence DOC dynamics. These drivers can control in-soil and in-stream DOC behavior in a catchment (Evans et al., 2005; Koprivnjak & Moore, 2006; de Wit et al., 2016). The type and properties of the catchment play a significant role in DOC concentration. In the study of boreal catchments, peatlands were found to be the major source of terrestrially derived DOC concentration due to slow water movement and slow decomposition of organic matter (Dillon & Molot, 1997). In peatlands, newer peat is easily mineralized compared to peat that has accumulated over many years (Dillon & Molot, 1997). Similarly, because of the high productivity of forested catchments, DOC concentrations are generally higher in forest dominated catchments than in those with rock covers (Moore, 1989).

Several studies have found catchment hydrological factors such as runoff, water table, and catchment connectivity as the significant drivers in determining DOC behavior in the catchment (Baker et al., 2006; Clair et al., 1999; Daniels et al., 2008; Evans et al., 2005). Increased runoff in the catchment can both increase and decrease DOC concentration depending upon the flow pathways (Evans et al., 2005; Walvoord & Striegl, 2007). The DOC concentration increases where flowpaths through the shallow organic soil layer are dominant, whereas it can decrease where the bulk of the water transits through the deep mineral layer (Clair et al., 1999; Valley & McDowell, 1988). The water table can also affect DOC concentration; decline in the water table in peatlands during dry periods can oxidize peat and lead to flushing of organic C during high flow events (Daniels et al., 2008; Petrone et al., 2006).

Additionally, understanding source connectivity is essential to understand DOC concentration in the stream (Baker et al., 2006). In wetter seasons, due to hydrological connectivity with C sources, high concentration of C can be seen; however, in dry seasons hydrological connectivity can be interrupted with C sources resulting in lower C concentrations (Dick et al., 2015; Spence et al., 2018). The hydrological disconnectivity is because of disrupted surface flow and high evaporation along the flow path which prevents runoff between upper and lower reaches (Dick et al., 2015). Thus, in dry periods, groundwater contributes to the DOC concentration (Dick et al., 2015).

Carbon concentration can be affected by changing climate. The catchments in the circumpolar north are estimated to have a total of 1,672 Pg C which accounts for approximately 50% of global below ground soil C (Tarnocai et al., 2009). With changing climate these catchments could release

a total of 162−288 Pg C by 2100 under RCP 8.5 (Schuur et al., 2013). There are many cases where DOC concentration is increasing with temperature (Chapman et al., 1995; Evans et al., 2005; Michalzik et al., 2003; Tipping & Hurley, 1988). Temperature increases can increase primary productivity (Striegl et al., 2005). Furthermore, the increased temperature can decrease water table position and can enhance oxygen availability in soil. Organic C mineralization in wetlands is highly sensitive to oxygen availability (Chapman et al., 2019). Although mineralization can occur under both aerobic and anaerobic conditions (Kane et al., 2019), aerobic soil conditions are found to mineralize 3.2 times more C comparing to anaerobic conditions (Schadel et al., 2016). In aerobic conditions, the presence of a strong electron acceptor (oxygen) deconstructs even strong enzymes such as oxidases and peroxidases in organic compounds (Sinsabaugh, 2010). Thus, aerobic respiration in microorganisms oxidizes C in organic matter into inorganic C (Lin et al., 2021). When microbial decomposition of the organic matter becomes sufficiently elevated, DOC concentration decreases (Weiman, 2015).

Increased evapotranspiration can also affect DOC concentration; in North America, an increase in summer temperature of catchments yields decreased soil moisture, increasing lake residence time and providing greater opportunity for DOC degradation (Hudson et al., 2003). The change in rainfall amount can also alter DOC concentration in catchments via dilution in surface water. Other drivers such as elevated atmospheric CO_2 (Clair et al., 1999; Freeman et al., 2004; Evans et al., 2005), sea salt deposition (de Wit et al., 2016), and acid deposition (Evans et al., 2005) can alter DOC concentration. Increasing trends in DOC concentration over the last few decades in northern Europe have been reported (Evans et al., 2006; Freeman et al., 2001; Monteith et al., 2014), whereas some authors have highlighted weak to no trends of DOC concentration in central Europe (Oni et al., 2012). Although in North America increasing DOC concentration trends have been observed, these trends are weak (Monteith et al., 2007; Oni et al., 2014). Drivers for the increasing trend in DOC concentration in catchments of North America and North Europe are due to change in runoff (Eimers et al., 2008; Oni et al., 2012), climate variability (Noacco et al., 2019; Striegl et al., 2005), and acid deposition (Monteith et al., 2007). In Norway, changes in climatic variables with sea salt deposition in catchments have changed DOC trends (de Wit et al., 2016). Thus, DOC behavior and pattern in catchment depends upon multiple catchment drivers.

1.2.2.3 DOC export under changing hydroclimatic regime

Understanding the export of C from the terrestrial ecosystem to the aquatic ecosystem is significant for knowing the sensitivity of the C cycle to changes in the hydroclimatic regime. Numerous studies have highlighted cases of DOC export with changing hydroclimatic regime (Clair et al., 1999; Futter et al., 2009; Ledesma et al., 2012; Noacco et al., 2019; Striegl et al., 2005). The drivers for DOC export such as runoff, hydrological connectivity, flow pathways, and soil moisture can be affected by changes in the hydroclimatic regime. For instance, an increase in temperature can increase evapotranspiration, decrease soil moisture, and decrease hydrological connectivity leading to lower flushing of C (Clair et al., 1999; Tranvik & Jansson, 2002).

Additionally, temperature increases can increase terrestrial C fixation, increasing C pools in the catchment (Freeman et al., 2004). Also, the increased temperature can increase the active layer of permafrost, enhancing oxidation of stored C in permafrost soil, which becomes the net source of DOC (Petrone et al., 2006). Permafrost thaw can also modify flow pathways; flow paths from shallow organic layer enhances DOC export whereas through deeper mineral layer can decrease export. Thus, overall C fluxes in the catchment are sensitive to hydroclimatic drivers.

1.2.3 Catchment biogeochemical modeling

Water quality in a catchment is determined by physical, chemical, and biological parameters in the system. As a result, complex water quality models are essential tools in predicting and simulating various mechanisms affecting water quality in a system (Tsakiris & Alexakis, 2014). Factors such as topography, vegetation type, land use, and landcover, as well as anthropogenic activities, all play a critical role in determining water quality (Tsakiris et al., 2009). Historically the development of water quality models has undergone three critical phases (Wang et al., 2013). The first phase (1925−1965), began with the development of the first water quality model to characterize water pollution in Ohio, USA (Streeter & Phelps, 1958; Wang et al., 2013). In this phase, a one-dimensional BOD-DO model was successful in understanding water pollution issues in water bodies such as rivers and estuaries (Burn & Mcbean, 1985; Bencala & Walters, 1983).

In the next phase, (1965−1995) two and three-dimensional models were developed (Wang et al., 2013). In this stage, catchment models were combined with water quality models to include more variables determining water quality (Tim & Jolly, 1994). In this phase, various models were developed: QUAL models for dendritic rivers and non-point source pollution by USEPA (Wang et al., 2013); WASP models developed by USEPA for rivers, lakes, wetlands, estuaries, and reservoirs (Robert et al., 1988); and MIKE11 by Denmark Hydrology Institute for rivers, tidal wetlands, and estuaries (Robert et al., 1988; Talebbeydokhti et al., 2017). Models at this stage were successful in providing detailed knowledge about non-point sources (Wang et al., 2013).

Another phase began where water quality models were integrated with air pollution models to include aerosol deposition in the surroundings of water bodies and indirect contamination in water bodies (Esterby, 1996). The water quality models developed in these phases are complex. The reason for this complexity is that these models consider the function of four parameters: spatial detail, temporal detail, water quality indicators, and complexity of water bodies (USEPA, 1998). At this stage, with the advancement of earlier models many new water quality models were developed, such as SWAT developed by the U.S. Department of Agriculture; the QUASAR model and BASINS models developed by USEPA (Wang et al., 2013); and the semi-distributed INCA model (Whitehead et al., 1998).

1.2.3.1. Water quality models for carbon

Water quality models for C are used to predict the concentration and transport of DOC in spatial or temporal scales. Different water quality models for C have been designed with different characteristics ranging from empirical to process-based models (Oni et al., 2012). These models

have various strengths and limitations for different applications. Empirical models are based on cause-effect relationships and identify drivers (Oni et al., 2012); however, these models fail to explain complex biogeochemical processes (Futter & de Wit, 2008) and they have significant limitations in forecasting scenarios for future conditions (Oni et al., 2012).

Limitations can be seen in the DOC model (DocMod), which uses C to nitrogen ratio of vegetation species and leachate quality and quantity to predict DOC fluxes (Currie & Aber, 1997). Similarly, drawbacks can be seen in the integrated biogeochemical model (PnET-BGC), which is a one-dimensional coupled model and works on monthly time series (Gbondo-Tugbawa et al., 2001), as does the ORCHIDEE-SOM model. Although the ORCHIDEE-SOM model is good at representing the DOC and Solid Organic Carbon (SOC) dynamics, it is not able to capture the processes beyond 2 m vertical discretized soil. The various biological, environmental, and geological factors result in soil heterogeneity leading to change in DOC concentration with time which is not captured by ORCHIDEE- SOM model (Camino-Serrano et al., 2018). Thus, it fails to capture the temporal dynamics of soil C concentration (Camino-Serrano et al., 2018).

Furthermore, some other process-based water quality models can simulate DOC behavior in catchments (Oni et al., 2012) such as the Dynamic DOC model (Michalzik et al., 2003) which is good at describing soil C processes but fails to describe the in-stream C process. The same is the case of landscape-scale C models (Hanson et al., 2004), which are adequate for understanding DOC patterns in the lake but fail to reproduce the terrestrial part of the catchment.

The Integrated Catchment Model for Carbon (INCA-C) was developed (Futter et al., 2007) to address the shortcomings of various water quality models for C. This model combines soil and stream parameters and projects long-term C dynamics at landscape scales. It was the first landscape-scale model designed to project temporal changes in DOC in forested, temperate, and boreal catchments (Futter et al., 2007). The INCA-C model helps to understand the mechanism controlling DOC concentration. Additionally, this model can simulate DOC concentrations under future climate scenarios (Futter & de Wit, 2008). This model has been successfully used to simulate observed DOC patterns, and subsequently used to explore future scenarios in headwater and larger catchments in Europe and Canada (Futter et al., 2007; Futter et al., 2009; Oni et al., 2012; Oni et al., 2014; de Wit et al., 2016; Xu et al., 2020). INCA-C consists of hydrological and biogeochemical sub-models. The C fluxes in soil and stream C pools (SOC, Dissolved Inorganic Carbon (DIC), Potentially Dissolved Carbon (PDC), and DOC) are shown in figure 1.2.

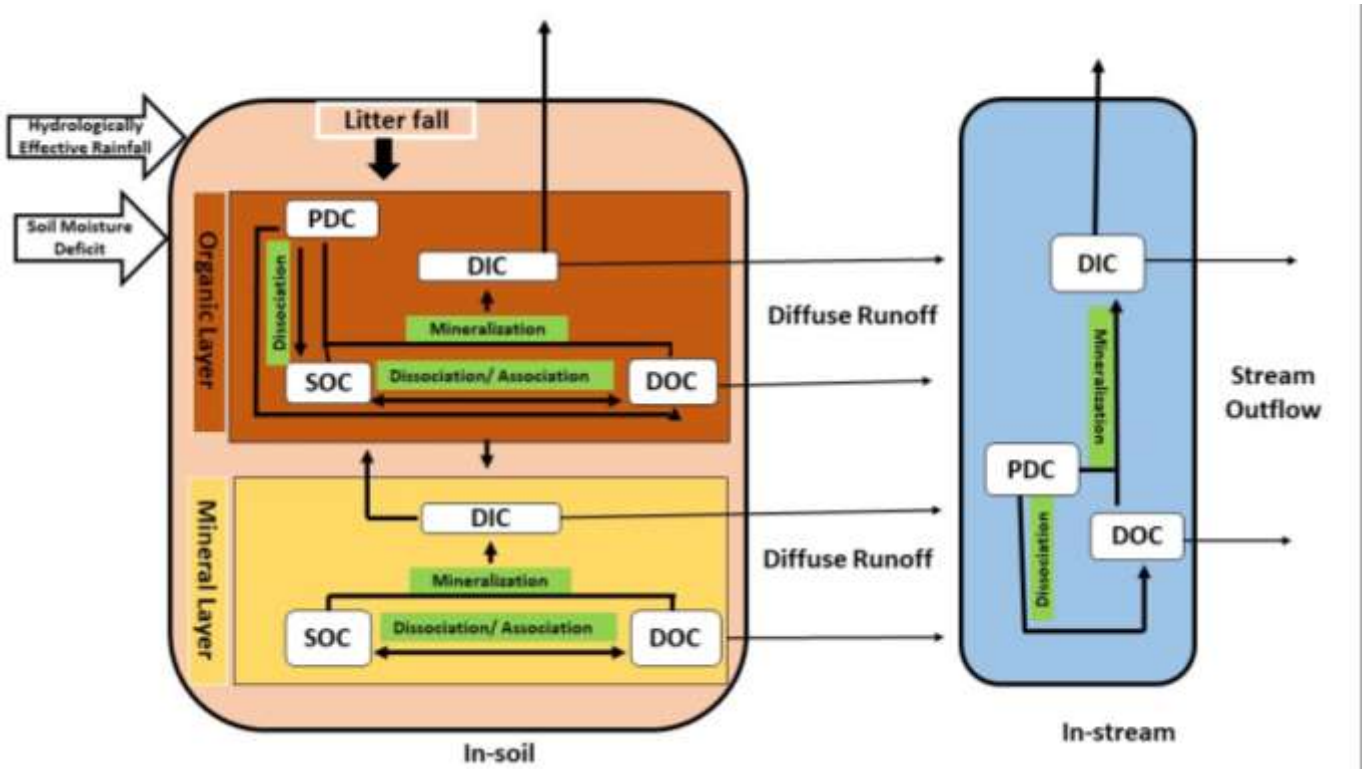

Figure 1.2: C pools and fluxes in soil and stream in INCA-C model (modified from Ledesma et al., 2012). Hydrologically Effective Rainfall (HER) and Soil Moisture Deficit (SMD) are hydrological inputs for INCA-C, litter fall represents C input, white boxes represent different C pools in soil and stream and green boxes show processes. Note that atmospheric deposition of C is not considered in the model.

1.2.4 Dissolved organic carbon as a mediator of contaminant transport

Baker Creek lies near the Giant Mine site. The lower part of the catchment has a history of contamination of arsenic, mercury, and other heavy metals from 1948 to 1980s due to untreated tailings and effluents being deposited (Baldwin, 2006; GMRP, 2013; Golder, 2018; Howell, 2014; Olivie-Lauquet et al., 2001; Wrye, 2008). Another source of contaminants to Baker Creek (upstream of Lower Martin) was atmospheric deposition (GMRP, 2013; Golder, 2018). Historically, the mine emitted 20,000 tonnes of arsenic during its operational period (Howell, 2014; Wrye, 2008) which was deposited up to 30 km from the historical roaster stack (Jamieson et al., 2017). In Baker Creek, a high concentration of bioavailable arsenic and mercury in whitefish (Cott et al., 2016), elevated sediment arsenic concentrations (GMRP, 2013; Golder, 2018) and high concentrations of total dissolved solids and heavy metals in downstream locations (2016−2018) (GNWT, 2017; Golder, 2018) were reported. The contaminants in the terrestrial part of the catchment could have impacts on aquatic and human health if exported to water bodies (Golder, 2018). It has been observed that DOC plays a major role in contaminant transport (Howell, 2014; Koprivnjak & Moore, 2006; McKnight et al., 1992; Mostofa et al., 2013). Thus, it is important to understand DOC export in Baker Creek to understand how this might be important

for metal mobility. At present there has been limited monitoring of DOC export. It remains uncertain how these patterns may change in response to changing hydroclimate and if DOC is sensitive to temperature and hydrological changes in the catchment. Thus, it is important to understand the behavior and pattern of DOC export as in Baker Creek under future hydroclimatic conditions.

1.3 Objectives

The purpose of this research is to understand how DOC responds to a changing hydroclimatic regime in the subarctic catchment. The specific objectives for this research are listed below.

Objective 1**:** Identify historical hydroclimatic trends in the catchment

Objective 2*:* Simulate catchment DOC export to understand landscape-scale factors controlling DOC

Objective 3*:* Forecast future catchment behavior and understand DOC response under a changing hydroclimatic regime

Chapter 2: Methodology

2.1 Description of the study site

The Baker Creek catchment is located in Canada's NWT on the northern side of Great Slave Lake near the city of Yellowknife. It is located between 62°45'00" N and 62° 30'00" N latitude, and 114°30'00" W and 114°20'00" W longitude (Figure 2.1), within a region of discontinuous permafrost. The catchment area is 165 km^2 and elevation ranges from 200 to 266 m (above sea level). Additionally, Baker Creek catchment is close (northwest within 30 km) to mining activities which are likely to have contributed to atmospheric deposition of metals including arsenic, copper, zinc, lead, nickel, cyanide, and chromium from the historic roaster stack (Baldwin, 2006; Galloway et al., 2012; Golder, 2013; Nasser, 2014; Nathan, 2018; Nasser et al., 2017).

The major land cover in Baker Creek catchment is exposed bedrock, which occupies 40% of the total area, followed by open water (23%), forest (21%), and wetlands and peatlands (16% combined) (Spence et al., 2018). The major soil types are derived from organic, sandy till, glaciofluvial deposits, with a trace amount of organic cryosols in poorly drained areas (Spence et al., 2010). The thickness of the organic soil layer ranges from less than a meter to more than 10 m (Spence & Hedstrom, 2018). The major flora of the region consists of Labrador tea (*Rhododendron groenlandicum*), black spruce (*Picea mariana*), paper birch (*Betula papyrifera*), jack pine (*Pinus banksiana*), and many species of moss and lichen with the majority of (*Sphagnum* spp. and *Cladonia* spp.).

Data from a climate station in the catchment (Vital Tower) and nearby stations characterize very long and cold winters with an average daily temperature in January of −24ºC and short, cool summers with an average daily July temperature of 17ºC. There is considerable interannual variability in temperature owing to the influence of oceanic-atmospheric circulation modes in western Canada (DeBeer et al., 2016). Average annual temperatures varied between −7ºC and −1ºC during the past 65 years (1955–2019). The average annual precipitation in the catchment is 249 mm, of which 36% falls as snow. Precipitation in the catchment typically falls as rain from May to September and snow from October to April. February–April are the driest months (average monthly precipitation: 35 mm) and July–September are the wettest months (average monthly precipitation: 103 mm). Annual precipitation ranged between 170 mm to 423 mm during the past 65 years (1955–2019).

The catchment contains 349 perennial lakes among which Duckfish is the largest headwater lake by area (6.2 km^2), followed by Martin Lake (3 km^2), Vital Lake (1.5 km^2), and Landing Lake (1.1 km^2) (Spence, 2006). The sub-catchments where these lakes are located demonstrate different physical features and hydrological behavior (Table 1), and during wet years, a greater proportion of the catchment contributes to discharge at the outlet of Lower Martin Lake (Spence, 2006). The outlet at Lower Martin Lake is gauged (Water Survey of Canada station: 07SB013) a short distance upstream of Great Slave Lake. There is a large variation in average annual discharge at the outlet of Lower Martin, ranging from 0.0009 to 0.43 $m^3 s^{-1}$. Maximum discharge occurs during snowmelt in spring (April–June).

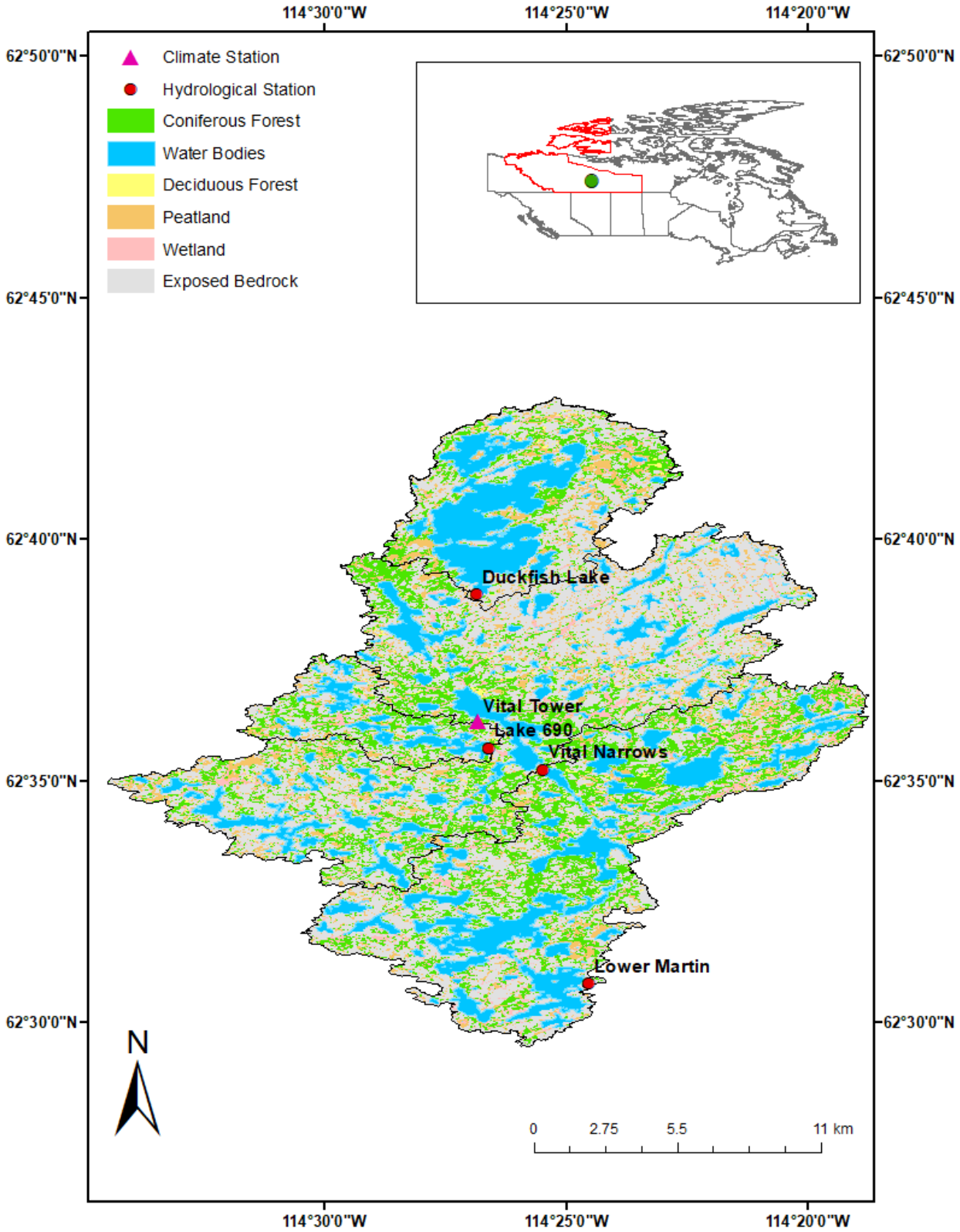

Figure 2.1: Baker Creek catchment showing land covers and hydrometeorological stations (Projection: NAD 1983, UTM 11N).

Table 2.1: Catchment characteristics for the Baker Creek catchment (Lower Martin Lake), and several of its sub-catchments (Spence & Hedstrom, 2018)

Name	Catchment area (km^2)	Land cover (%)				Average annual runoff (mm)
		Surface water	Forest	Wetland	Bedrock	
Duckfish Lake	25	34	17	16	33	40
Lake 690	9	21	25	15	39	115
Vital Lake	102	22	19	16	43	108
Lower Martin Lake	153	23	21	16	40	49

2.2 Modelling approach

A coupled model framework using PERSiST and INCA-C was used in this research (Figure 2.2). PERSiST is a semi-distributed hydrological model designed for modeling rainfall-runoff patterns for the INtegrated CAtchment (INCA) family of models (Futter et al., 2014). Input data for PERSiST consists of daily temperature and precipitation (Futter et al., 2014; de Wit et al., 2016). PERSiST has been used in all scales of catchments from small headwater boreal systems in Sweden (Salmonsson, 2013), to moderate-sized temperate catchments in Norway (Couture et al., 2014) and the UK (Futter et al., 2014), as well as in large sub-tropical catchments like the upper Ganga and Brahmaputra (Futter et al., 2015). PERSiST is used to generate time series of daily HER and SMD for use in INCA. PERSiST calculates HER as precipitation minus the sum of evapotranspiration and interception. PERSiST model version 1.6.4 was used in this study.

The semi-distributed, processed-based INCA-C model was used in this study to simulate DOC behavior. This model is based on the Integrated Catchment Model for Nitrogen, developed in Europe with the aim of understanding catchment nutrient budgets (Whitehead et al 1998). The model integrates hydroclimatic processes with terrestrial components and simulates DOC fluxes (Futter et al., 2007; Oni et al., 2012) at daily time steps. It incorporates information about in-soil C processes, surface water processes, and landscape-scale water movement (Futter et al., 2007). The model represents the transfer of organic C between terrestrial and surface water environments, with sub-catchments used as the basis for model parameterization (Futter et al., 2007). The terrestrial part of the model has up to six land cover classes consisting of up to three soil compartments. The surface water environment (stream) is modeled as a single stream reach or a branched stream network. The model is run using daily HER and SMD as inputs and operates at a daily time step. This study used the new branching version of INCA-C (Version: Branching_INCA-C_v2.0.0_BETA_14) to model C behavior in Baker Creek sub-catchments.

As shown in figure 2.2, PERSiST model was run using daily temperature and precipitation data of Vital Tower station and calibrated using observed stream flow data. Flow in the catchment from

headwater lake (Duckfish) to outlet of Lower Martin were directed by using structure file as input. Model was calibrated in sub-catchments scale using streamflow observations of sub-catchments (Duckfish Lake, Lake 690, Vital Narrows, and Lower Martin). The generated HER and SMD from best parameter set of PERSiST model were used as input for INCA-C model. INCA-C model was calibrated by using observed stream flow and DOC concentration in sub-catchments. Both manual and Monte Carlo calibration were conducted to obtain best performing parameter set. The best parameter set obtained by running INCA-C was used for simulating future DOC simulations.

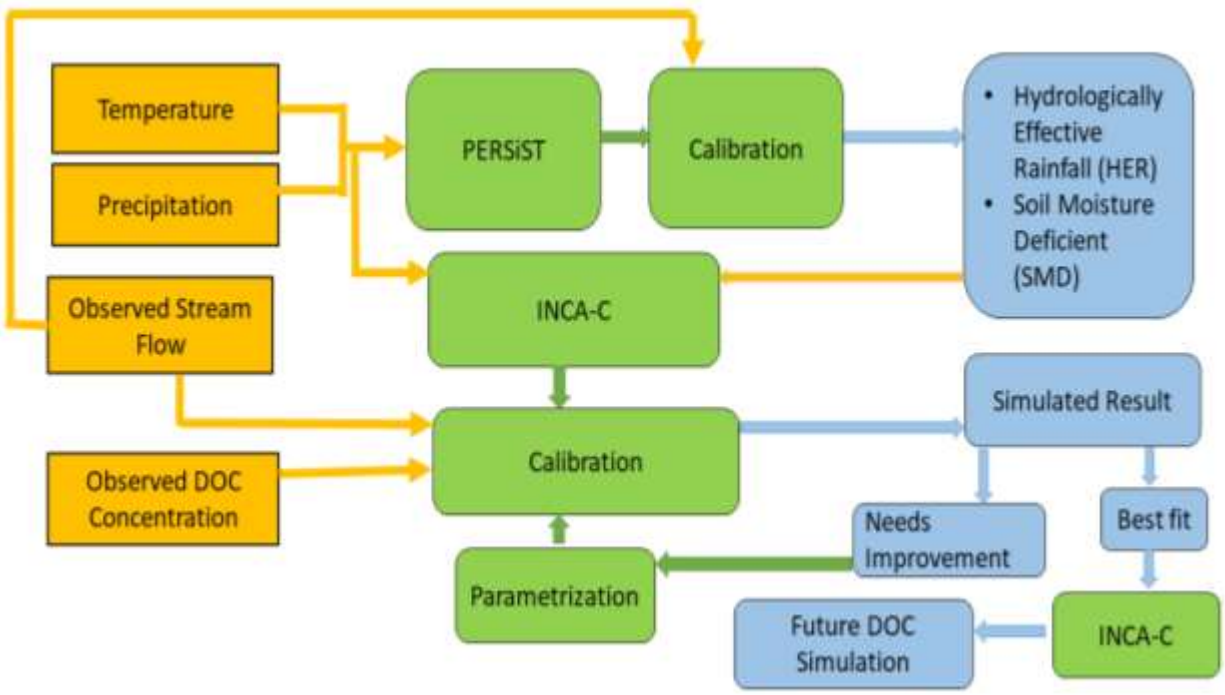

Figure 2.2: Modelling approach (gold colour represents the input, green represents method, and blue colour represents output). Note: Daily temperature and precipitation data of Vital Tower station was used as input for PERSiST. Output from PERSiST (SMD and HER) were used as input for INCA-C. PERSiST model was calibrated using streamflow data. INCA-C model was calibrated by streamflow and available observed DOC concentration data of Baker Creek sub-catchments.

2.3 Data sources

Most of the data collected in the catchment to date have been previously published as a dataset (Spence and Hedstrom, 2018), which is used extensively here (details below).

2.3.1 Topography and Land Cover

Digital elevation and land cover data were obtained from Spence & Hedstrom (2018). Recent available elevation data were collected on August 21, 2007, using Light Detection and Ranging (LiDAR) at 10 m resolution. The elevation data uses the NAD1983 UTM Zone 11N Projection

system (Spence et al., 2010). Land cover classification data were collected via the SPOT5 MS satellite image at 10 m resolution (May 24, 2008–June 20, 2009; Spence & Hedstrom, 2018). Imaging was mapped using the maximum likelihood of supervised classification of a composite image of two satellite images using Normalized Difference Vegetation Index and multispectral bands as input (Spence & Hedstrom, 2018).

2.3.2 Climate and Hydrology

Temperature and precipitation data for Vital upland (2005−2016) were obtained from Spence & Hedstrom (2018) and by retrieving data (package: 'weathercan'; LaZerte & Albers, 2018) for Meteorological Service of Canada Yellowknife (YKA) station #1706 (1955−2013) and station #51058 (2013−2019) (http://www.climate.weather.gc.ca). At Vital tower (VT), temperature data were obtained with a Vaisala HMP45C thermohygrometer, and rainfall data were collected with a Texas Instruments TE-525M tipping bucket rain gauge (Spence & Hedstrom, 2018). The Vital station operates from ~early April until ~early October annually. Gaps in the Vital temperature and precipitation data, due to intermittent or seasonal gaps in sensor recordings, were addressed using data from YKA, which lies ~5 km from the southern end of the catchment (see section 2.4). End of winter snow on the ground (November−March) in the catchment was estimated using annual snowpack surveys in April (2003−2016) (Spence & Hedstrom, 2018).

Hydrological data at the outlet of Lower Martin Lake collected by WSC (1983−2017) was retrieved from https://wateroffice.ec.gc.ca/search/historical_e.html. Hydrological data of three other stations (Figure 2.1), i.e. Duckfish Lake (2009−2016), Lake 690 (2008−2016), and Vital Narrows (2005−2016), operated by the Science and Technology Branch of Environment and Climate Change Canada, were available from Spence & Hedstrom (2018).

2.3.3 Organic Carbon Chemistry

Water samples for DOC analysis were collected approximately biweekly (during open-water season) by the Government of the Northwest Territories Water Resource Division, at the footbridge downstream of the outlet of Baker Creek at Lower Martin Lake (April 2010 to November 2019). Similarly, for two other sites, Lake 690 (2010−2014) and Vital Narrows (2015−2019), grab samples were taken each spring and summer. These water samples were analyzed for DOC using infrared combustion (detection limit 0.5 mg L^{-1}) at the Taiga Environmental Laboratory, NWT. Additionally, DOC samples collected in Duckfish Lake and analyzed by Shimadzu Total Organic Carbon combustion analyzer at the Environmental Geochemistry Laboratory (University of Waterloo) in the summer of 2019 were used in this study.

2.4 Data processing

Data processing, data visualization, and statistical analyses were all performed using R: A Language and Environment for Statistical Computing, 2017 (R Core Team 2020; version 3.6.3). Half-hourly temperature and rainfall over 2005–2016 at VT were processed to daily average temperature and total daily precipitation. We used a two-step approach to infill temperature and precipitation data.

The half-hourly temperature was converted into daily values and missing values in temperature data were filled using data of the YKA station; linear regression of daily observations (package: 'stats'; function 'lm') was used to infill the VT record. After infilling missing values in VT, the small number of remaining missing values (days when data was missing in both stations) were infilled by using the predictive mean matching method (package: 'imputeTS'; function 'mice').

For precipitation data, warm-season half-hourly rainfall for VT was converted into daily values, and missing values in daily rainfall were infilled using nearby YKA station data according to linear regression (package: 'stats'; function 'lm'). Likewise, for the winter period outside of normal tipping bucket operation at VT, rainfall amounts for days with an average temperature above zero degrees were estimated as above, assuming precipitation under these conditions falls as rain. Winter period days with an average temperature above zero when data were missing in both stations were infilled by using the predictive mean matching method (package: 'imputTS'; function 'mice'). Daily snowfall accumulation during the period when rainfall gauges were not in operation was estimated by interpolation, according to the snow water equivalent (SWE) amount measured in April. The snowpack data (SWE) had a missing value (for the year 2006), which was filled by a predictive mean matching method (package: 'imputeTS'; function 'mice'). Total daily precipitation at VT (2005–2016) was taken as the sum of these rainfall and snowfall reconstructions.

2.5 Model Calibration

2.5.1. PERSiST

The PERSiST model was first calibrated manually using daily discharge data for four sub-catchments (Duckfish Lake, Lake 690, Vital Narrows, and outlet at Lower Martin). Initially, parameter values were set according to default recommended values from PERSiST applications in other catchments. Landscape-scale parameters were set according to Table 2.1. The main focus of manual calibration was to get appropriate water balance parameters and water routing matrix (partition of runoff generation between soil boxes (Ledesma & Futter, 2020)). In PERSiST, water is routed directly from each land cover to the stream reach. Soil buckets in each land cover receive water (HER) and the flux of water through each compartment (bucket) is calculated by water routing matrix. The elements of the water routing matrix (i, j) represents the fraction of water leaving a bucket "i" and adding to another bucket "j" (Ledesma & Futter, 2020). Water fluxes in buckets ($m^3\,d^{-1}$) are calculated at 1 km^2 area in each land cover and total fluxes from sub-catchment to reach are calculated by multiplying fluxes with catchment area (Futter et al., 2014). For the Baker Creek catchment, to simulate discharge sensibly, PERSiST was parameterized to allow water to move quickly with low water loss by evapotranspiration; much of the water was routed via the faster layer to streamflow. The influential parameters were updated iteratively when a better-simulated result than the previous starting point was obtained. When model performance wasn't improved with the adjusted values, the parameters were reset to the previous values. The parameter ranges were explored until no further improvement in model performance was obtained.

Model performance at each iteration was estimated by goodness-of-fit metrics. Pearson Correlation coefficient (R^2), Nash-Sutcliffe (NS), Log Nash Sutcliffe (Log (NS)), the absolute proportional difference (AD), and the ratio of variances (Var) were evaluated, considering the optimal values (Table 2.2) for these metrics. A quasi-nested approach to manual calibration was used, where headwater catchments (Duckfish and Lake 690) were calibrated first. After obtaining a satisfactory fit for these records, the downstream stations at Vital Narrows and Lower Martin were calibrated.

After getting the best performance set from manual calibration, Monte Carlo (MC) analysis with 25 parameter sets, each chain consisting of 500 model runs, was applied to explore parameter space and generate behavioral parameter sets. The MC tool uses tolerance windows (minimum and maximum) for sensitive catchment-scale parameters (degree day melt factor, growing degree threshold, time constant, and evapotranspiration adjustment), sub-catchment parameters (precipitation multipliers), and reach scale parameters (flow parameters: a, b, c, f) (Table A.1). Tolerance windows were set as ± 25% of the values obtained through manual calibration. Differential weights were assigned for different parts of the catchment. Higher weights (five) were assigned to the Lower Martin stations, because it had the most complete observational record available, whereas lower weights (one) were used for Vital Narrows and Lake 690. Although, there was not specific guideline for selecting weighing values, we evaluated alternate weighting ratios (1:5 and 1:10), and found that this did not influence the results. Similarly, a higher weight (two) was given to NS in an effort to better-capture flow peaks which the manual calibration was less successful in reproducing, while Log (NS), Var, and AD were assigned weights of one. The MC analysis gave one best-performing parameter set for each iteration. The best-performing parameter set from all iterations was evaluated by checking goodness-of-fit metrics and by visual time-series assessment. The best-performing parameter set from the MC analysis was used to generate SMD and HER for input to INCA-C.

Table 2.2: Optimal values of the goodness of fit metrics used to evaluate model performance (Ledesma & Futter, 2020)

Performance indicator	Range
R^2	0 (No match) to 1 (Perfect match)
NS	0 (Fitting mean value) to 1 (Perfect match)
Log (NS)	0 (Fitting mean value) to 1 (Perfect match)
AD	Closer to zero (Perfect match); Positive value (under prediction); Negative value (Over prediction)
Var	1 (Perfect match)

2.5.2. INCA-C

The INCA-C model was calibrated manually using daily discharge and DOC data for four sub-catchments (Duckfish Lake, Lake 690, Vital Narrows, and the outlet of Lower Martin Lake). Initially, parameter values were set according to default recommended values from the INCA-C application to other catchments. Available sub-catchment parameters (area and land cover) were set according to Table 2.1. The remaining sub-catchment, reach, instream, and land phase groups of parameters were adjusted in order, moving on to the next group of parameters when no further improvements were achieved. The initial focus of manual calibration was streamflow, to achieve similar or better performance than obtained from PERSiST. After calibrating for streamflow, the in-soil parameters related to C processes (C input, transformation, and processes) were calibrated to model DOC concentration. INCA-C has two soil boxes in each land cover type (upper organic and lower mineral). Each soil box has four C pools (SOC, PDC (Potentially Dissolved Carbon), DOC, and DIC). Carbon input occurs through litter fall, root breakdown, and microbial death and transported from soil to stream through diffuse flow (Futter et al., 2007).

Model performance for discharge and DOC simulations was evaluated by the goodness of fit metrics (Pearson Correlation coefficient (R^2) and Nash-Sutcliffe (NS)). At Baker Creek, there were several DOC observations at Lower Martin each year, while Vital Narrows had sparse observations of only two years. Observations were not available at Duckfish in the calibration period, however a single observation for 2019 and anecdotal observations were used to inform the calibration. Visual assessment was used for this sub-catchment in an effort to simulate higher DOC levels anticipated for this location. In addition to evaluating discharge and DOC, the manual calibration was also evaluated for the behavior of PDC fluxes (direct runoff layer) and DOC (organic and mineral layer) pools. In instances where the calibration did not yield relatively constant pools (which leads to unstable forecast simulations), further calibration was performed. Land phase (fast pool fraction in organic and mineral layer, organic and mineral layer retention

volume, PDC to DOC processes, threshold soil zone flow) and reach parameters (DOC to DIC self-shading factor, radiation multiplier, and microbial degradation) were calibrated to ensure the stability of PDC and DOC. This proved to be important, as the first iteration of the manual calibration and MC analysis failed to be robust enough to generate forecast simulations.

After getting the best performance set from manual calibration, MC analysis was carried out, as described above but using parameter specific tolerance windows for sensitive parameters (Table A.2). As above, differential weights were assigned to favor calibration performance for different processes and parts of the catchment. The highest weight (two) was assigned to Lower Martin which had the most complete record of observed DOC. Carbon process parameters were assigned weights of five while parameters controlling hydrology were assigned a weight of one. The best performing parameter set from the 25 MC-derived parameter sets was identified by visual assessment and assessment of goodness-of-fit metrics for DOC and discharge; this was used to simulate future catchment behavior.

2.6 Historic trend analysis and future hydroclimatic scenarios

The temperature and precipitation data of nearby climate station YKA (1955−2019) located 5 km from the southern end of the catchment, and discharge data at the outlet of Lower Martin (1983−2017) were used for historic trend analysis. Historic annual trends analysis of temperature and precipitation was done by non-parametric Mann-Kendall test (package: Kendall; function: 'MannKendall'). Trend analysis of discharge was done by using modified Mann-Kendall test (package: modifiedmk; function: 'mmky1lag'). Seasonal and monthly trend analysis of temperature, precipitation, and discharge was done by using seasonal Mann-Kendall test (package: trend; function: 'smk.test'). Seasonal trend analysis was done for early winter (October–December), late winter (January–March), spring (April–June), and summer (July–September). The historical trend analysis for discharge was done in the hydrological year (September–August). The Mann-Kendall test was performed using alpha = 0.05, but the p-value was Bonferroni adjusted in cases where multiple comparisons were made (e.g. seasonal and monthly tests).

Future catchment behavior was simulated by running PERSiST and INCA-C for three 30-year scenarios. Daily temperature and precipitation for input to PERSiST were generated using the package CoSMoS (Strnad et al., 2020), which is used to extend or generate time-series data by preserving the probability distribution and linear autocorrelation structure. The baseline scenario was generated using the data record for VT, extended to 30 years. The baseline scenario was created as a reference to evaluate the future scenarios. Future scenarios for a warmer (elevated temperature) and a warmer and wetter climate (elevated temperature and precipitation) were also generated using this method. To derive these scenarios, it was assumed that temperature and precipitation increased linearly according to the trends (+0.52°C per decade, +6.5% precipitation per decade) reported by DeBeer et al. (2016) through 2080. Using these temperature and precipitation levels projected for 2080, 30-year (nominally ~2066–2095) time-series for temperature and precipitation were created using CoSMoS, preserving the probability distribution and linear autocorrelation structure from the observed record. Note that this approach does not

account for seasonal changes in precipitation or temperature patterns reported by DeBeer et al. (2016).

Future discharge under baseline and future climate scenarios was simulated by INCA-C. The projected total annual runoff (obtained from simulated discharge) and projected total annual precipitation were used to calculate the annual runoff ratio under baseline and future scenarios. Similarly, annual C fluxes under baseline, elevated temperature, and elevated temperature and precipitation scenario were calculated as the sum of daily fluxes, which were estimated as the product of simulated daily DOC concentration and flow divided by catchment area given below:

$$C\ \ export = \frac{Q * C}{A} \qquad (2.1)$$

where *C export* is average daily C export (g m^{-2} d^{-1}), *Q* is average daily simulated discharge (m^3 d^{-1}), *C* is average daily simulated DOC concentration (mg L^{-1}), and *A* is the area (m^2) of the catchment. To understand the certainty of projection of average annual discharge and DOC flux, 95% confidence interval values were calculated for baseline, elevated temperature, and elevated temperature and precipitation scenario over 30 years at Duckfish, Vital Narrows, and Lower Martin station. Additionally, 5^{th} percentile (Q5) and 95^{th} percentile (Q95) values were calculated for average discharge, DOC concentration, and DOC flux

Chapter 3: Results

3.1 Historical Trend Analysis

3.1.1 Temperature

Historic trend analysis of temperature was done with 65 years of temperature data from the Yellowknife station (1955−2019; Figure 3.1). The Mann-Kendall test result showed a statistically significant positive trend for average annual temperature (p-value: 9.8×10^{-6}; Kendall's Tau: 0.41), average annual maximum temperature (p-value: 7.7×10^{-7}; Kendall's Tau: 0.45), and average annual minimum temperature (p-value: 7.5×10^{-5}; Kendall's Tau: 0.38) (Table 3.1; Figure B.1; B.2). Also, test analyzing seasonal average temperature have shown significant trends in all of four seasons (Table 3.1). Monthly average temperature showed no significant trends; however monthly temperature had shown significant values before Bonferroni correction in January, February, March, June, July, and December (Table B.1).

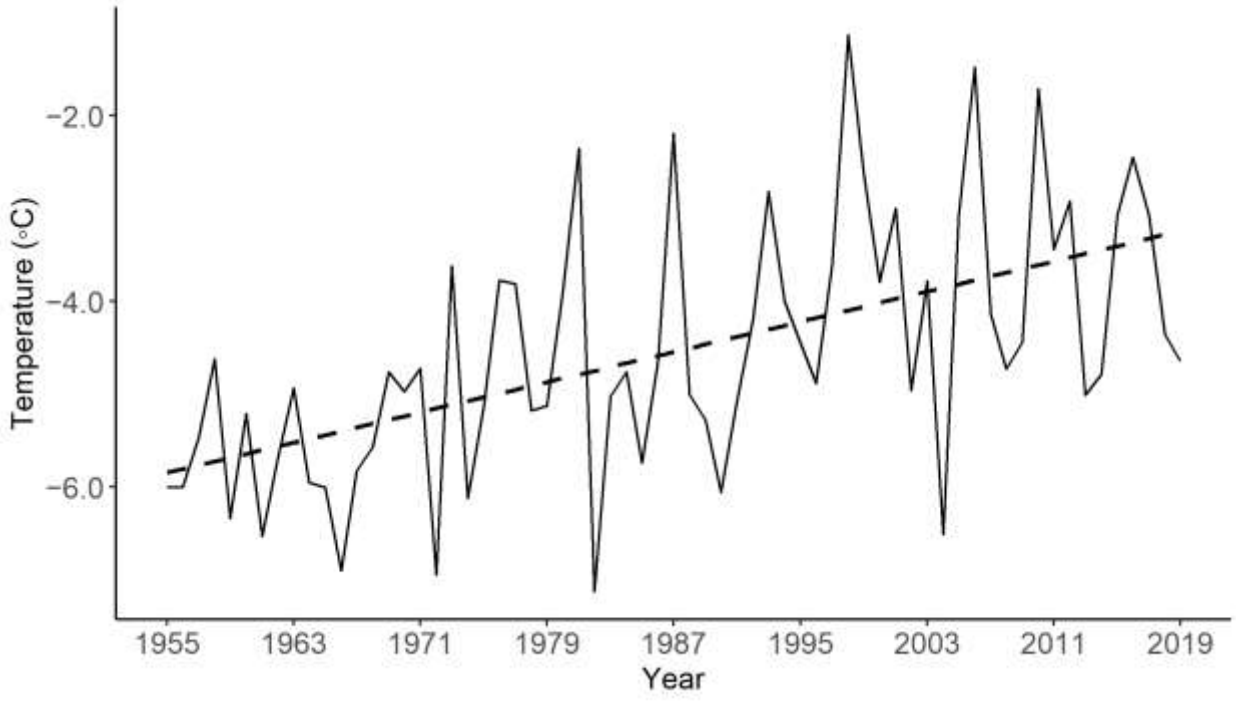

Figure 3.1: Average annual temperature (1955–2019) at Yellowknife station (located 5 km from the southern end of the Baker Creek catchment). Note: Black dashed line is trend line.

Table 3.1: Mann-Kendall test results for annual and seasonal temperature (Early winter: October–December, Late winter: January–March, Spring: April–June, and Summer: July–September) trend at Yellowknife station (1955−2019).

Parameter	Tau	p-value	Interpretation
Average annual temperature	0.41	2.4×10^{-6}	Positive trend
Average annual maximum temperature	0.45	5.6×10^{-8}	Positive trend
Average annual minimum temperature	0.37	4.5×10^{-5}	Positive trend
Average late winter temperature	0.03	1.8×10^{-3}	Positive trend
Average early winter temperature	0.03	9.6×10^{-4}	Positive trend
Average spring temperature	0.03	1.9×10^{-3}	Positive trend
Average summer temperature	0.02	0.03	Positive trend

3.1.2 Precipitation

Historic trend analysis of precipitation was done with 65 years of precipitation data from the Yellowknife meteorological station in hydrological years (1954−2018; Figure 3.2). Significant trends for total annual precipitation, total annual rainfall, and total annual snowfall were not detected (Table 3.2; Figure B.3; B.4). There was no significant trend for monthly and seasonal average precipitation, rainfall, and snowfall (Table B.2; B.3) except spring rainfall, which exhibited a significant positive trend. Moreover, the long-term data for precipitation (Figure 3.2) showed periodic cycles of wet and dry years.

Table 3.2: Mann-Kendall test results for annual precipitation trends at Yellowknife station (1954−2018) in hydrological years

Parameter	Tau	p-value	Interpretation
Total annual precipitation	6×10^{-3}	0.9	No trend
Total annual rainfall	0.13	0.1	No trend
Total annual snowfall	0.02	0.8	No trend

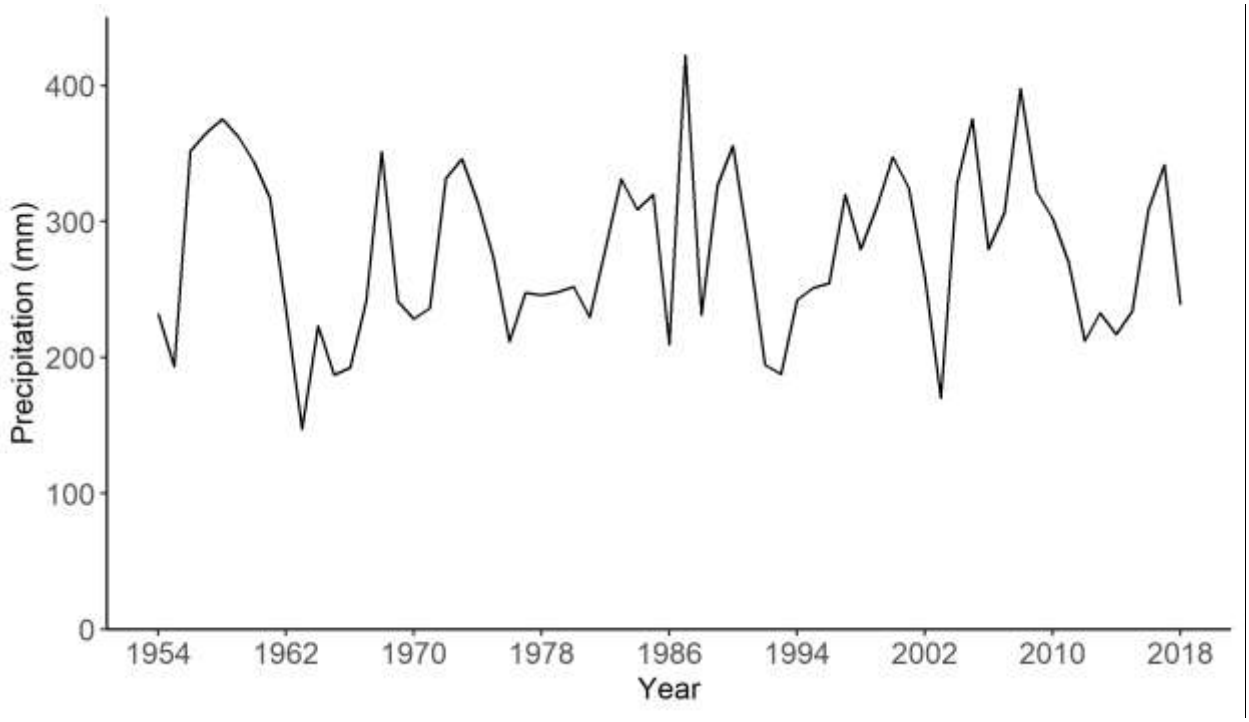

Figure 3.2: Total annual precipitation in hydrological years (1954–2018) at Yellowknife station (located 5 km from the southern end of the Baker Creek catchment).

3.1.3 Discharge

Annual discharge at Lower Martin during 1983−2017 (hydrological years) was demonstrated to have no significant trend (p-value: 0.7; Kendall's tau: 0.03; Table 3.3), whereas seasonal discharge has shown significant positive trends in all of four seasons. Additionally, we note that as with precipitation, interannual variability in discharge is high (Figure 3.3).

Table 3.3: Mann-Kendall test results for annual and seasonal discharge (Early winter: October–December, Late winter: January–March, Spring: April–June, and Summer: July–September) observed at Lower Martin Lake (1983−2017) in hydrologic years.

Parameter	Tau	p-value	Interpretation
Average annual discharge	0.03	0.7	No trend
Average late winter discharge	0.03	0.04	Positive trend
Average early winter discharge	0.03	0.03	Positive trend
Average spring discharge	0.03	0.03	Positive trend
Average summer discharge	0.03	0.04	Positive trend

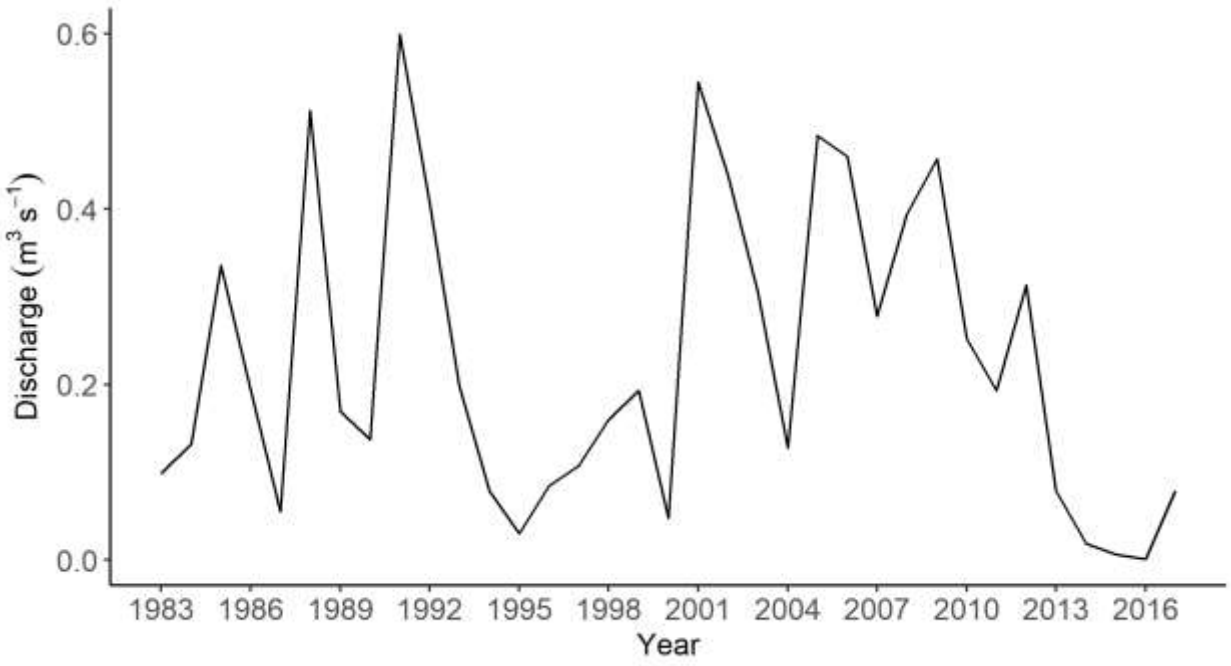

Figure 3.3: Average annual discharge (m^3 s^{-1}) from Lower Martin Lake (1983–2017) in hydrological years.

There were significant trends for average seasonal discharge in all four seasons (Table 3.3). The observational record coincided with natural dry and wet cycles may influence trend detection. Moreover, there were no significant trends for average monthly discharge (Table B.4). The average annual discharge at Lower Martin station during this period ranged from 8 x 10^{-4} to 0.59 $m^3 s^{-1}$.

3.2 Model Calibration

3.2.1 PERSiST manual calibration

Initially, PERSiST was manually calibrated for the full period for which temperature, precipitation, and discharge data were available (2005–2016) (Figure 3.4). The period consists of high-quality continuous discharge measurement at Lower Martin with discontinuous records in the other three sub-catchments. Duckfish Lake and Lake 690 have seasonal discharge measurements (spring to fall) whereas Vital Narrows has continuous discharge measurements with few missing values. The record consists of both hydrologically wet (2005–2007, 2009–2011) and dry (2013–2016) years.

For the period (2005–2016), model performance was generally good for Duckfish Lake and Lower Martin; however, simulations of the hydrological behavior of Lake 690 and Vital Narrows were much poorer (Table 3.4, Figure 3.4). Lake 690 is a small reach, and thus despite the poor model performance here (NS: 6 x 10^{-3}), the impact on calibration for the Baker Creek catchment (NS: 0.74 at Lower Martin) is small. Thus, simulated and observed fits of main catchments were the primary focus during calibration. Simulated discharge at Duckfish suggests the model somewhat overestimated high flow during dry years while underestimating peak flow during wet years. Similarly, simulation of discharge at both Vital Narrows and Lower Martin shows the model

underestimated high flow during wet years while overestimating base flow and high flow periods during dry years. For all three stations, the model overestimated discharge in the drier period at the end of the record.

Table 3.4: PERSiST and INCA-C manual calibration results for discharge in four sub-catchments of Baker Creek catchment.

Model	Sub-catchment	R^2	NS	Log(NS)	Var	AD
PERSiST	Duckfish	0.76	0.68	0.68	0.79	0.04
(2005–2016)	Lake 690	0.32	6×10^{-3}	−0.05	3.71	0.59
	Vital Narrows	0.42	0.18	0.02	1.98	0.56
	Lower Martin	0.77	0.74	0.75	1.56	0.08
PERSiST	Duckfish	0.91	0.89	0.89	1.03	−0.17
(2012–2016)	Lake 690	0.67	0.6	0.59	1.04	0.21
	Vital Narrows	0.87	0.82	0.8	1.64	0.33
	Lower Martin	0.94	0.91	0.82	1.43	−0.29
INCA-C	Duckfish	0.8	0.79			
(2012–2016)	Lake 690	0.55	0.51			
	Vital Narrows	0.8	0.72			
	Lower Martin	0.87	0.85			

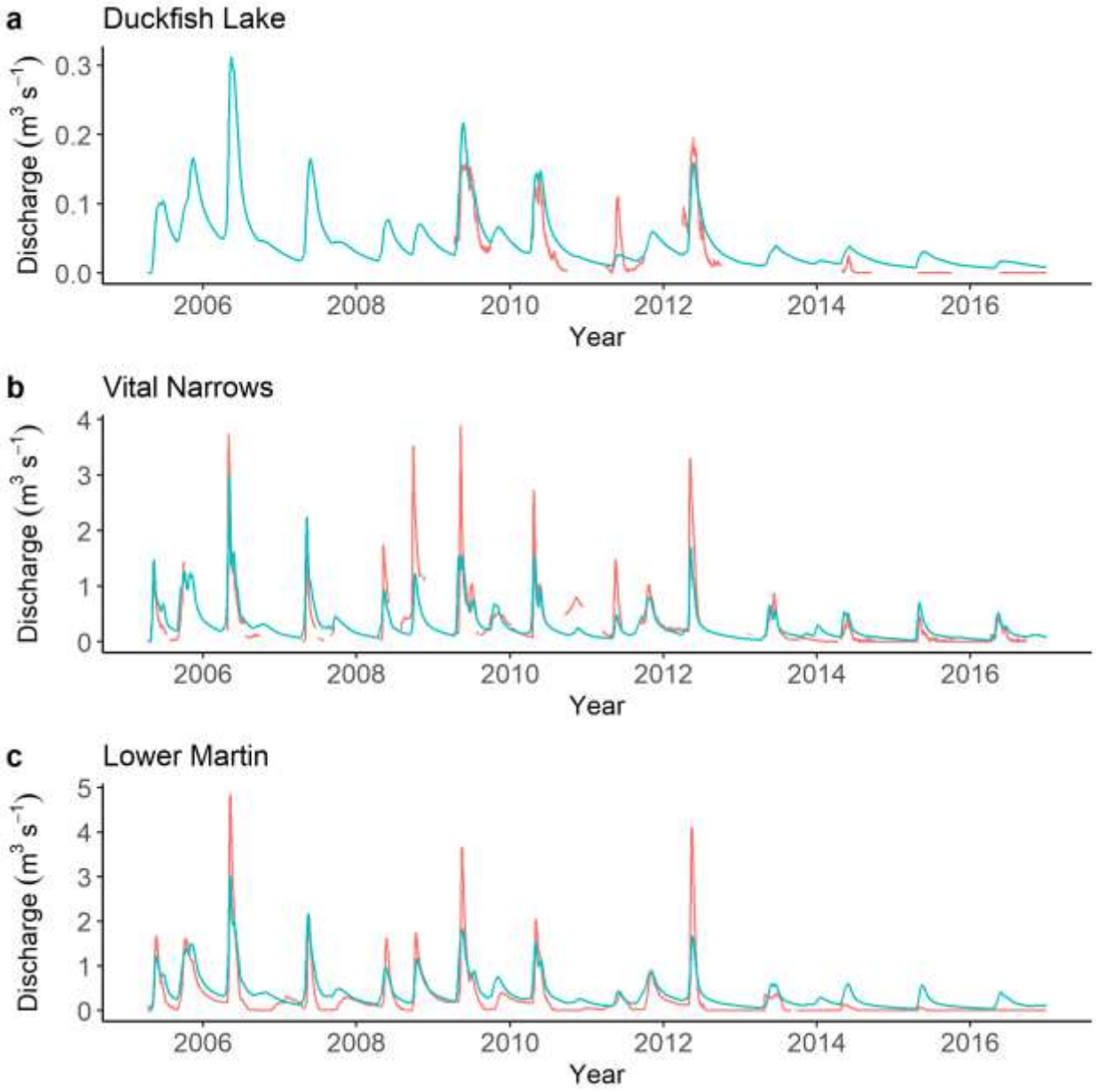

Figure 3.4: PERSiST simulated (blue) and observed (red) discharge (m^3 s^{-1}) (2005–2016) at Duckfish Lake (top), Vital Narrows (middle), and Lower Martin (bottom). Note that the y-axis scale varies by catchment and that discharge monitoring is limited to warm seasons at Duckfish Lake and Vital Narrows.

The overestimated discharge in drier records and data availability of DOC being limited to the later, drier part of the record presents a challenge for modeling DOC behavior. Thus, this drier part of the record (2012–2016) for which DOC observations were available was used in a second calibration (Figure 3.5). Calibration for this shorter record indicated an improved fit between observed and simulated discharge (Table 3.4). The calibration did an adequate job of reproducing discharge peaks with the Var (~1) for all four sub-catchments. Discharge was overestimated for Duckfish Lake (AD: −0.17) and Lower Martin (AD: −0.29) and underestimated for Lake 690 (AD: 0.21) and Vital Narrows (AD: 0.33). Peak flows were reasonably simulated in a high flow year (2012) and NS showed overall good performance at Duckfish Lake (0.89), Vital Narrows (0.82), and Lower Martin (0.91), but not at Lake 690 (0.6). Low flows were also better captured and Log (NS) showed reasonable performance at Duckfish Lake (0.89), Vital Narrows (0.8), and Lower Martin (0.82), but was weaker for Lake 690 (0.59).

Though the model has slightly overestimated discharge in low flow periods, this nonetheless represents an improvement over performance achieved using the longer-term record. Simulated peak flow at Vital Narrows (2013) and Lake 690 (2013; Figure B.5) was somewhat early, while at Lower Martin simulated peak flow was delayed relative to observations in some years. The overall timing of streamflow was well-captured at Duckfish Lake (R^2: 0.91), Vital Narrows (R^2: 0.87), and Lower Martin (R^2: 0.94).

3.2.2 INCA-C manual calibration

3.2.2.1 Discharge

The INCA-C model indicated a good fit between observed and simulated discharge (Figure 3.6) with similar model performance as PERSiST (Table 3.4). The manual calibration did an adequate job of reproducing discharge peaks. Simulations of peak flows were reasonable at Duckfish Lake (NS: 0.79), Vital Narrows (NS: 0.72), and Lower Martin (NS: 0.85) but problematic at Lake 690 (NS: 0.51).

Compared to PERSiST, the INCA-C model better reproduced the magnitude of peak flow (Figure 3.6) at Duckfish Lake (2012) and Vital Narrows (2014, 2015). Peak flow at Duckfish and Vital Narrows was underestimated in some years and generally overestimated in dry years at Lower Martin (2014–2016). As was the case with PERSiST, INCA-C simulated peak flow tended to be slightly late in some cases (e.g. Vital Narrows: 2012, 2015; Lower Martin: 2012–2014). Overall, it was possible to reasonably capture different hydrological behaviors such as peak flow in spring, hydrological drought after 2012, variation in flow amount in wet and dry years using INCA-C (Figure 3.6).

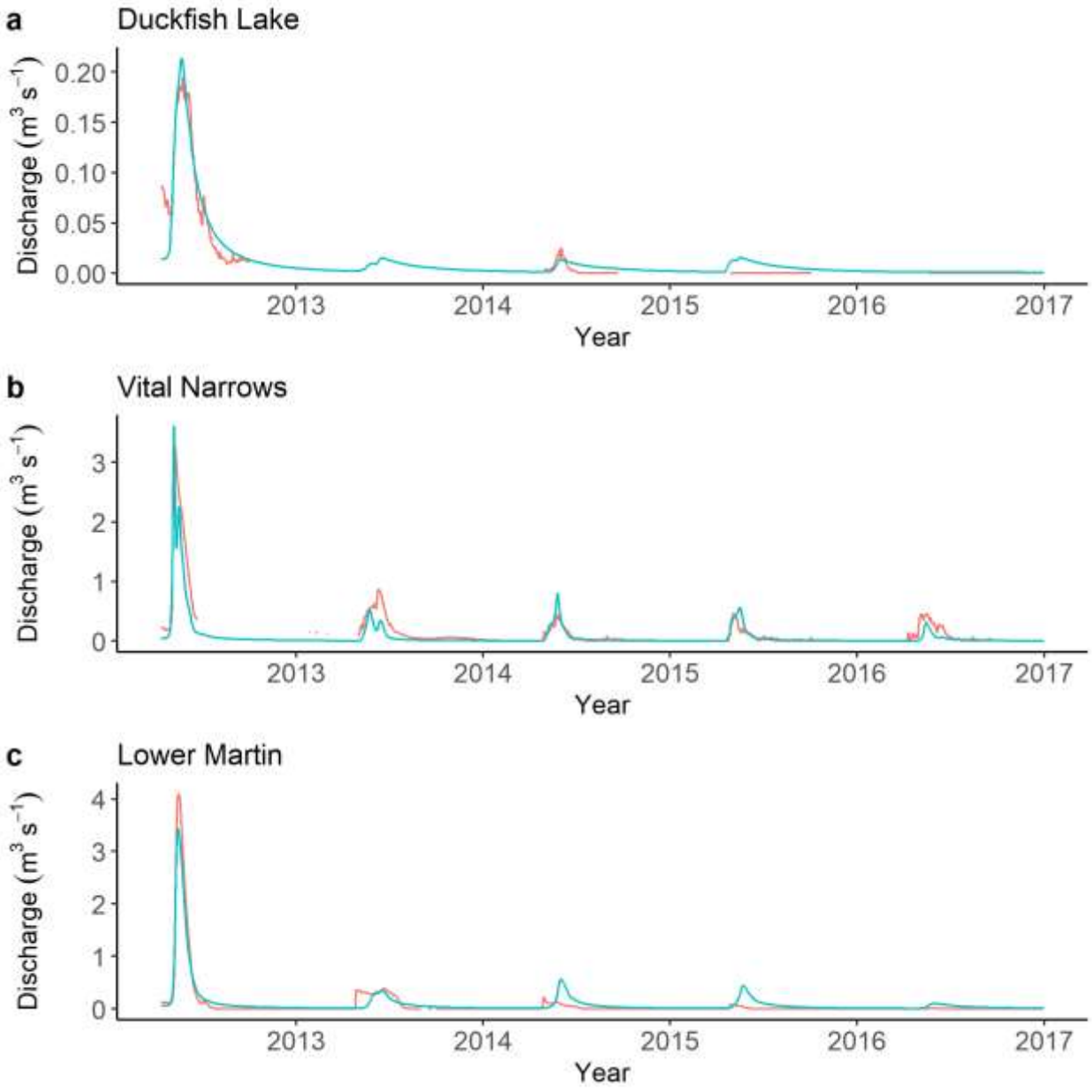

Figure 3.5: PERSiST simulated (blue) and observed (red) discharge (m^3 s^{-1}) (2012–2016) at Duckfish Lake (top), Vital Narrows (middle), and Lower Martin (bottom).

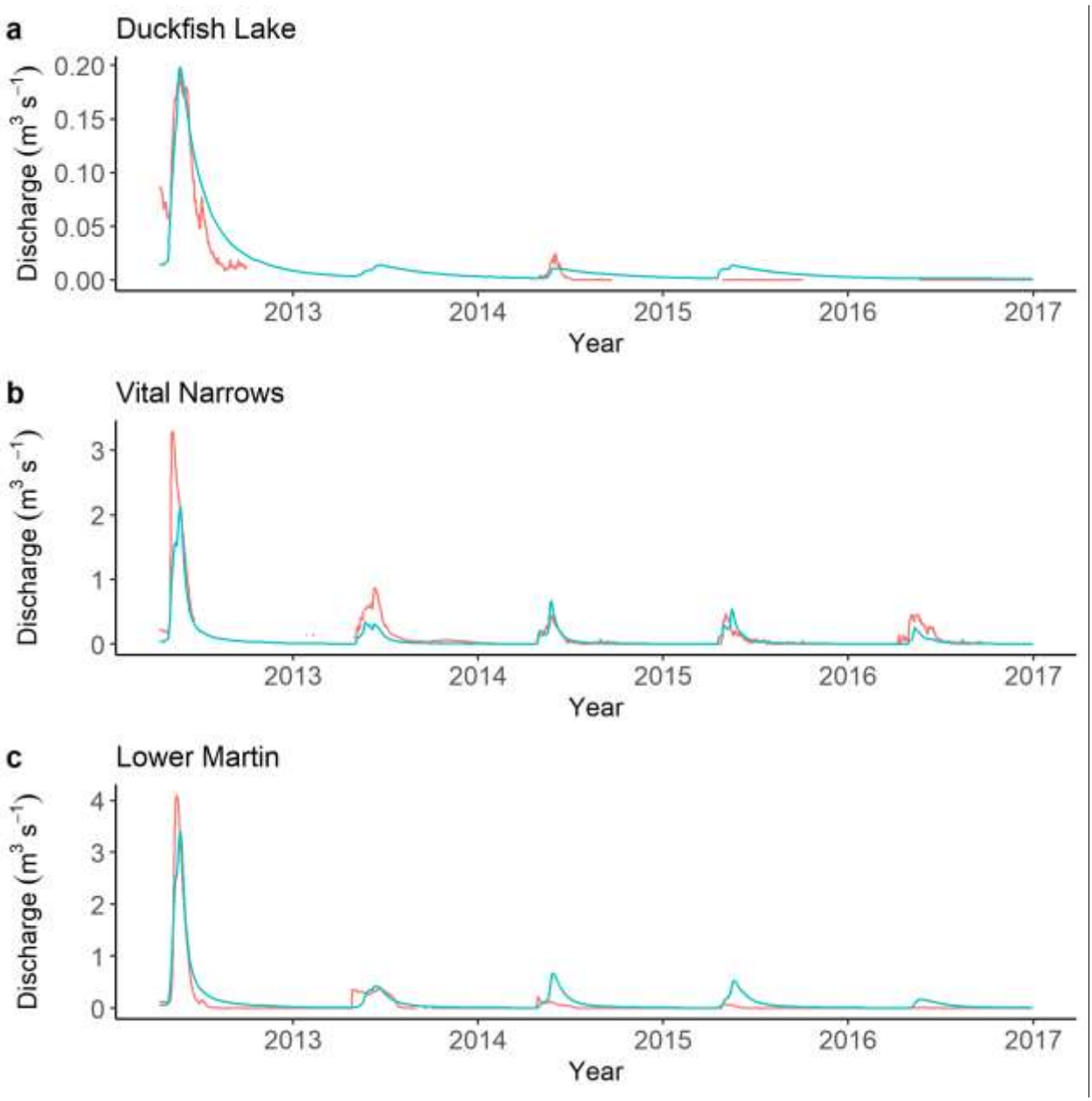

Figure 3.6: INCA-C simulated (blue) and observed (red) discharge ($m^3 s^{-1}$) at Duckfish Lake (top), Vital Narrows (middle), and Lower Martin (bottom) (2012–2016).

3.2.2.2 Dissolved organic carbon

Manual calibration of INCA-C was able to provide a reasonable simulation of DOC dynamics in sub-catchments (Figure 3.7). Both high and low DOC concentrations after 2014 at Lower Martin were captured. Simulated DOC concentrations at Duckfish Lake were higher compared to Vital Narrows and Lower Martin.

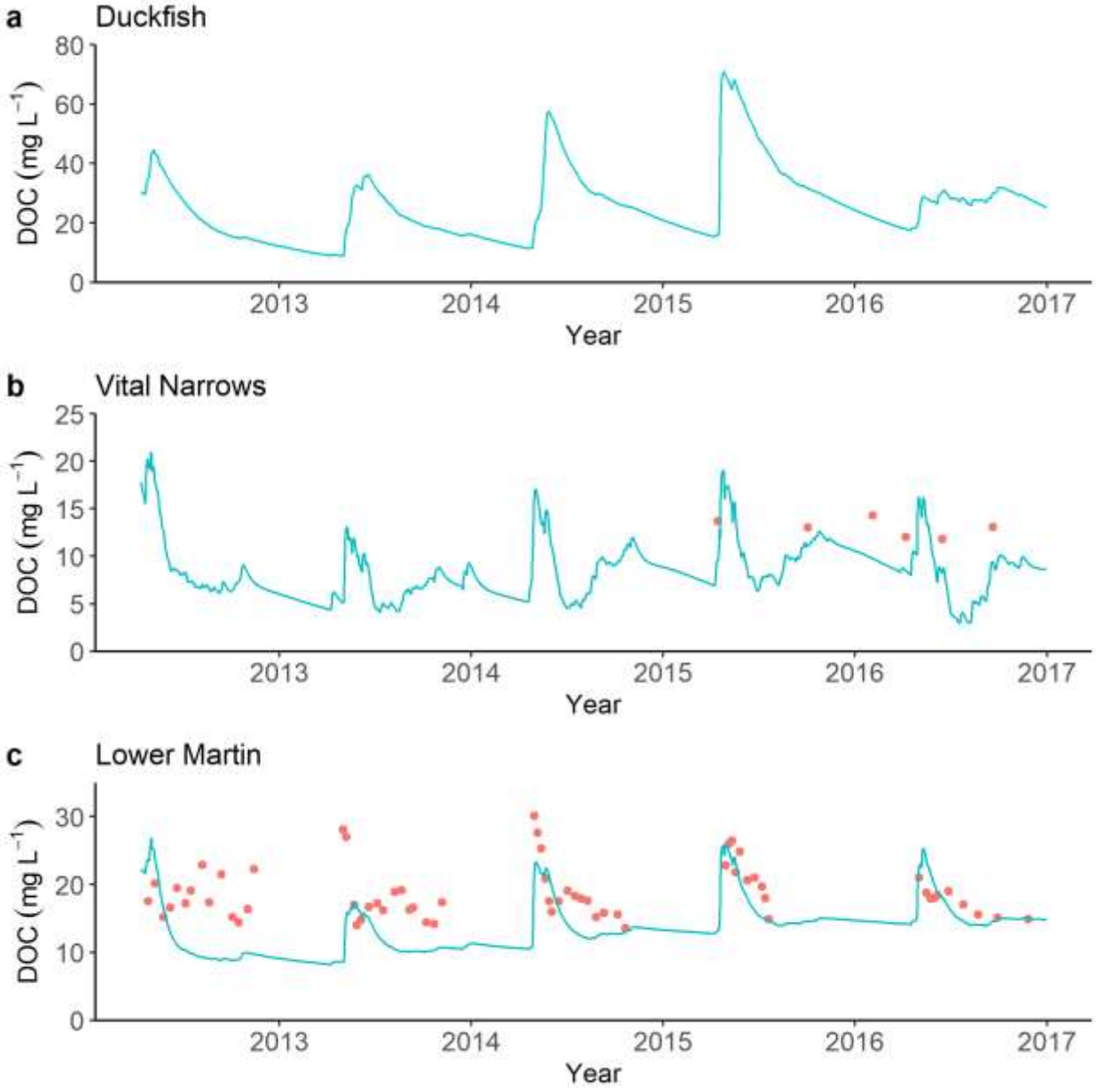

Figure 3.7: INCA-C simulated (blue) and observed (red) DOC (mg L^{-1}) at Duckfish (top), Vital Narrows (middle), and Lower Martin (bottom) (2012–2016) from the manual calibration. Note: Regular DOC observations were available only at Lower Martin whereas irregular grab sampling is conducted elsewhere, and Duckfish was not sampled during this period.

At Duckfish Lake, observed DOC concentration is higher in the post-drought period (52 mg L^{-1} in 2019), while visual observations suggest different colour of water in downstream reaches when it is connected (C. Spence, pers. comm.). Together, this suggests that the connectivity of Duckfish Lake can be important for downstream DOC patterns in Baker Creek. Low R^2 for DOC concentration at both Vital Narrows (0.31) and Lower Martin (0.19) were reported. The best model fit is observed in dry years (2014 and 2015) when the catchment was more disconnected. In Baker Creek, although we have robust record of observations only at Lower Martin (2012–2016) we are still modelling other parts of catchment to get the better simulations in lower part. As, observed data at Duckfish is missing, simulations were compared with single year data in 2019.

Evaluation of weekly C fluxes (2012−2016; Figure 3.8) for Lower Martin shows evidence that DOC can be both underestimated and overestimated at times during the calibration period. Except few observations in 2013 and 2014, the overall tendency was for DOC flux to be overestimated (Figure 3.8), despite DOC concentrations being underpredicted overall (Figure 3.8). The overestimated DOC flux was because of overestimated discharge in that period.

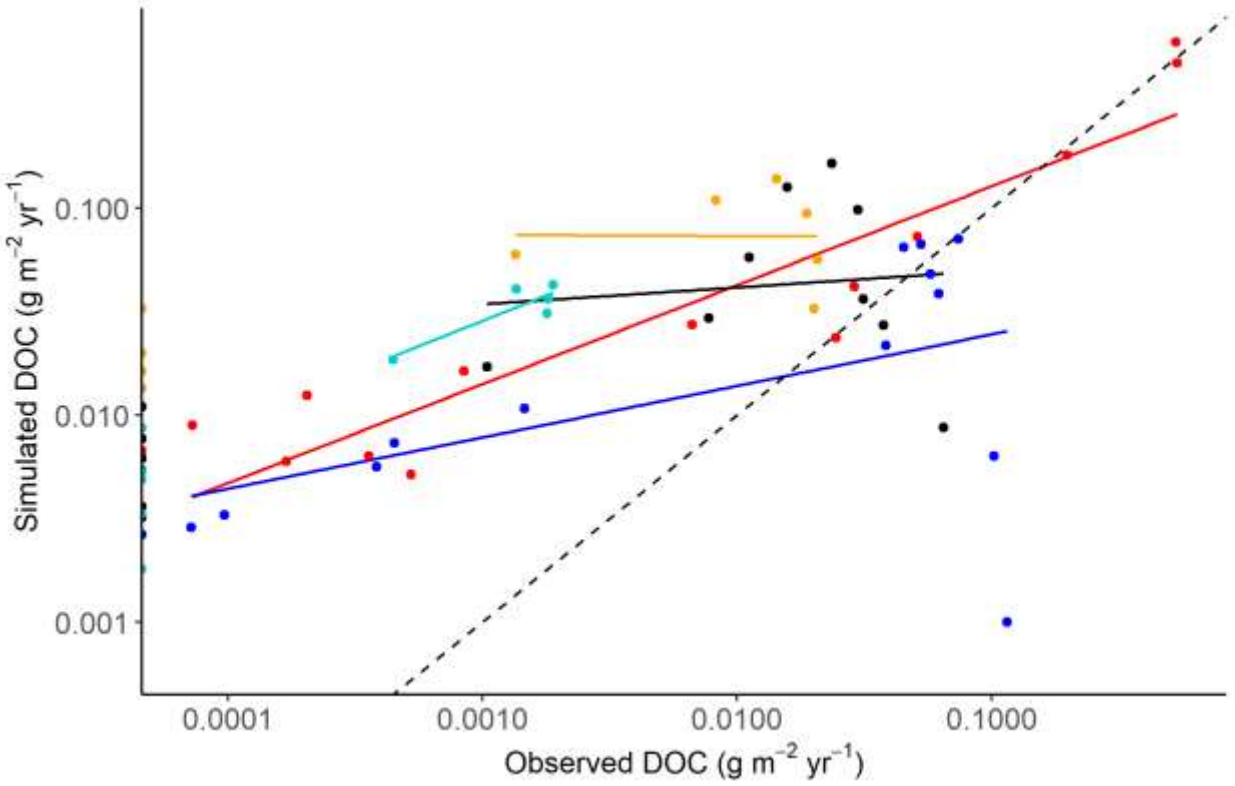

Figure 3.8: INCA-C simulated and observed weekly DOC flux (g m^{-2} yr^{-1}) at Lower Martin (2012–2016). The color lines (red: 2012, blue: 2013, black: 2014, orange: 2015, cyan: 2016) represent a regression line of the weekly observations (when available) in a given year (colored points; red: 2012, blue: 2013, black: 2014, orange: 2015, cyan: 2016). The dashed black line represents 1:1 line of overall data.

The discharge was a major control on annual DOC export in the Baker Creek catchment (Figure 3.9). For instance, at Lower Martin flow weighted mean DOC export in wet year (2012) was 0.36 g m^{-2} yr^{-1} and in dry years (2013−2016) was 0.05 g m^{-2} yr^{-1} on average. High DOC export in 2012 and low export in the other dry year shows the importance of hydrological connectivity with C rich sources for C export. This is further explained by the connectivity of Duckfish Lake to the lower reaches. In 2012, Duckfish Lake was connected to lower reaches for a prolonged period when DOC concentrations remained elevated; however, in dry years surface flow from Duckfish Lake (Figure 3.9) was interrupted and DOC concentrations decreased more rapidly on the falling limb of the hydrograph (2014, 2015, 2016).

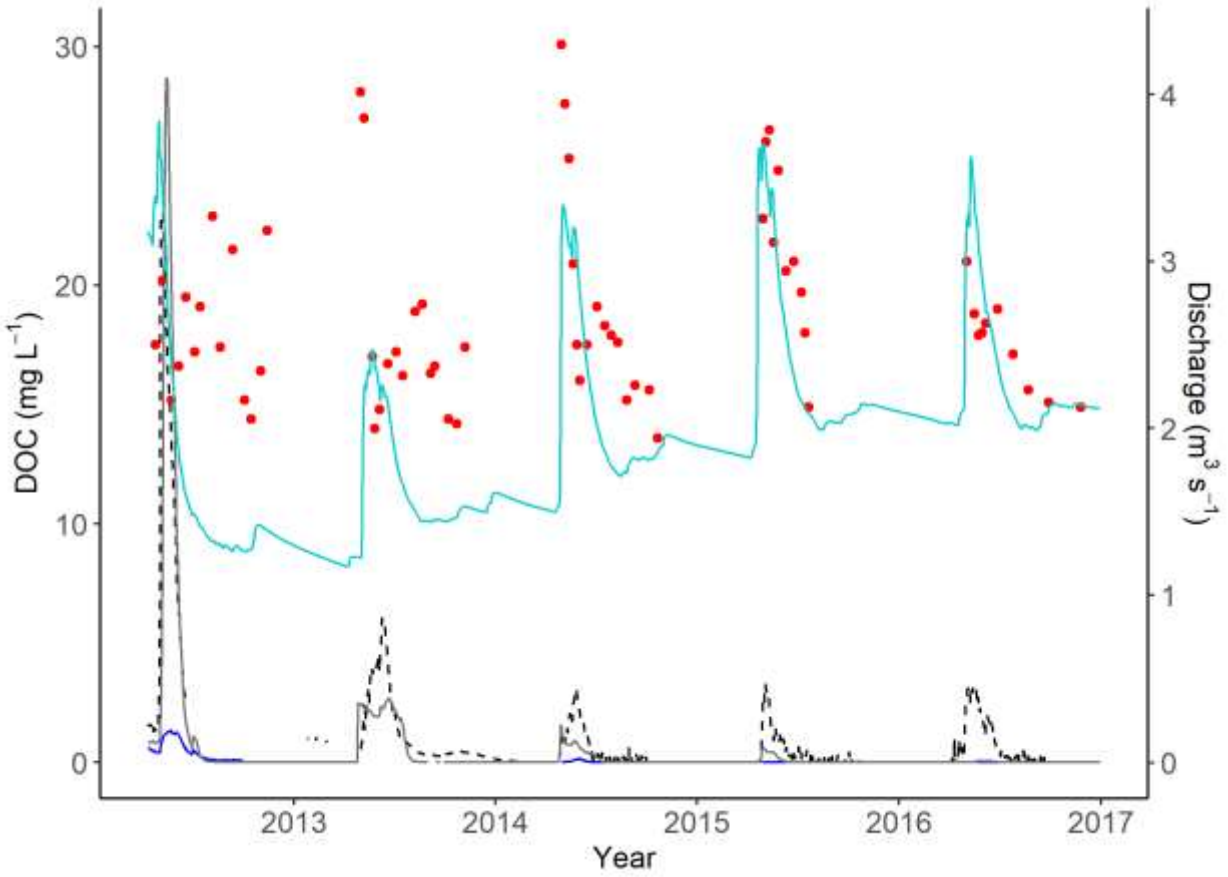

Figure 3.9: Runoff control on DOC (2012−2016). The plot shows observed DOC (red), simulated DOC (light blue), observed discharge at Lower Martin (grey), Vital Narrows (black dashed), and Duckfish (blue) colour.

3.2.3 Monte Carlo analysis

The MC tool for INCA-C generated 24 best parameter sets (one was not behavioural). Exploring the performance results and time-series plots helped to select the best-performing parameter set (Figure 3.10). The best performing parameter set was identified based on performance metrics (R^2 and NS) for Lower Martin, where the most complete record of DOC was available.

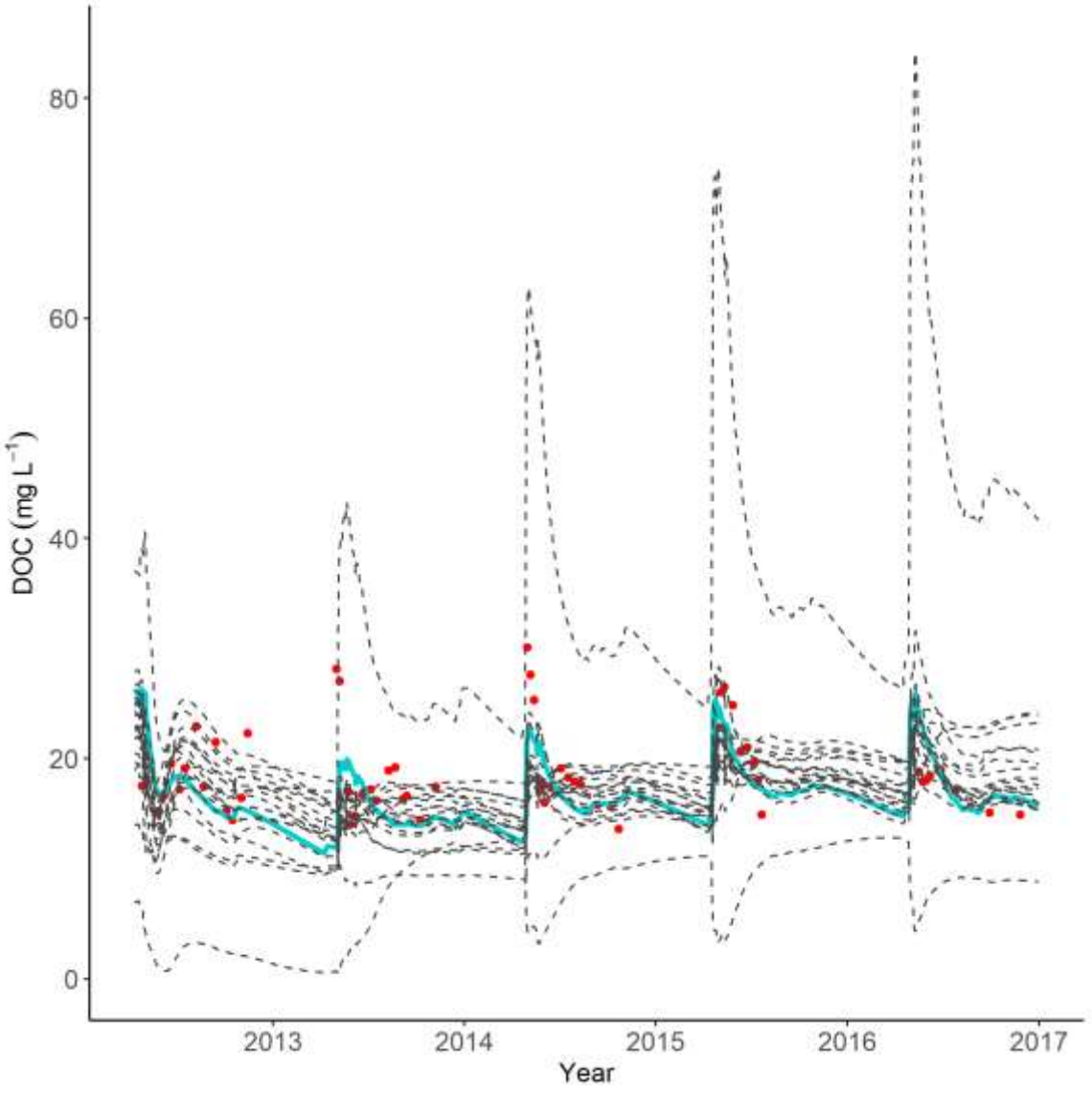

Figure 3.10: INCA-C simulated DOC (mg L^{-1}) from 24 (excluding one which was not behavioral) Monte Carlo generated parameter sets at Lower Martin (2012–2016). Note: light blue solid line indicates DOC from the best performing parameter set, dashed lines represent 23 other parameter sets and red points indicate observed DOC concentration.

The parameter set showing the best fit between observed and simulated discharge and DOC and have R^2 and NS values closer to one was selected as the best parameter set. The best parameter set obtained from the MC tool showed a similar fit for discharge as the best parameter set from manual calibration in all parts of the catchment (Figure 3.11) except at Duckfish Lake in 2012 where the MC parameter set slightly overestimated the discharge (Figure 3.11a).

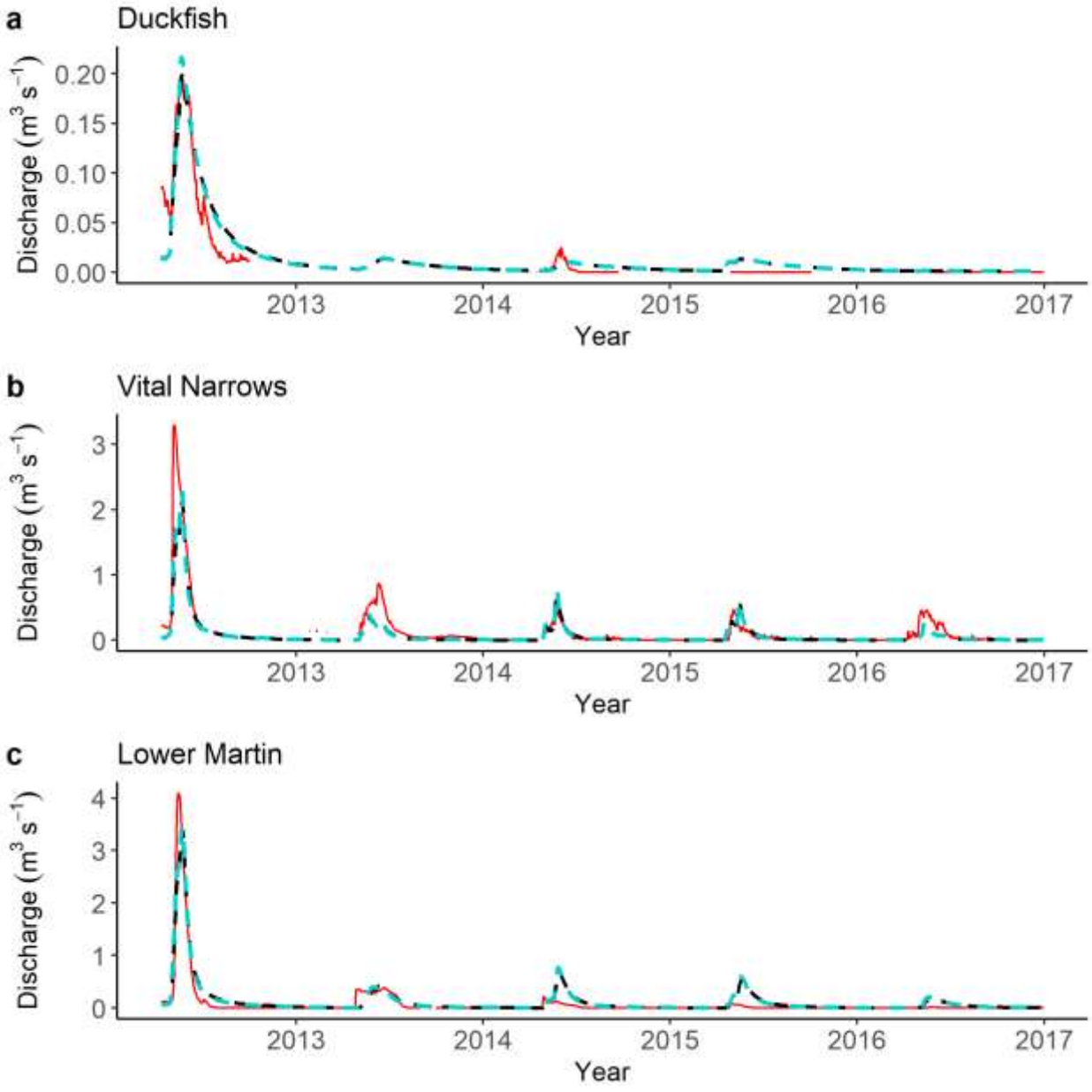

Figure 3.11: Plot comparing INCA-C simulated discharge ($m^3\ s^{-1}$) from manual calibration (black dashed), best Monte Carlo parameter set (light blue dashed), and observed discharge (red) at Duckfish (top), Vital Narrows (middle), and Lower Martin (bottom) (2012–2016).

The model performance result for discharge at Duckfish, Lake 690, and Vital Narrows was comparatively good from the MC parameter set whereas the model performance result from the manual calibration at Lower Martin was slightly better (Table 3.5).

For DOC concentration, both manual calibration and MC calibration gave a similar R^2 (0.19). Although the R^2 value for Lake 690 and Vital Narrows is slightly better in the manual calibration, there were few observations used to calculate the metrics. Due to available long-term DOC observations at Lower Martin, our main focus while selecting model performance was based on Lower Martin. The MC calibration was comparatively better at capturing higher DOC concentration (2015) and late summer DOC concentration at Lower Martin (2012–2014) than the manual calibration (Figure 3.12c) and produced a better simulation of Vital Narrows (Figure 3.12b). Thus, together the performance metrics and time series suggest that the MC approach yields a somewhat better simulation of the observational record.

Table 3.5: Performance indicators for INCA-C Monte Carlo and manual calibration in Baker Creek catchment (2012−2016). Note: Only Lower Martin has a long record of DOC observations.

Indicators	**Monte Carlo Calibration**				**Manual Calibration**			
	Duckfish Lake	**Lake 690**	**Vital Narrows**	**Lower Martin**	**Duckfish Lake**	**Lake 690**	**Vital Narrows**	**Lower Martin**
R^2 (Flow)	0.83	0.57	0.83	0.86	0.8	0.55	0.8	0.87
NS (Flow)	0.80	0.53	0.76	0.84	0.79	0.51	0.72	0.85
R^2 (DOC)		0	0.17	0.19		6×10^{-3}	0.31	0.19

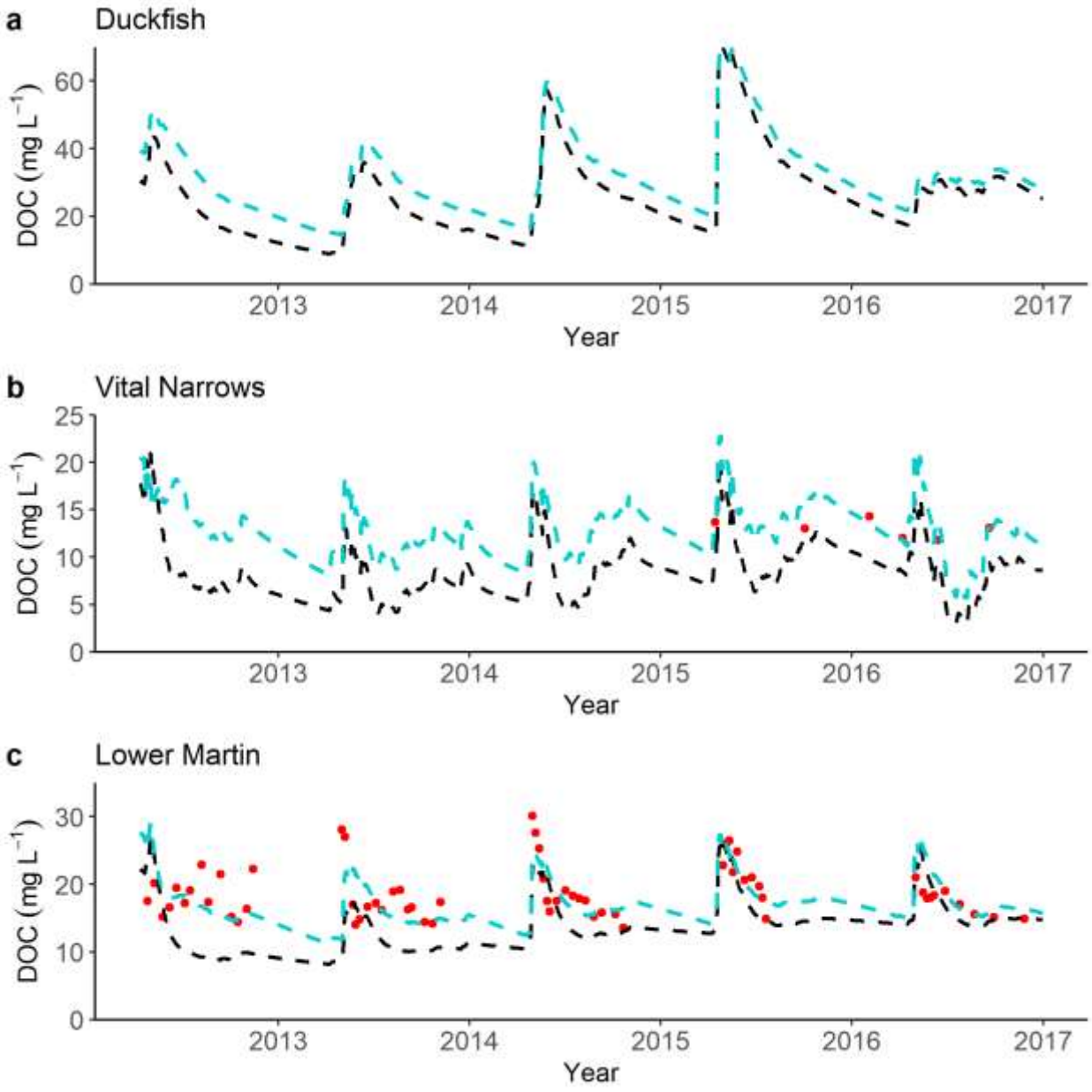

Figure 3.12: Plot comparing INCA-C simulated DOC (mg L^{-1}) from manual calibration (black dashed), best Monte Carlo parameter set (light blue dashed), and observed DOC (red) at Duckfish (top), Vital Narrows (middle), and Lower Martin (bottom) (2012–2016).

3.3 Forecasting future catchment behavior

Initially, the best MC parameter set was selected for simulating future catchment behavior, as there was minimal functional difference in performance for discharge (Table 3.5), but DOC was better for this MC derived parameter set (Figure 3.12). While the best MC parameter set was capable of simulating discharge in the sub-catchments under these scenarios; simulations of DOC (at Vital Narrows and Lower Martin) were problematic and suggested instability of C pools under these parameterizations. Thus, the manually calibrated best parameter set was used for simulating future catchment behavior under future scenarios.

3.3.1 Discharge

Simulated average annual discharge at the Baker Creek catchment (for the 30-year) under baseline, elevated temperature, and elevated temperature and precipitation scenarios revealed important differences (Figure 3.13). The simulated annual average discharge at Duckfish (9×10^{-3}–0.1 $m^3 s^{-1}$), Vital Narrows (0.01–0.4 $m^3 s^{-1}$), and Lower Martin (0.03–0.7 $m^3 s^{-1}$) under the baseline scenario were highly variable, reflecting the contrasting wet and dry conditions observed for Lower Martin Lake during the operation of the WSC gauge. Under the elevated temperature scenario, annual average discharge ranges at Duckfish (4×10^{-3}–0.07 $m^3 s^{-1}$), Vital Narrows (9×10^{-3}–0.37 $m^3 s^{-1}$), and Lower Martin (0.02–0.6 $m^3 s^{-1}$) demonstrated an absolute decline in discharge relative to the baseline. Under the elevated temperature and precipitation scenario, annual average discharge ranges at Duckfish (0.03–0.27 $m^3 s^{-1}$), Vital Narrows (0.2–0.98 $m^3 s^{-1}$), and Lower Martin (0.3–1.6 $m^3 s^{-1}$) were notably higher than the baseline condition.

Average annual discharge under elevated temperature scenario shows less interannual variability, whereas under elevated temperature and precipitation scenario the range in annual average discharge in all three catchments increases (Figure 3.13). The 90th percentile of discharge under elevated temperature scenario is less than the 25th percentile of discharge under elevated temperature and precipitation scenario.

The 5th percentile (high flow) and 95th percentile (low flow) annual discharge are projected to decrease under elevated temperature scenario, and increase under elevated temperature and precipitation scenario (Table 3.6). Annual high flows under the elevated temperature scenario are projected to decrease by 33% at Duckfish, 25% at Vital Narrows, and 25% at Lower Martin. Similarly, annual low flows under this scenario are projected to decrease by 37% at Duckfish, 22% at Vital Narrows, and 24% at Lower Martin. In contrast, under the elevated temperature and precipitation scenario high flows at Duckfish, Vital Narrows, and Lower Martin will increase by 133%, 150%, and 150% respectively. Likewise, low flows will increase by 137% at Duckfish, 93% at Vital Narrows, and 73% at Lower Martin.

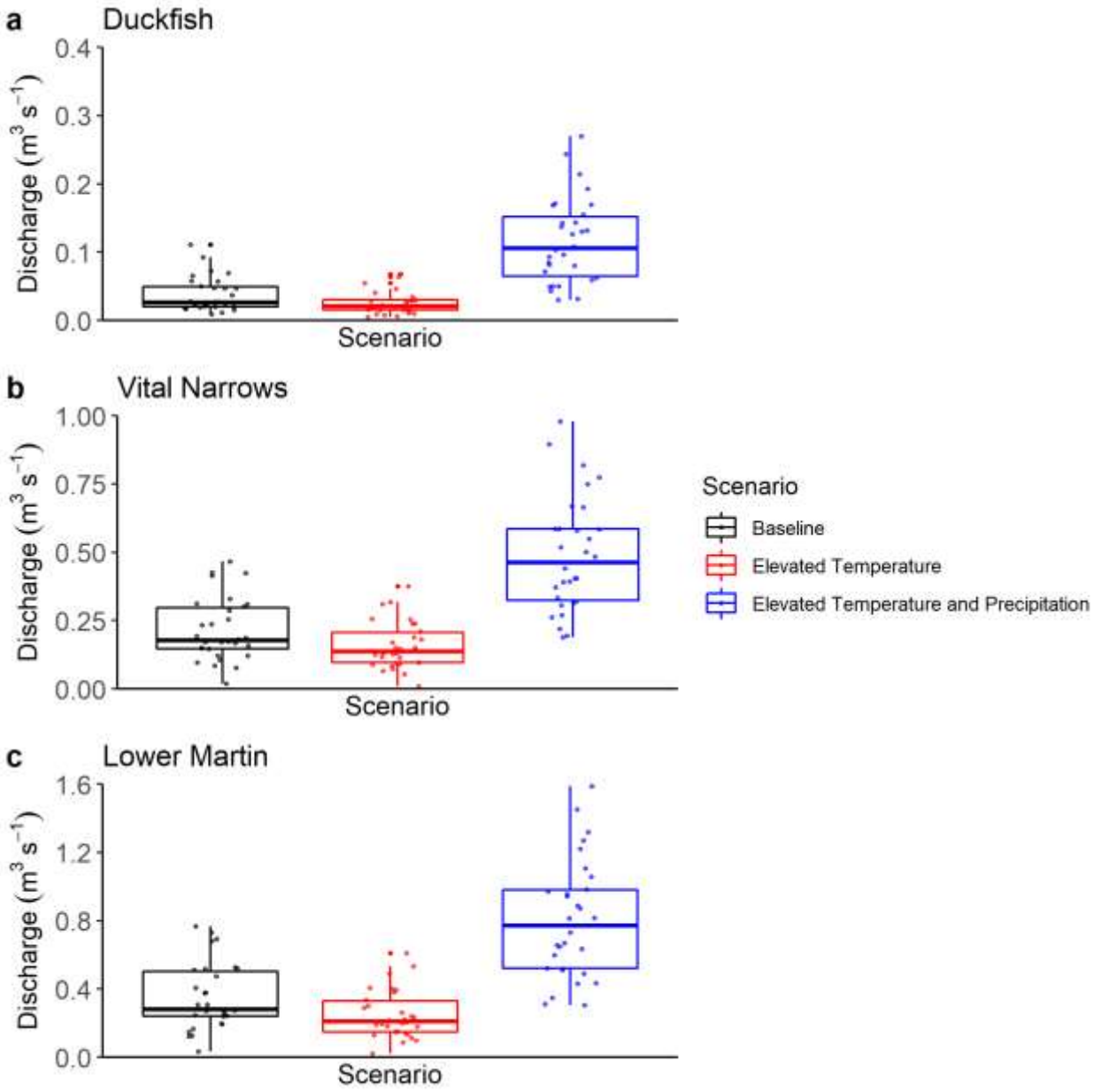

Figure 3.13: Boxplot showing INCA-C simulated average annual discharge ($m^3 s^{-1}$) under baseline (black), elevated temperature (red), and elevated temperature and precipitation (blue) for the 30-year scenarios at Duckfish Lake (top), Vital Narrows (middle), and Lower Martin (bottom). Note: Points shown in box plot are average annual discharge in individual years for each scenario.

Table 3.6: INCA-C model projected average annual Q5, Q95, average annual discharge ($m^3\ s^{-1}$) with 95% confidence interval (in parentheses) under baseline, elevated temperature, and elevated temperature and precipitation scenarios. Change in discharge from baseline (in % with confidence interval) over 30 years at Duckfish, Vital Narrows, and Lower Martin is also shown.

Scenario	Statistics	Duckfish	Vital Narrows	Lower Martin
Baseline	Q5	3×10^{-03}	0.08	0.12
	Q95	0.16	0.44	0.75
	Average	0.040 (0.030–0.050)	0.22 (0.18–0.27)	0.37 (0.29–0.44)
Elevated Temperature	Q5	2×10^{-03}	0.06	0.09
	Q95	0.10	0.34	0.57
	Average	0.030 (0.020–0.039)	0.17 (0.13–0.21)	0.27 (0.20–0.33)
	Change (%)	−25 (−33, −22)	−22 (−27, −22)	−27 (−31, −25)
Elevated Temperature and Precipitation	Q5	7×10^{-03}	0.2	0.3
	Q95	0.38	0.85	1.3
	Average	0.11 (0.09–0.13)	0.49 (0.42–0.56)	0.80 (0.68–0.92)
	Change (%)	175 (200, 160)	122 (133, 115)	116 (126, 119)

The projected average annual discharge under the baseline scenario at Duckfish Lake is 0.04 $m^3\ s^{-1}$, Vital Narrows is 0.22 $m^3\ s^{-1}$, and Lower Martin is 0.37 $m^3\ s^{-1}$ over 30 years (Table 3.6). As with the patterns for low and high flows, the annual average discharge will decrease under elevated temperature and increase under elevated temperature and precipitation scenarios. The 95% confidence interval for discharge under elevated temperature and elevated temperature and precipitation scenario in parts of catchment are shown in table 3.6. The annual runoff ratio under the baseline scenario at Duckfish Lake is 0.17, Vital Narrows is 0.24, and Lower Martin is 0.26 over 30 years. The runoff ratio will decrease under elevated temperature (Duckfish: 0.13, Vital Narrows: 0.18, Lower Martin: 0.19) and increase under elevated temperature and precipitation scenarios (Duckfish: 0.35, Vital Narrows: 0.37, Lower Martin: 0.4).

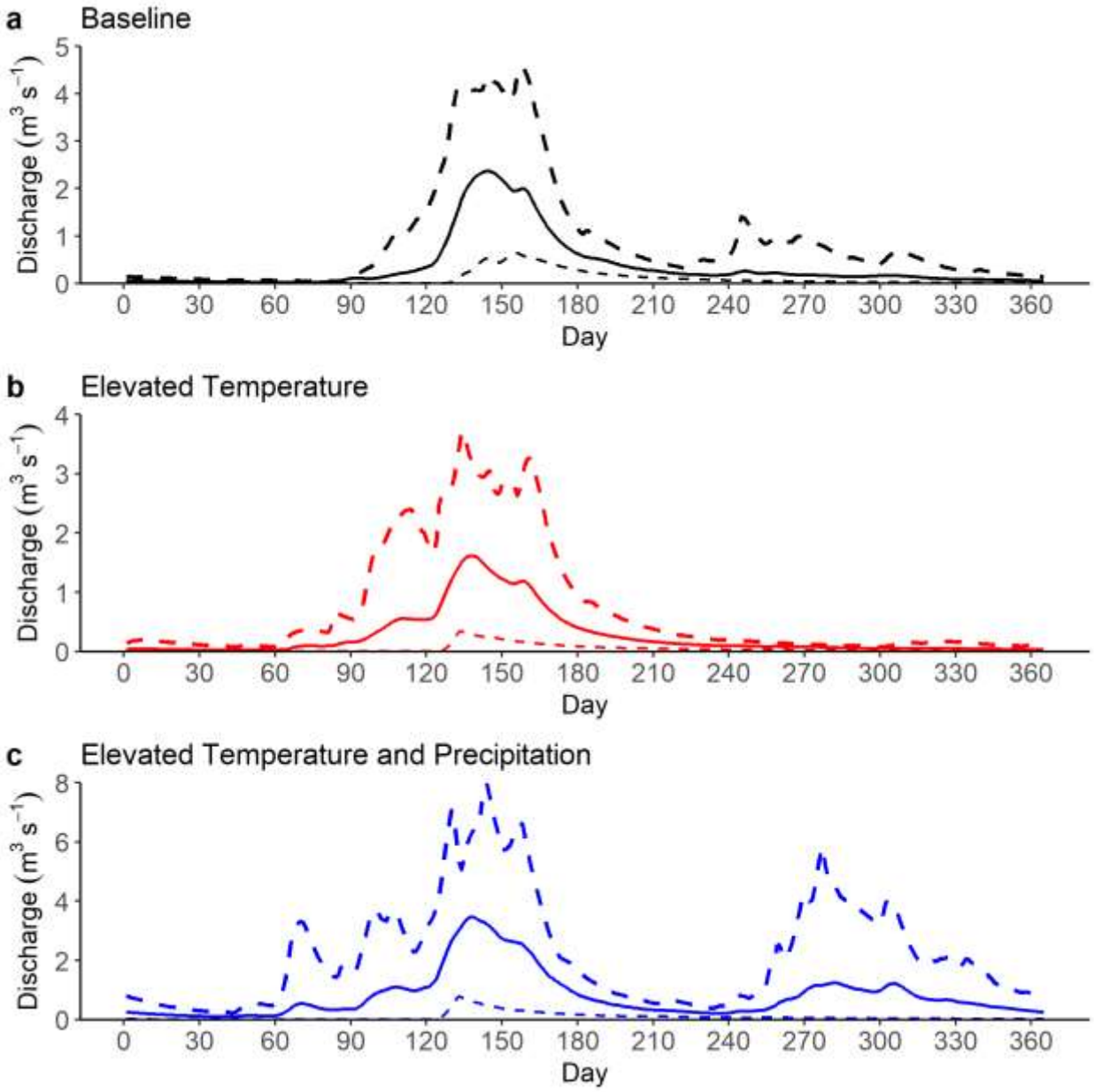

Figure 3.14: Average daily discharge ($m^3 s^{-1}$), Q5 (thin dashed line), and Q95 (thick dashed line) over 30 years under baseline (a), elevated temperature (b), and elevated temperature and precipitation (c) scenario at Lower Martin.

At Lower Martin, under the elevated temperature scenario average daily discharge is projected to increase in March and April and decrease from May to November (Figure 3.14). Under the elevated temperature and precipitation scenario, average daily discharge and Q95 values of average daily discharge is projected to increase throughout the year, although the magnitude of increase varies seasonally (Figure 3.14). Under this scenario, a pronounced secondary peak of discharge in early winter is predicted.

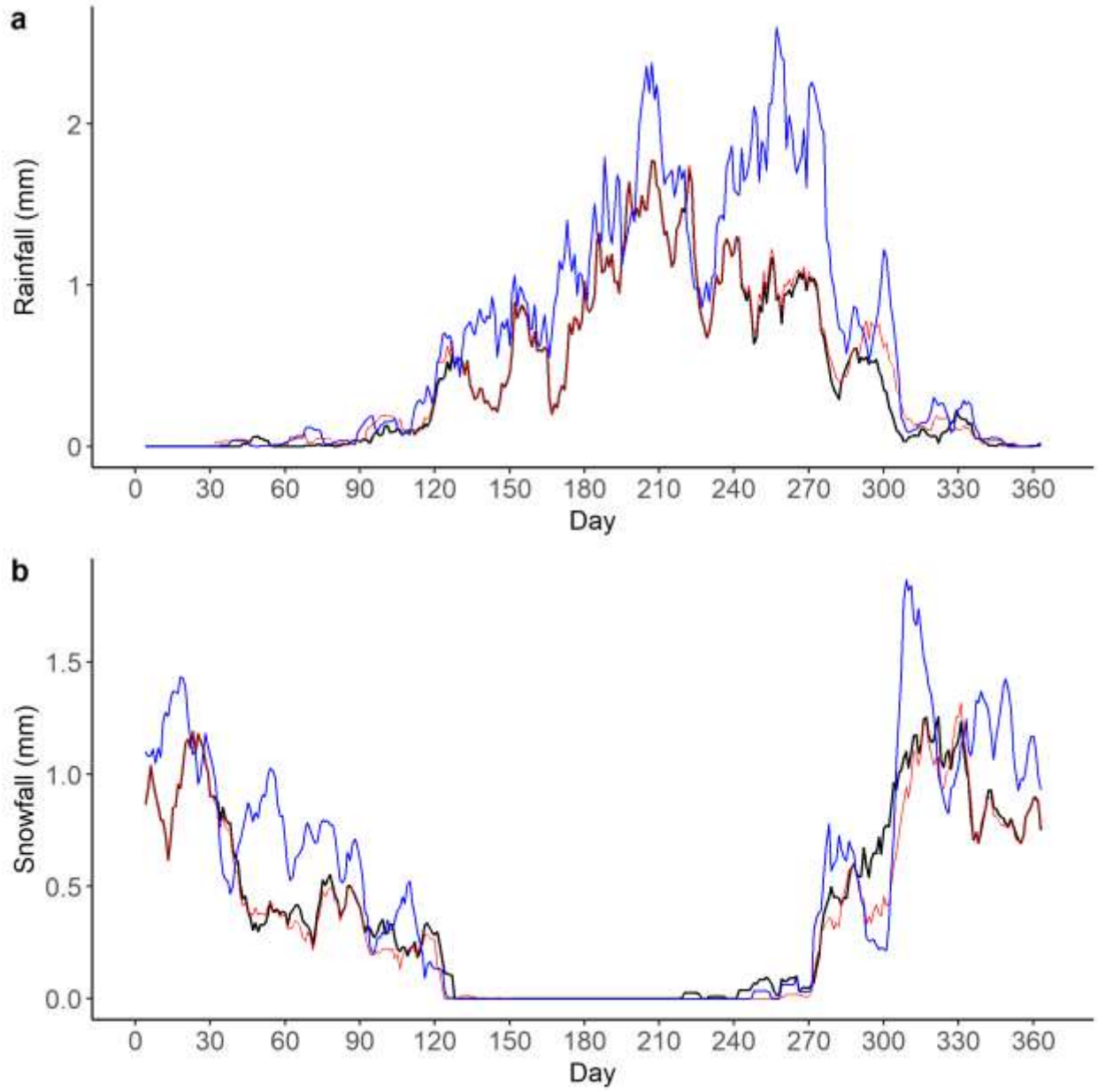

Figure 3.15: Seven days moving average rainfall (3.15a) and snowfall (3.15b) at Lower Martin station over 30 years under baseline (black), elevated temperature (red), and elevated temperature and precipitation (blue) scenario. Note: Average daily rainfall and average daily snowfall is calculated as average of 30 years.

The average daily rainfall is projected to increase under elevated temperature scenario from March to mid-May and from mid-October to November whereas snowfall from mid-October to mid-November is projected to decrease (Figure 3.15). Under the elevated temperature and precipitation scenario, both rainfall and snowfall are projected to increase with the shift in the highest rainfall peak from July to September (Figure 3.15). This shifted rainfall peak in September is the likely driver of the secondary discharge peak from September to November.

3.3.2 Dissolved organic carbon

INCA-C simulated average annual DOC concentration at the Baker Creek catchment over 30 years under baseline, elevated temperature, and elevated temperature and precipitation scenarios revealed key differences (Figure 3.16). The simulated annual average DOC concentration at Duckfish (15−31 mg L^{-1}), Vital Narrows (5−12 mg L^{-1}), and Lower Martin (7−15 mg L^{-1}) under the baseline scenario were highly variable, but Duckfish was notably higher, consistent with observations of colour of water and a single observation collected in 2019. Under the elevated temperature scenario, annual average DOC concentration at Duckfish (14−36 mg L^{-1}), Vital Narrows (4−12 mg L^{-1}), and Lower Martin (6−15 mg L^{-1}) demonstrated concentrations similar to the baseline scenario. Under the elevated temperature and precipitation scenario, annual average DOC concentration at Duckfish (8−19 mg L^{-1}), Vital Narrows (4−8 mg L^{-1}), and Lower Martin (6−12 mg L^{-1}) demonstrated an absolute decline in DOC concentration relative to the baseline condition. Moreover, average daily DOC concentration under the elevated temperature scenario is predicted to increase transiently in March and April and decrease from October to December at Lower Martin (Figure 3.17).

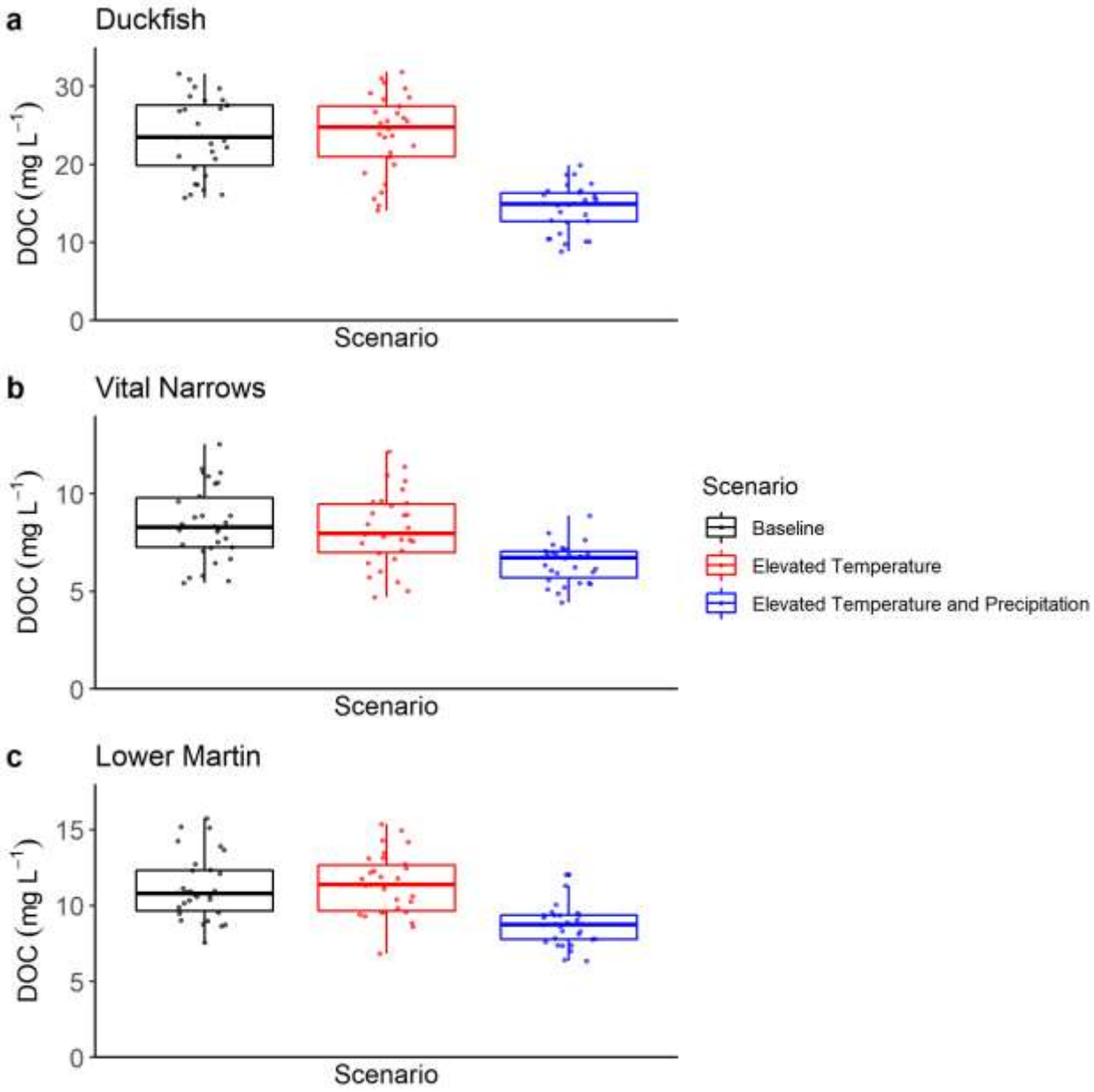

Figure 3.16: Boxplot showing INCA-C simulated average annual DOC concentration (mg L^{-1}) under baseline (black), elevated temperature (red), and elevated temperature and precipitation (blue) scenarios at Duckfish (top), Vital Narrows (middle), and Lower Martin (bottom) over 30 years. Note: Points shown in box plot are average annual DOC concentration in individual year simulated for each scenario.

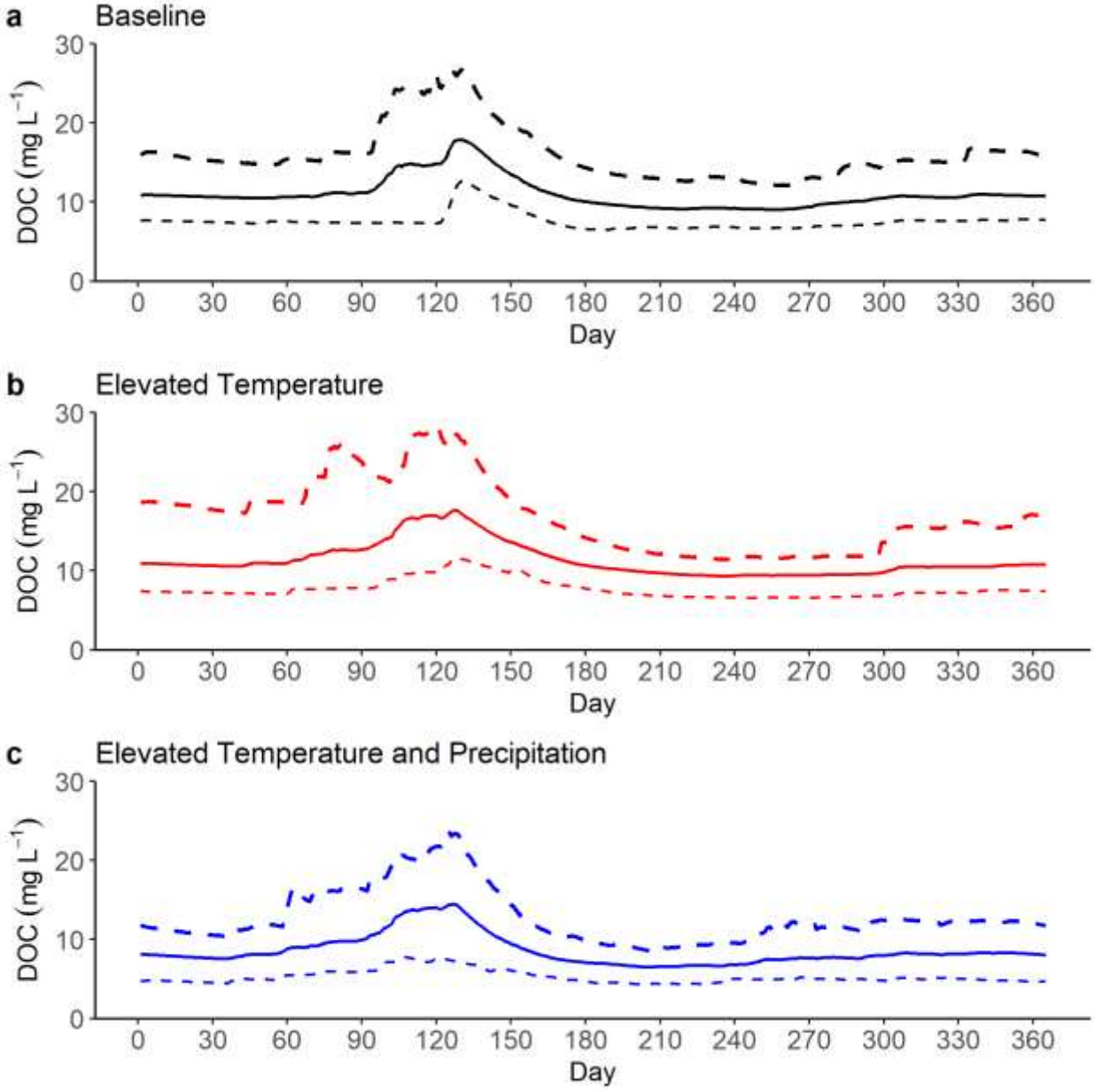

Figure 3.17: Average daily DOC concentration (mg L^{-1}), Q5 (thin dashed line), and Q95 (thick dashed line) over 30 years under baseline (a), elevated temperature (b), and elevated temperature and precipitation (c) scenario at Lower Martin.

Calculation of DOC export at the Baker Creek catchment over 30 years under baseline, elevated temperature, and elevated temperature and precipitation scenarios assisted understanding C dynamics (Table 3.7). The average DOC export under the baseline scenario at Duckfish is 1.10 g m^{-2} yr^{-1}, Vital Narrows is 0.90 g m^{-2} yr^{-1}, and Lower Martin is 2.51 g m^{-2} yr^{-1}. DOC export is projected to decrease (Duckfish: 0.80 g m^{-2} yr^{-1}; Vital Narrows: 0.67 g m^{-2} yr^{-1}; Lower Martin: 1.89 g m^{-2} yr^{-1}) under the elevated temperature scenario compared to the baseline scenario. Under conditions of elevated temperature and precipitation, however, DOC export is projected to increase (Duckfish: 2.0 g m^{-2} yr^{-1}; Vital Narrows: 1.48 g m^{-2} yr^{-1}; Lower Martin: 4.19 g m^{-2} yr^{-1}). The 95% confidence interval for DOC export under elevated temperature and elevated temperature and precipitation scenario in parts of catchment are shown in table 3.7. At Lower Martin, the average daily DOC export and Q95 values for DOC export are projected to increase from March to May and October to December under elevated temperature and precipitation scenario (Figure 3.18); however, under elevated temperature scenario, it is projected to increase in April and noticeably decrease in May and June.

Table 3.7: Average DOC flux (g m^{-2} yr^{-1}) with 95% confidence interval range (in parentheses) under baseline, Elevated temperature, and Elevated temperature and precipitation scenario and change in DOC export (comparing to baseline scenario in %) over 30 years at Duckfish Lake, Vital Narrows, and Lower Martin.

Scenario	**Statistics**	**Duckfish**	**Vital Narrows**	**Lower Martin**
Baseline	Average	1.1 (0.8–1.4)	0.90 (0.72–1.08)	2.51 (2.03–2.99)
Elevated Temperature	Average	0.8 (0.6–1.1)	0.67 (0.52–0.82)	1.89 (1.49–2.28)
	Change (%)	−27 (−25, −21)	−25 (−27, −24)	−24 (−26, −23)
Elevated Temperature and Precipitation	Average	2.0 (1.6–2.3)	1.48 (1.24–1.71)	4.19 (3.56–4.82)
	Change (%)	81 (100, 64)	64 (72, 58)	67 (75, 61)

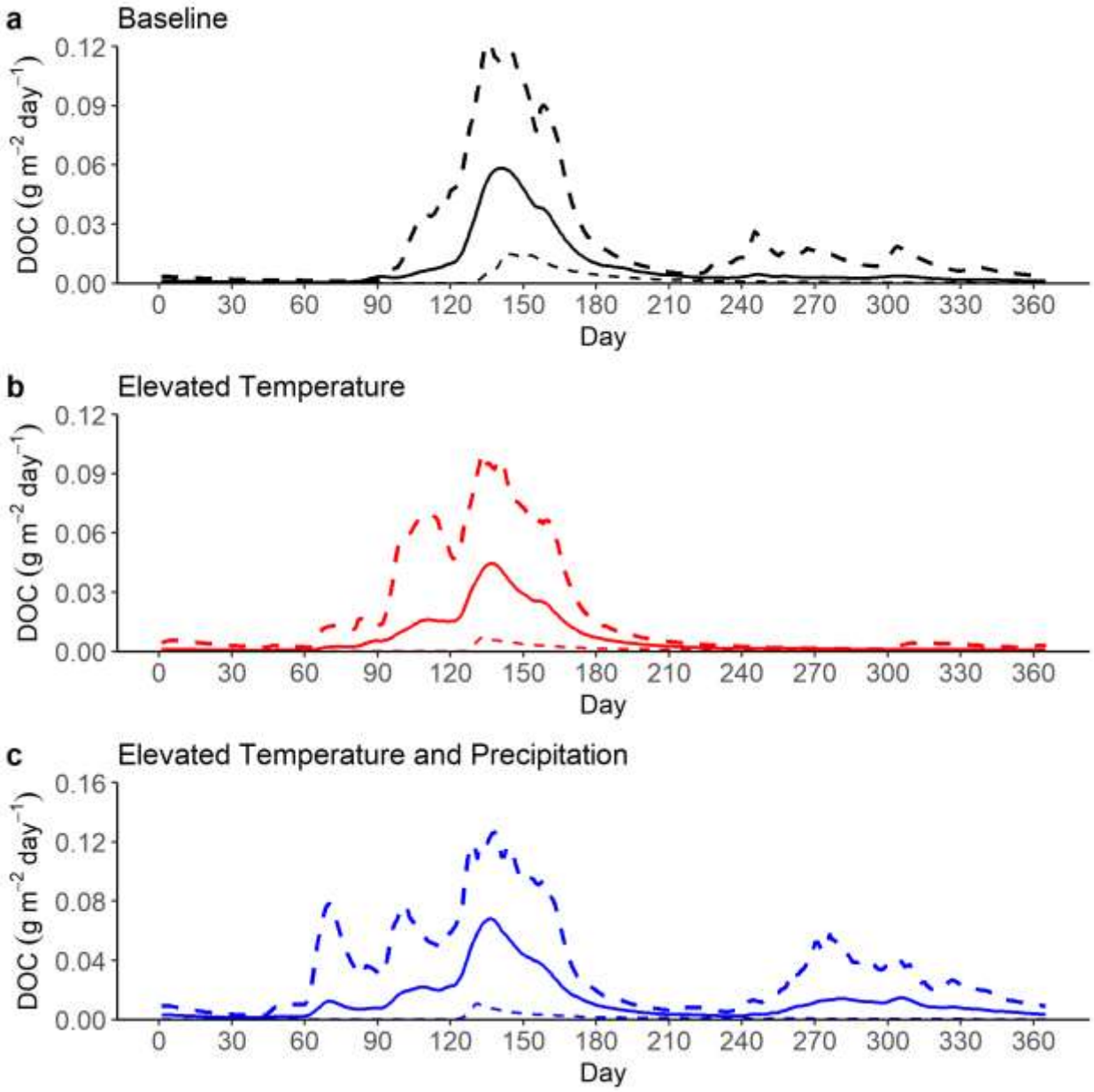

Figure 3.18: Average daily DOC export (g m^{-2} day^{-1}), Q5 (thin dashed line), and Q95 (thick dashed line) over 30 years under baseline (a), elevated temperature (b), and elevated temperature and precipitation (c) scenario at Lower Martin.

Chapter 4: Discussion

Baker Creek is a complex and fascinating catchment to study with diverse hydrological behavior. Despite a complex catchment, overall catchment behaviour was captured. However, there was a tendency for the models to overestimate the flow and underestimate concentration in certain years. PERSiST simulations of hydrology and INCA-C simulations of both hydrology and DOC patterns, were reasonable but not particularly strong. Exploration of hydroclimatic control on DOC export using INCA-C has highlighted the importance of understanding the present and future hydroclimatic changes in the catchment. Historic hydroclimatic data have shown evidence of climate warming and future climate scenarios reflect changes in the hydroclimatic regime. The changing hydroclimatic behavior can be important for future DOC fluxes, which could contribute to changing patterns of metal export.

4.1 Catchment hydrology and response to changing hydroclimate

Historic temperature records nearby YKA meteorological station (1955−2019) have shown evidence of climate warming. Analysis of available temperature data over the past 65 years showed statistically significant annual and seasonal warming. The annual warming signals were similar to changes since 1950 summarized by DeBeer et al., (2016) for western Canada. Assessment of basins in northern Canada has also shown strong signals of climate warming with extreme warm winters (Furgal & Prowse, 2007; Gillet et al., 2019). Analysis of available precipitation data over the past 65 years at the YKA station detected no significant change in annual and seasonal precipitation except spring rainfall. The average annual precipitation trend result is different from other observations (1950−2018) in North America (Douville et al., 2021) and western Canada (1950−2012) (DeBeer et al., 2016), which showed an increasing trend in annual precipitation. As, there was only single station available long-term data (YKA), it might not be robust comparing to multi-station analyses.

Changing climate can play a significant role in changing catchment hydrology (Dery et al., 2016; Rood et al., 2017). For example, increasing precipitation in northern Eurasia (Smith et al., 2007), increasing active layer thickness due to warming in Sweden (Akerman & Johansson, 2008); permafrost melting in the Yukon river basin (Walvoord & Striegl, 2007) were observed changing discharge. In the Baker Creek catchment, a large number of lakes are connected by short channels (Spence, 2006). The catchment has maximum discharge in spring freshet (peak in May). The fill-spill process of lakes affected by climate variables controls discharge in the catchment (Spence et al., 2013; Spence & Woo, 2003). The connectivity of part of the catchment has a significant role in the outflow amount in the outlet of Lower Martin. For example, Duckfish shows attenuating behavior, while the eastern part of Vital Narrows shows flashy nature. In spring and summer, connectivity of sub-catchments through surface runoff controls discharge (Phillips et al., 2011) whereas base flow from lake storage controls runoff in the winter (Aukes, 2019; Jacques & Sauchyn, 2009). In winter, although air temperature remains lower than freezing temperature, soil temperature below 40 cm remains above freezing, which maintains sub-surface flow (Spence et

al., 2013). However, during dry periods, the upper part of the catchment dries, interrupting connectivity, and the contributing area contracts.

Whereas there is no evidence of changes in annual streamflow via available long-term flow records (Table 3.3), seasonal discharge has shown significant positive trends. Additionally, future discharge projection for Baker Creek under an elevated temperature scenario suggested a decrease in average annual discharge. Decreased average annual discharge is projected in other subarctic catchments such as northern Fennoscandia (Lotsari et al., 2010). In Baker Creek, decrease in runoff ratio (Duckfish Lake: –23.5%; Vital Narrows: –25%; Lower Martin: –27%) over 30 years is associated with a decline in discharge under elevated temperature scenario. The increased temperature can decrease snowfall amount and change the form of precipitation from snow to rain which is already observed (Bintanja, 2018; Bintanja & Andry, 2017). The decreased snowfall amount can decrease total annual runoff and groundwater recharge (Jenicek & Ledvinka, 2020).

At Baker Creek, daily discharge in early spring is projected to increase in the future as peak discharge shifts earlier in the year under warmer conditions that prompt earlier snowmelt. The decrease in discharge during the remainder of the year is linked with increased evapotranspiration, as it has been shown that increased rainfall is balanced by increased evapotranspiration in the circumpolar north (Vihma et al., 2016). Moreover, increasing evapotranspiration has the potential to decrease the contribution of discharge from upstream lakes such as Duckfish, which ultimately limits the active stream network and lowers contributing area (Phillips et al., 2011; Spence et al., 2010).

Predictions of elevated discharge under the elevated temperature and precipitation scenario are similar to observations for other subarctic catchments such as in northern Sweden (Andreasson et al., 2004). The increase in precipitation and temperature in the catchment can affect hydrological drivers such as runoff contributing area, effective precipitation, active stream networks, permafrost melting, hydrological storage, and baseflow (Connon et al., 2014; Phillips et al., 2011; Spence et al., 2010; Morse et al., 2016). In Baker Creek, a projected increase in discharge over 30 years is linked with projected increase in runoff ratio (Duckfish Lake: increased by 106%; Vital Narrows: increased by 54%; Lower Martin: increased by 54%) under the elevated temperature and precipitation scenario.

Another important projection is a shift in a flow regime from nival to combined nival and pluvial. The elevated temperature and precipitation scenario had a projected secondary discharge peak in early winter at Lower Martin (Figure 3.14). Spence et al. (2011) have reported evidence of this shift in flow regime in Baker Creek for a recent wet period. The shift in regime from nival to combined nival and pluvial was attributed to a shift in timing and form of precipitation (Spence et al., 2011), mainly a shift in precipitation from snowfall to rainfall and increasing rainfall in fall (Figure 3.15). The elevated temperature and precipitation scenario predicted high rainfall in summer and fall, with fall rainfall being larger. This projected shift in the flow regime in Baker Creek coincides with the studies in other subarctic catchments such as northern Fennoscandia

(Lotsari et al., 2010), northern Sweden (Bergström et al., 2001), and Norway (Beldring et al., 2008).

4.2 Carbon Flux

Changing hydroclimatic patterns could have major control on C concentration in catchments. However, in Baker Creek, the projected annual DOC concentration under the elevated temperature scenario is similar to the baseline scenario. This finding contrasts with cases where DOC concentration increased with temperature (Evans et al., 2005; Xu et al., 2020); however, it is consistent with other observations from northern Europe (Oni et al., 2012) where no increase in DOC concentration was observed. In contrast, the DOC concentration is predicted to decrease under the elevated temperature and precipitation scenario. This finding is consistent with Clair et al. (2008) in catchments in Nova Scotia where the decreasing trend of DOC concentration was observed with enhanced surface flow resulting in DOC dilution in water bodies. Another important finding of this study is the changes in C export under both climate scenarios. The DOC export in Baker Creek catchment showed that C export would decrease if temperature increases occur in the absence of changes in precipitation. The predicted decrease in C export was similar to the projection of Lake Simcoe catchment in Canada (Oni et al., 2011). Decreased DOC export under elevated temperature scenario is related to a projected decrease in discharge (due to increased temperature) and hydrological connectivity with C rich sources such as Duckfish Lake. Export of DOC is projected to increase under the elevated temperature and precipitation scenario in all three study locations at Baker Creek which supports the previous projections of an increase in DOC export in northern catchments (Clair et al., 1999).

In Baker Creek, the lakes are oligotrophic, and likely act as sinks, rather than sources of C. The major source of aquatic C in Baker Creek is terrestrial C. Elevated warming can increase permafrost melting which can enhance allochthonous C sources to the aquatic system (Roiha et al., 2016). The extent of permafrost immediately north of Great Slave lake (including Baker Creek) has been found to align with the distribution of forest types (Morse et al., 2015). Permafrost occurs in hillslopes, peat bogs, and plateaus where organic material lies over glaciolacustrine clays (Morse et al., 2015). Permafrost is absent from areas of exposed bedrock and well-drained coarse thin overburden. In Baker Creek, since lakes and exposed bedrock comprise ~60% of the catchment; permafrost would cover less than 40%. Projected enhanced temperature can increase the active layer thickness of permafrost soil. Thus, the net flux of C also depends upon the active layer thickness. In Baker Creek, flow pathways are projected to be proportionally similar under elevated temperature and elevated temperature and precipitation scenario comparing to baseline scenario (~80% flow from organic layer). However, the flow amount from organic horizon is projected to be two times higher under elevated temperature and precipitation scenario (Table B.5) and ~0.75 times lower under elevated temperature scenario compared to the baseline scenario. Thus, under elevated temperature and precipitation scenario, increased flow amount can increase the flux owing to a much greater volume of water, while at the same time being more dilute with respect to DOC concentration. Moreover, in the model representation is not necessarily flowing along a

catena from upland to forest and forest to wetland and finally to water bodies. The water from bedrock moves directly to the water bodies. The consequence could be low stream concentrations even with more flow under this scenario. However, the projected increase in DOC flux could be because of longer connectivity due to longer periods of DOC flushing from the organic layer.

Simulations of DOC concentration in Baker Creek show sensitivity to parameters that can be affected by the change in temperature and precipitation such as terrestrial productivity, residence time, and microbial mineralization. DOC concentration in the catchment is rather insensitive to change in the productivity of wetland and forest areas. For example, a five-fold increase in the productivity of wetland and forest areas of the catchment results in only a three-fold increase in DOC concentration. Nonetheless, under an elevated temperature scenario, the productivity of the catchment can increase (Striegl et al., 2005), which could increase DOC concentration. Water residence time also increases with the increased temperature (Weiman, 2015), however, increasing the potential for aquatic DOC degradation to occur. The residence time of C-rich locations such as Duckfish Lake (140 d) and other lakes (Vital Narrows: 19 d; Lower Martin: 54 d) is projected to increase under elevated temperature scenario and projected to decrease (Duckfish: 86 d, Vital Narrows: 14 d, Lower Martin: 31 d) under elevated temperature and precipitation scenario compared to baseline scenario (Table B.6).

Microbial mineralization in lakes is greater under the elevated temperature and precipitation scenario (Table B.7) as more DOC is being flushed in from the catchment and the rate of mineralization has a strong positive relationship with temperature (Gudasz et al., 2010). The increased mineralization explains the reason behind the projected decline in DOC concentration under elevated temperature and precipitation scenario. In contrast, less mineralization is projected under elevated temperature scenario (Table B.7). Under an elevated temperature scenario, less DOC is being flushed into the lakes from the catchment due to projected decline in runoff. Under an elevated temperature scenario, the actual rates of microbial mineralization (% DOC mineralized per day) are going to be higher because the water will be warmer for longer, but because the amount of total amount of DOC received by the lakes is less, the total amount mineralized is predicted to be lower.

Additionally, climate scenarios in Baker Creek support evidence from numerous previous observations where runoff-driven control in DOC export was observed (Creed et al., 2008; Grant et al., 2008; Worrall & Burt, 2007). For instance, the elevated temperature scenario has projected a decrease in C flux (24–27%) under similar DOC concentration but lower discharge (22–27%). Similarly, the elevated temperature and precipitation scenario projected an increase in C flux (64–81%) under decreased DOC concentration and increased discharge (116–175%) projection. Both climate projections have highlighted the control of discharge on C fluxes. Similarly, runoff control in seasonal C load has also been projected in the catchment. A secondary DOC export peak is projected in winter in Baker Creek under warmer and wetter climate conditions, which coincides with the winter discharge peak. Spence et al. (2015) previously observed this type of seasonal C export behavior in Baker Creek during an exceptionally wet fall.

Thus, under an elevated temperature and precipitation scenario, increased dilution (with increased precipitation) and increased microbial mineralization appear to control the C concentration, suggesting the potential for lower DOC concentration (Figure 3.16) compared to the baseline scenario. Increased runoff, flow amount from organic soil column, and connectivity for a longer period has projected higher DOC export under elevated temperature and precipitation scenario. Under an elevated temperature scenario, the decreased mineralization appears to balance the increased C concentration (by increased productivity and/or active layer of permafrost) keeping DOC concentration similar to the baseline scenario. Decreased runoff, specifically lower flow amount from the organic column and therefore less connectivity with C sources, and mineralization for longer time due to higher residence time appear to contribute to a decline in DOC export under elevated temperature scenario compared to baseline scenario.

4.3 Model performance

4.3.1 PERSiST

The PERSiST model was successful in simulating inter and intra-annual patterns in Baker Creek and its sub-catchments. Among the four sub-catchments, PERSiST captured discharge in three locations (Duckfish Lake, Vital Narrows, and Lower Martin), reasonably well. In these locations, model performance was better during the shorter (2012−2016), dry portion (period with available DOC observations) of the record (R^2 ranging from 0.87 to 0.94 and NS ranging from 0.82 to 0.91) compared to the longer (2005−2016) record (R^2 ranging from 0.42 to 0.77 and NS ranging 0.18 to 0.74) (Table 3.4). In previous applications of hydrological models, NS performance (>0.5) is considered good (Moriasi et al., 2007). Previous applications of the model have also observed better simulations in shorter records compared to longer ones (Futter et al., 2014). In the longer record, capturing a wider range of conditions such as wet and dry cycles (as observed in Baker Creek) using a single parameter set was challenging. However, in shorter record there is lesser likelihood of having extreme conditions and can be more easily simulated by using single parameter set (Ledesma et al., 2012).

Higher flow years with high precipitation (e.g. 2012) were better captured; however, during dry periods (after 2012), discharge at Duckfish was intermittent or zero, and the model was not able to represent these periods of disconnectivity, and also overestimated baseflow. Moreover, external disturbance in the hydrological system by beaver activities (Spence & Hedstrom, 2018) which lead to transient changes in connectivity, could be another challenge in accurately simulating flow.

4.3.2 INCA-C

Simulations of discharge and C processes in sub-catchments of Baker Creek with INCA-C were reasonable. Although the model performance (R^2 ranged from 0.19 to 0.31) was not strong as other INCA-C applications in northern catchments (de Wit et al., 2016; Futter et al., 2011; Ledesma et al., 2012; Oni, et al., 2012; Oni et al., 2014; Xu et al., 2020), it has done a good job in capturing DOC concentration in three sub-catchments of the rather complex Baker Creek catchment.

The performance of the INCA-C model is affected by data availability (available observations), characteristics of the catchment (such as connectivity, flow pathways, C content in soil layers), and calibration process (initial parameter values, parameter adjustment, and selection). Among sub-catchments of Baker Creek, model performance was comparatively better at Vital Narrows. This could be due to the limited number of observations at Vital Narrows compared to Lower Martin. With a lower number of observations, the chance of having extreme conditions is lessened, which improves the chance of getting a better model fit (Ledesma et al., 2012; de Wit et al., 2016). Simulated DOC concentration was much lower than measured values in the period when catchment is connected (2012–2014) and was well captured in the period when catchment was disconnected (after 2014). Accurate discharge simulation is crucial for the simulation of DOC concentration. At Lower Martin, where discharge is overestimated, simulated DOC concentration is underestimated (2012–2014). In the wet hydrological year (2012), 83% (at Duckfish), 93% (at Vital Narrows) and 94% (at Lower Martin) of water travels through the organic layer and in dry hydrological years (2013–2015), 82% (at Duckfish), 93% (at Vital Narrows) and 94% (at Lower Martin) of water travels through the organic layer. This suggests the same source of DOC in dry and wet years; however, the difference in the amount of DOC export could be because of the difference in the amount of water flowing.

The hydrological complexity could be another reason behind lower model performance for DOC concentration. For instance, during wet periods, some sub-catchments with (at least intermittently) high organic C (Duckfish) are connected. Connectivity of such lakes with different DOC characters can be an important influence on C concentration in lower reaches, making it necessary to accurately represent both the magnitude and timing, as well as the DOC concentrations in these waters, to effectively represent the larger catchment. Additionally, the presence of large number of lakes in Baker Creek and uncaptured permafrost processes in catchment could be another reason for lower model performance.

Calibration of INCA-C requires initial values of some parameters. Due to the lack of actual data of those parameters, estimated values were used. Although estimations were done in a sensible way to get better performing result and represent the real conditions such as high SOC and DOC in organic layer than a mineral layer, and high SOC and DOC in wetland and forest than bedrock and water bodies, there remains the risk of not adequately characterizing these parameters. A more robust representation of catchment hydrological behavior is also crucial for better simulation of DOC concentration by INCA-C. In Baker Creek, the inability to simulate discharge peaks has also affected the performances of DOC simulations. For instance, INCA-C had overestimated peak discharge at Lower Martin in later dry years (2014−2016). The overestimated discharge could have diluted DOC concentration and lead to underestimated DOC concentration during that period. Thus, further improved discharge simulation could improve DOC simulation.

4.3.3 Model sensitivity, uncertainty, and limitations

Sensitive PERSiST and INCA-C parameters for discharge and DOC simulations in the calibration period were identified (Table A.1; Table A.2). The precipitation-related parameters such as

precipitation multipliers, flow velocity parameters, time constant and temperature-related parameters such as degree-day melt factor, growing degree threshold, and evapotranspiration adjustment were most sensitive in discharge modeling. The precipitation multipliers (rain multiplier and snow multiplier) are adjustment factors used to represent potential differences in rainfall and snowfall across sub-catchments. Flow velocity parameters are empirical scaling factors used for the calculation of streamflow velocity, and the time constant is the residence time of water in a soil column as a proxy of hydrological connectivity. Degree-day melt factor adjusts the temperature-dependent rate of snowmelt, growing degree offset is threshold temperature above which evapotranspiration occurs and evapotranspiration adjustment is the factor to limit water loss by evapotranspiration. These parameters have been demonstrated to play a strong role in discharge simulation for other catchments (e.g. Oni et al., 2012; Xu et al., 2020).

Simulated DOC concentration in the catchment was sensitive to both hydrological and chemical parameters (Table A.2) such as flow velocity (controlling streamflow velocity), partitioning (controlling flow through organic/mineral layer as shown in Table B.5), and residence time (Table B.6) and microbial degradation (Table B.7) which can control DOC mineralization. DOC simulation was also sensitive to litterfall (controlling C input) and C processes in the soil layers, which determines DOC absorption and desorption rates. These sensitive chemical parameters control C production and transformations in soil, which is governed by temperature whereas hydrological parameters control DOC export mainly governed by precipitation. Thus, the combination of higher temperature and precipitation in future simulations suggests the potential for higher DOC export.

Model simulations have some limitations related to model input and calibration strategy. For instance, in PERSiST model, temperature and precipitation data of a single station were used throughout the catchment. During calibration, specific rainfall and snowfall multipliers were used to improve model performance, but the true nature of variability in precipitation amount across the catchment is not well known. Additional precipitation time series of upstream and downstream reaches could have helped to get a more robust model performance, or at least reduced the need to rely on these parameter adjustments during calibration. In INCA-C, DOC input from aerial source is not considered. Although, there could be many sources for aerial DOC, one major source is forest fire. However in Baker Creek there is no evidence of forest fire since 1960s (Spence et al., 2020). Thus, aerial deposition of C in Baker Creek could be less in amount. Furthermore, the calibration period of record selected was dry and did not capture the full range of hydrological variability exhibited over the last several decades, thus the model performance during wetter periods remains unknown. In PERSiST and INCA-C, equifinality was another challenge where multiple sets of parameters with different parameter spaces were showing equivalent calibration performance. Previous modeling applications have highlighted over-parameterization and compensatory behavior in parameter space as reasons for equifinality (Beven & Binley, 1992; Futter et al., 2007). Despite improved DOC simulations by MC analysis, there were some mathematically possible but scientifically implausible simulations. For example, the MC

calibration of INCA-C had two different best parameter sets with the same model efficiency. However, one among them had unstable PDC in direct runoff and organic layer and it was losing C in the soil and was deemed implausible. As model simulations don't capture the permafrost processes in the catchment, incorporating the permafrost processes in a new version of model could help to better simulate uncaptured C processes and improve model performance.

4.4 Contaminants transport under changing scenario

Future climate scenario projections indicated the potential for both increases or decreases in DOC export from Baker Creek. These future changes in DOC export can affect bioavailability, toxicity, and mobility of historically stored heavy metals in the catchment (Koprivnjak & Moore, 2006; Ledesma et al., 2012; McKnight et al., 1992). The organic acid present in DOC acts as chelators and binds with metal, making organic complexes (Hudson et al., 2003). For instance, studies have found evidence of soil contamination (up to 20 to 30 km) from the historic roaster stack of Giant Mine, and contamination was mainly found in the shallow soil of forest and wetland areas (GNWT, 2019; Jamieson et al., 2017).

In Baker Creek, organic C input in the upper soil column is approximately 10 times higher than organic C input in the lower soil column. For example, under the baseline scenario, at Lower Martin, Simulated C in upper soils is 10 times higher than lower soils (49.7 vs 4.8 g m^{-2}). With elevated temperature and precipitation scenario, C input in both soil columns at Lower Martin is projected to increase (upper soil column: 69.9 g m^{-2}; lower soil column: 6.9 g m^{-2}). With the increase in C input, DOC export from the upper soil column to streams is projected to increase. The projected increase in DOC export from the upper soil column under warmer and wetter future conditions can make organic complexes with metal contaminants present in the upper soil layer (in wetland and forest areas) and can enhance the mobility of stored metals. For example, copper present in soil can bind with DOC and form the Cu-DOC complex which enhances the desorption of copper in soil (Ashworth & Alloway, 2007). The formation of Cu-DOC complexes with increased DOC export can increase the concentration and mobility of stored copper from the outlet of Baker Creek. Moreover, DOC have multiple functional groups that can bind with metals such as amino, carboxyl, phenolic, thiols (Smith et al., 2002). It also shows polyelectrolyte nature such as it carries either positively or negatively charged ionizable groups. For instance, humic substance have a strong negative charge at their outer surface due to which they love to bind with metal cations. Thus, it easily makes complexes with alkali and alkaline earth metals. However, some metalloids such as arsenic behave differently. Arsenic forms an anion with –3 charge (arsenate) which can bind with amine groups on humic acids, allowing DOC to complex these anions. Additionally, with the projected increase in DOC mineralization under elevated temperature and precipitation scenario in land covers such as wetland area, more oxygen is consumed and can undergo redox reactions with metal pollutants binding protons.

Additionally, sediment analysis in Baker Creek has shown five contaminants of potential concern: arsenic, chromium, copper, manganese, and nickel (Golder, 2013). The projected increase in DOC export may increase the transport of these metal contaminants and increase the bioavailability of

metals. For example, in natural bodies, initially, mercury is available in an ionic state. DOC facilitates the conversion of ionic mercury to methylmercury and makes it bioavailable in the food chain. The evidence of arsenic concentration in tissues of benthic organisms and fish species have already been reported in the area (Cott et al, 2016; Golder, 2013; 2018). With increased DOC export, the bioavailability of heavy metals could increase and can accumulate in the food chain. Thus, the projected increase in DOC export could increase the transfer of heavy metal pollutants (Palmer et al., 2019) raising the risk of impacts to aquatic and human health.

Chapter 5: Conclusions

In summary, Baker Creek is a fascinating catchment and one that proves challenging to simulate. Historic hydroclimatic data in Baker Creek has shown evidence of climate warming and seasonal hydrological changes. Understanding past and present hydroclimatic patterns have assisted in the simulation of future hydrological behavior and C export (over 30 years). The hydrological model PERSiST and biogeochemical model INCA-C were used to simulated discharge and DOC patterns in sub-catchments of Baker Creek. A shorter calibration record (2012–2016) worked well in model simulations, with the R^2 and NS for discharge 0.87–0.94 and 0.82–0.91, respectively. Well-simulated hydrological processes helped in capturing DOC concentration. While INCA-C captured broad DOC patterns in Baker Creek (R^2: 0.19–0.31), there is room to improve. Nonetheless, because the models were calibrated to the driest period on record, there remains uncertainty about how these models as currently calibrated, and how well they will represent longer-term periods that exhibit greater hydrologic variability. Simulated future discharge over 30 years suggests that both increases (under elevated temperature and precipitation scenario) and decreases (under elevated temperature scenario) in annual discharge are possible. The changes in runoff ratio i.e. decreased runoff ratio under elevated temperature scenario and increased runoff ratio under the elevated temperature and precipitation scenario has contributed to changes in discharge, respectively. Additionally, simulations of daily discharge under the elevated temperature and precipitation scenario demonstrate increased winter discharge and a shift in hydrological regime from nival to combined nival and pluvial.

In Baker Creek, the temperature had a positive effect on terrestrial productivity, microbial activities, and water residence time, which resulted in negligible change in DOC concentration under the elevated temperature scenario. The decrease in DOC concentration under the elevated temperature and precipitation scenario is related to the negative effect of precipitation on DOC concentration. Despite this, DOC export in Baker Creek was highest under this future scenario; increased connectivity with C rich parts of the catchment and increased flow amount through the C-rich upper organic layer are likely important for this pattern. Furthermore, with the shift in the hydroclimatic regime, the catchment is projected to have increased DOC export in winter. Thus, this research highlights the control of hydroclimatic drivers on inter and intra annual patterns of DOC export.

An increase in DOC export in the Baker Creek catchment can increase the mobility of historically deposited metal contaminants in soil and sediments. Overall, contaminant transport could increase under elevated temperature and precipitation scenario and could decrease under elevated temperature scenario. These projected patterns of discharge, DOC concentration, and DOC export could be a launching point for future research to formulate hypotheses to examine patterns of contaminant transport under projected conditions. Findings from this research could be a good source of knowledge for understanding the impact of changing hydroclimatic regime on C export in this and similar sub-arctic catchments. These findings could assist policymakers more generally in thinking through adaptation measures for predicted water contamination, which could affect

aquatic health and the health of nearby aboriginal communities that are exposed to contaminated water and fish from Baker Creek. Further research using a coupled model for both DOC and metal fluxes together could help in watershed and water quality management planning for possible future impacts.

Appendix A: Supplemental information for chapter 2

Table A.1: Tolerance window for sensitive PERSiST parameters used in the Monte Carlo analysis.

Parameter	Unit	Value
a		0.01–2.7
b		0.67–0.99
c		75 x 10^{-3}–0.12
Rain Multiplier		0.8–1.1
Snow Multiplier		0.8–1.1
Degree day melt factor	(mm $^{\circ}C^{-1}$)	0.5–3
Growing degree threshold	($^{\circ}C$)	−0.6–1.62
Time Constant (Quick box)	days	0.78–3.5
Time Constant (Fast box)	days	4–32
Time Constant (Slow box)	days	7.8–52
Evapotranspiration Adjustment		0.075–0.55

Table A.2: Tolerance windows for sensitive INCA-C parameters used in the Monte Carlo analysis.

Parameter	**Unit**	**Value**
a		0.75–2.25
b		0.33–1.18
c		75×10^{-6}–25×10^{-4}
f		0.17–0.75
DOC → DIC microbial	day^{-1}	75×10^{-6}–0.11
SOC → DOC (Organic layer)	day^{-1}	1×10^{-4}–0.012
PDC → DOC (Organic layer)	day^{-1}	7×10^{-3}–0.1
DOC → DIC (Organic layer)	day^{-1}	8×10^{-4}–0.012
DOC → SOC (Organic)	day^{-1}	1×10^{-4}–13×10^{-4}
Retention volume (Organic)	m^3	18700–69835
Runoff layer residence time	days	0.75–1.25
Organic layer residence time	days	1.5–3.7
Mineral layer residence time	days	15–31
Litter fall	$kg\ ha^{-1}\ d^{-1}$	0.07–1.7
Partitioning (Organic/Mineral layer)		0.45–0.75

Appendix B: Supplemental information for chapter 3

Table B.1: Result of Mann-Kendall test for average monthly temperature (1955–2019) at Yellowknife station (1706 and 51058).

Parameter	Tau	p-value	Adjusted p-value	alpha	Interpretation
January	0.03	0.01	0.2	0.05	No trend
February	0.03	0.01	0.1	0.05	No trend
March	0.03	0.03	0.3	0.05	No trend
April	0.02	0.05	0.6	0.05	No trend
May	0.02	0.05	0.6	0.05	No trend
June	0.03	0.03	0.3	0.05	No trend
July	0.03	0.04	0.4	0.05	No trend
August	0.02	0.07	0.8	0.05	No trend
September	0.02	0.1	1	0.05	No trend
October	0.02	0.05	0.6	0.05	No trend
November	0.02	0.03	0.3	0.05	No trend
December	0.03	0.3		0.05	No trend

Table B.2: Mann-Kendall test result for seasonal precipitation, rainfall, and snowfall (1955–2019) at Yellowknife station (1706 and 51058).

Reach	**Precipitation**		**Rainfall**		**Snowfall**	
	Tau	**p-value**	**Tau**	**p-value**	**Tau**	**p-value**
Late Winter	−0.01	0.2	0.01	0.03	−0.01	0.1
Spring	-6×10^{-3}	0.5	0.03	3×10^{-3}	−0.01	0.1
Summer	-6×10^{-3}	0.6	0.02	0.1	−0.01	0.1
Early Winter	-5×10^{-3}	0.5	0.01	1	-9×10^{-3}	0.3

Table B.3: Mann-Kendall test result for average monthly precipitation, rainfall, and snowfall (1955–2019) at Yellowknife station (1706 and 51058).

		Precipitation		**Rainfall**		**Snowfall**	
Month	**alpha**	**Tau**	**p-value**	**Tau**	**p-value**	**Tau**	**p-value**
January	0.05	−0.01	0.5	0.03	0.9	−0.01	0.3
February	0.05	0.01	0.4	0.02	1	-6×10^{-3}	0.7
March	0.05	-2×10^{-3}	0.8	0.03	0.3	-8×10^{-3}	0.6
April	0.05	0.02	0.2	0.01	1	-7×10^{-3}	0.6
May	0.05	−0.01	0.5	0.01	1	−0.01	0.5
June	0.05	−0.01	0.5	0.04	0.1	−0.01	0.2
July	0.05	−0.02	0.2	0.03	0.6	−0.02	0.1
August	0.05	−0.02	0.1	0.003	1	-7×10^{-3}	0.6
September	0.05	−0.01	0.5	0.01	1	−0.01	0.3
October	0.05	−0.01	0.3	0.03	0.6	−0.02	0.1
November	0.05	0.00	0. 9	−0.01	1	−0.01	0.5
December	0.05	-9×10^{-3}	0.5	0.016	1	−0.01	0.4

Table B.4: Result of Mann-Kendall test for average monthly discharge (1983–2017) at Lower Martin station (07SB013).

Parameter	**Tau**	**Adjusted p-value**	**alpha**	**Interpretation**
January	0.032	0.14	0.05	No trend
February	0.034	0.12	0.05	No trend
March	0.035	0.11	0.05	No trend
April	0.033	0.12	0.05	No trend
May	0.032	0.14	0.05	No trend
June	0.033	0.13	0.05	No trend
July	0.032	0.14	0.05	No trend
August	0.032	0.14	0.05	No trend
September	0.033	0.12	0.05	No trend
October	0.031	0.15	0.05	No trend
November	0.032	0.14	0.05	No trend
December	0.031	0.15	0.05	No trend

Table B.5: Projected flow ($m^3 s^{-1}$) from organic layer and mineral layer under baseline, elevated temperature, and elevated temperature and precipitation scenario over 30 years at Duckfish, Vital Narrows, and Lower Martin.

	Duckfish Lake		Vital Lake		Lower Martin	
	Organic Layer	Mineral Layer	Organic Layer	Mineral Layer	Organic Layer	Mineral Layer
Wetland						
Baseline	1.5×10^{-3}	2.9×10^{-4}	2.0×10^{-3}	2.3×10^{-4}	2.2×10^{-3}	2.1×10^{-4}
Elevated Temperature	1.1×10^{-3}	2.1×10^{-4}	1.4×10^{-3}	1.7×10^{-4}	1.6×10^{-3}	1.5×10^{-4}
Elevated Temperature and Precipitation	4.6×10^{-3}	8.8×10^{-4}	4.8×10^{-3}	6.1×10^{-4}	5.3×10^{-3}	5.3×10^{-4}
Forest						
Baseline	1.5×10^{-3}	2.9×10^{-4}	2.4×10^{-3}	1.6×10^{-4}	2.7×10^{-3}	1.6×10^{-4}
Elevated Temperature	1.1×10^{-3}	2.1×10^{-4}	1.8×10^{-3}	1.2×10^{-4}	1.9×10^{-3}	1.1×10^{-4}
Elevated Temperature and Precipitation	4.6×10^{-3}	8.8×10^{-4}	4.9×10^{-3}	3.4×10^{-4}	6.1×10^{-3}	3.6×10^{-4}

Table B.6: Average residence time (days) under baseline, elevated temperature, and elevated temperature and precipitation scenario over 30 years at Duckfish, Vital Narrows, and Lower Martin.

Scenario	Duckfish Lake	Vital Narrows	Lower Martin
Baseline	127	18	49
Elevated Temperature	140	19	54
Elevated Temperature and Precipitation	86	14	31

Table B.7: Average microbial mineralization of DOC (kg d^{-1}) of 30 years in lake under baseline, elevated temperature, and elevated temperature and precipitation scenario at Duckfish, Vital Narrows, and Lower Martin.

Scenario	Duckfish Lake	Vital Narrows	Lower Martin
Baseline	40	117	0.37
Elevated Temperature	37	100	0.36
Elevated Temperature and Precipitation	45	174	0.47

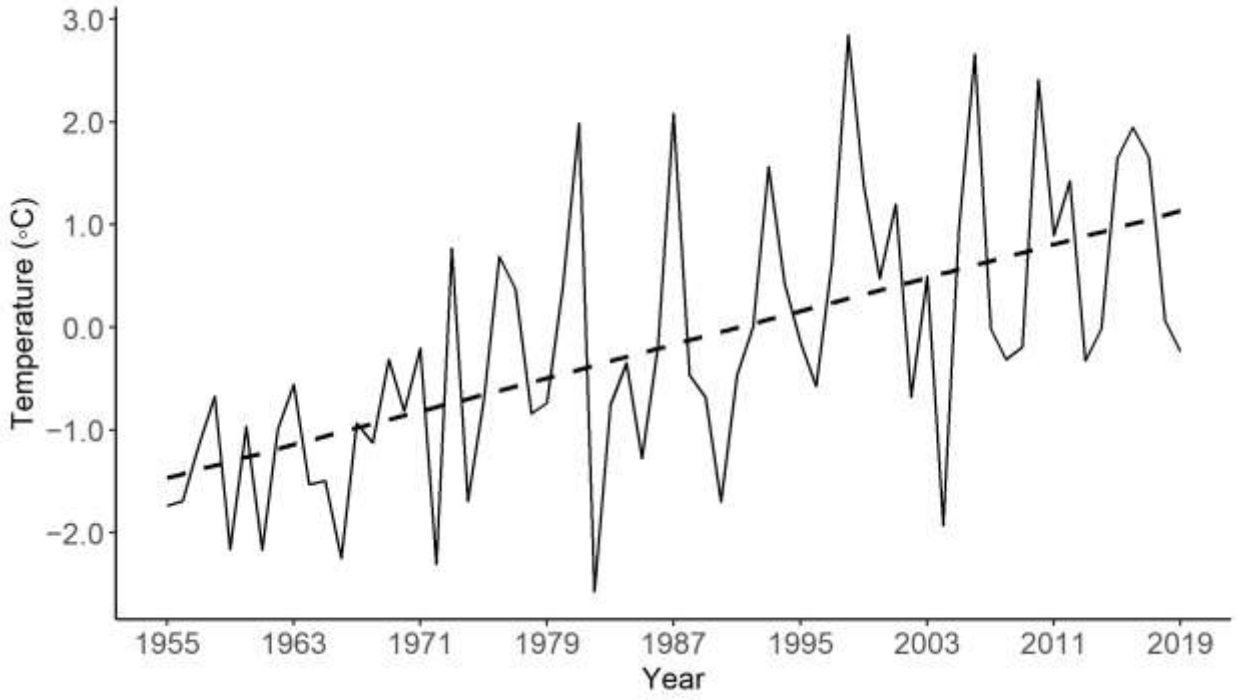

Figure B.1: Average annual maximum temperature (1955–2019) at Yellowknife station (located 5 km from the southern end of the Baker Creek catchment). Note: Black dashed line is a trend line.

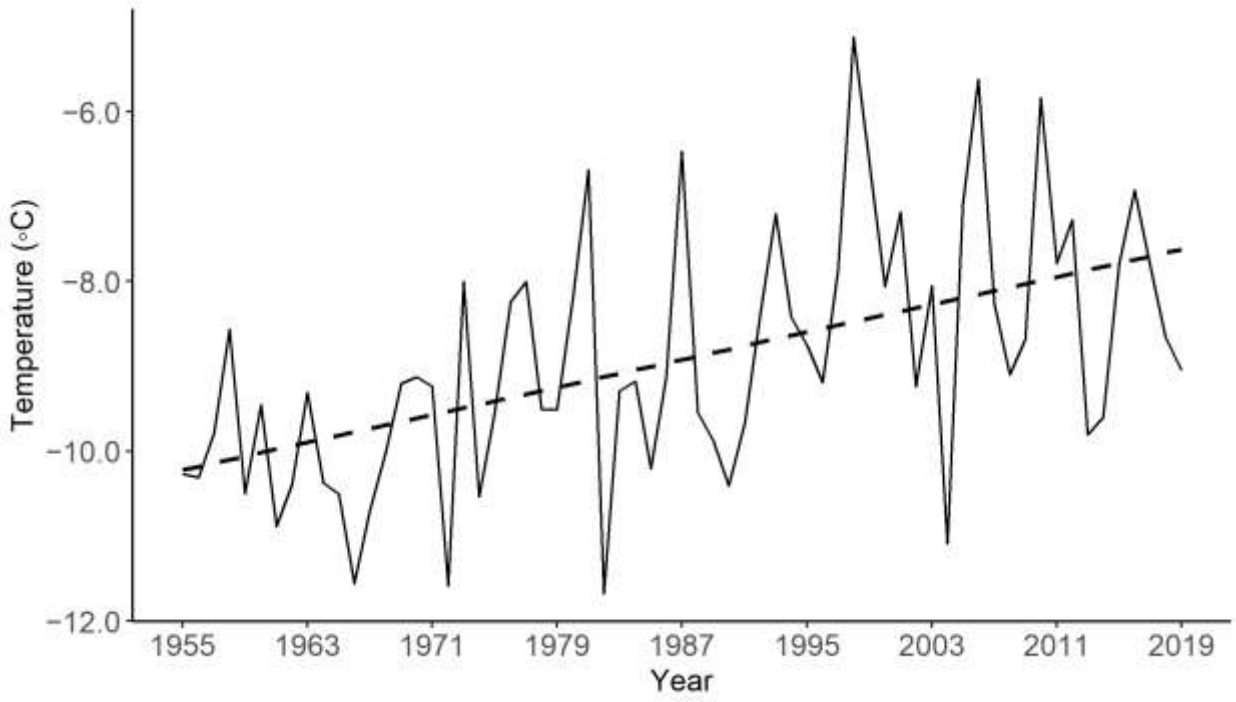

Figure B.2: Average annual minimum temperature (1955–2019) at Yellowknife station (located 5 km from the southern end of the Baker Creek catchment). Note: Black dashed line is a trend line.

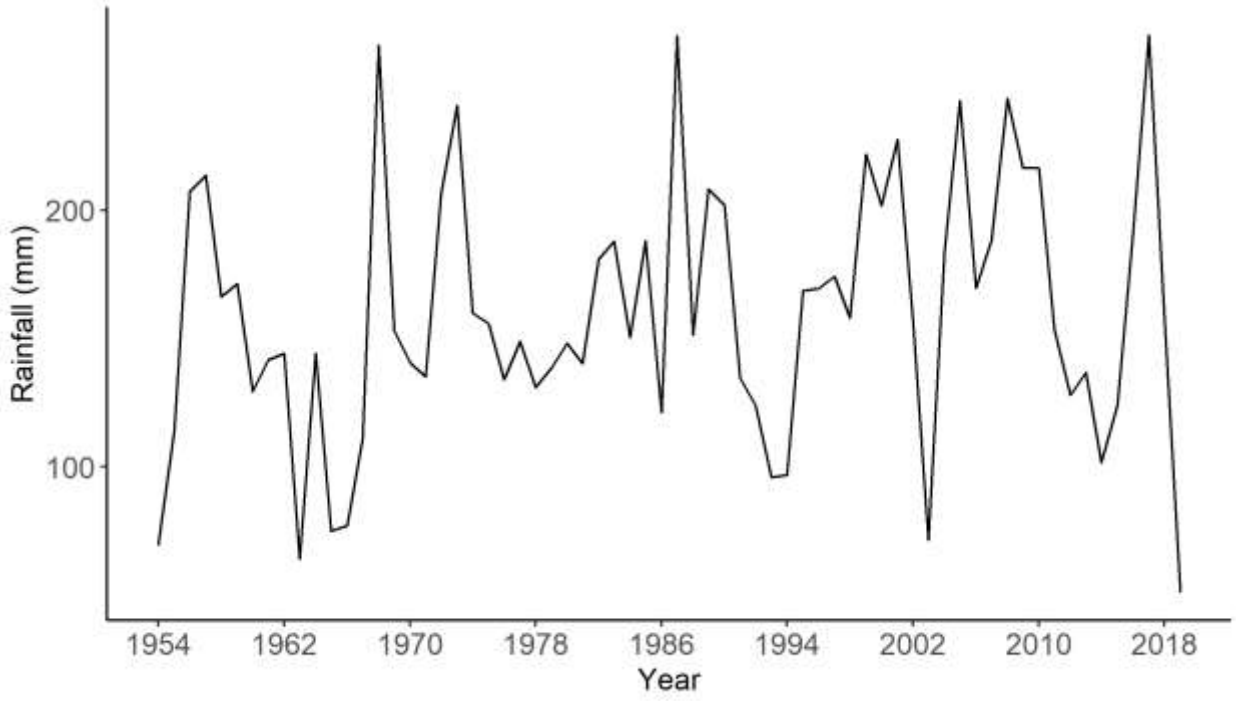

Figure B.3: Total annual rainfall (mm) (1954–2019) at Yellowknife station (located 5 km from the southern end of the Baker Creek catchment)

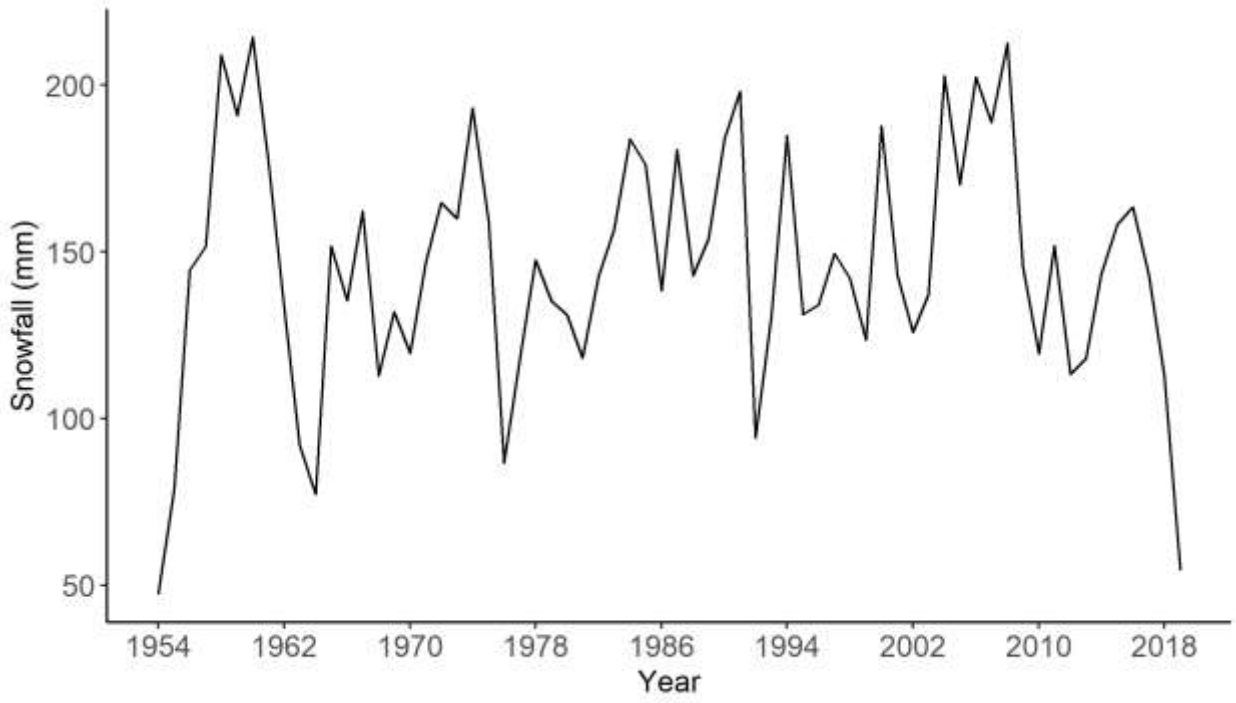

Figure B.4: Total annual snowfall (mm) (1954–2019) at Yellowknife station (located 5 km from the southern end of the Baker Creek catchment)

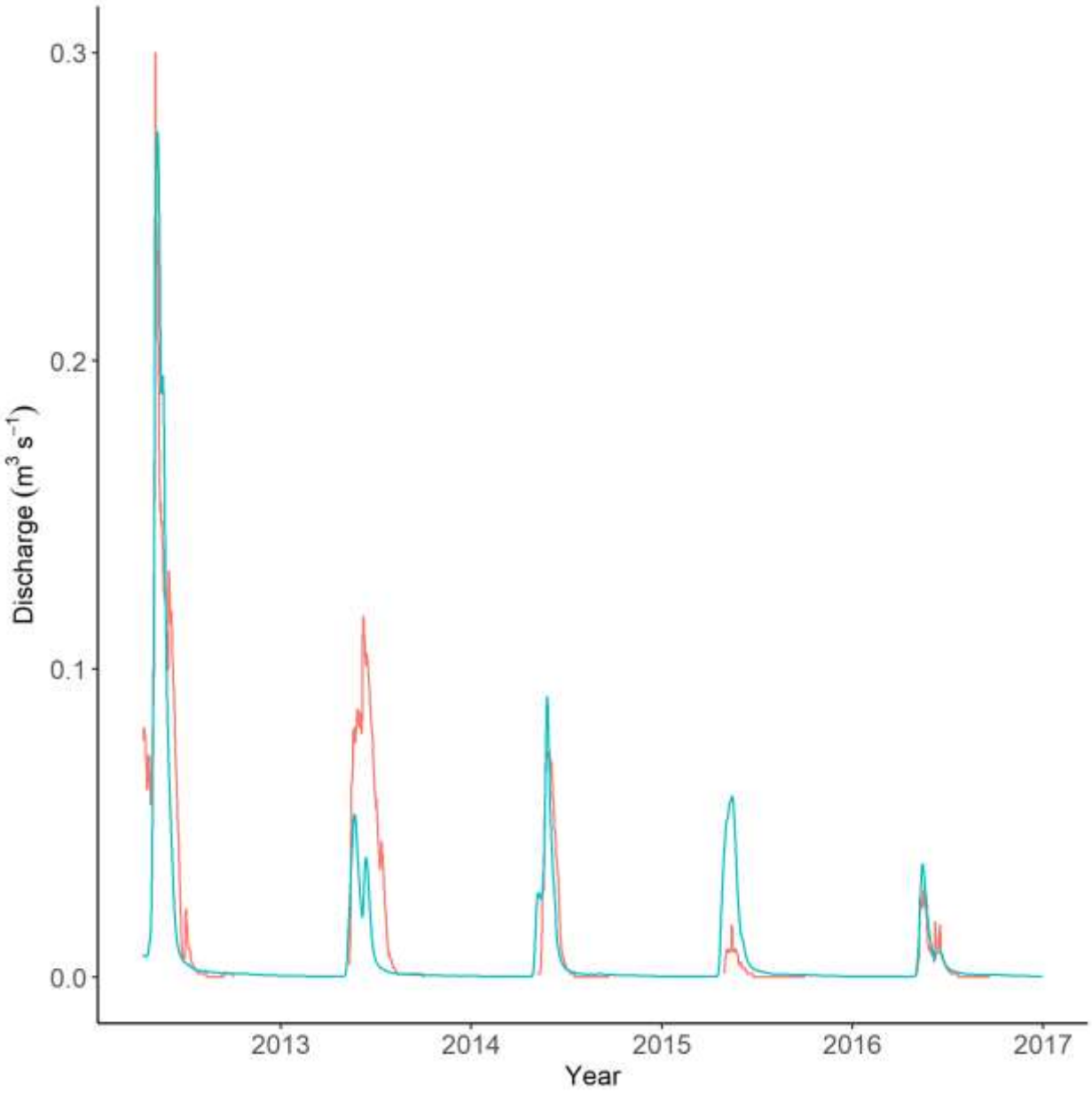

Figure B.5: PERSiST simulated (blue) and observed (red) discharge (m^3 s^{-1}) (2012–2016) at Lake 690.

References

ACIA. (2004). Impact of a Warming Arctic: Arctic Climate Impact Assessment. Cambridge University Press. Retrieved from http://www.acia.uaf.edu

ACIA. (2005). Arctic Climate Impact Assessment. Cambridge University Press. Retrieved from http://www.acia.uaf.edu

Åkerman, H. J., & Johansson, M. (2008). Thawing permafrost and thicker active layers in sub-arctic Sweden. Permafrost and Periglacial Processes, 19(3), 279–292. https://doi.org/10.1002/ppp.626

Al-Reasi, H. A., Wood, C. M., & Smith, D. S. (2013). Characterization of freshwater natural dissolved organic matter (DOM): Mechanistic explanations for protective effects against metal toxicity and direct effects on organisms. Environment International, 59, 201–207. https://doi.org/10.1016/j.envint.2013.06.005

Andréasson, J., Bergström, S., Carlsson, B., Graham, L. P., & Lindström, G. (2004). Hydrological change - Climate change impact simulations for Sweden. Ambio, 33(4–5), 228–234. https://doi.org/10.1579/0044-7447-33.4.228

Ashworth, D. J., & Alloway, B. J. (2007). Complexation of copper by sewage sludge-derived dissolved organic matter: Effects on soil sorption behaviour and plant uptake. Water, Air, and Soil Pollution, 182(1–4), 187–196. https://doi.org/10.1007/s11270-006-9331-7

Aukes, P. J. K. (2019). Dissolved Organic Matter in the Canadian Arctic & Sub-Arctic. University of waterloo.

Baken, S., Degryse, F., Verheyen, L., Merckx, R., & Smolders, E. (2011). Metal complexation properties of freshwater dissolved organic matter are explained by its aromaticity and by anthropogenic ligands. Environmental Science and Technology, 45(7), 2584–2590. https://doi.org/10.1021/es103532a

Baker, M. E., Weller, D. E., & Jordan, T. E. (2006). Improved methods for quantifying potential nutrient interception by riparian buffers. Landscape Ecology, 21(8), 1327–1345. https://doi.org/10.1007/s10980-006-0020-0

Baldwin, S. A. (2006). Northern Hard Rock Mining : Effects on Riparian Zones and Passive Biological Treatment of Impacted Waters.

Bauwens, A., Sohier, C., & Degré, A. (2013). Impacts of climate change on hydrological regimes and water resources management in the Meuse catchment. A review. Biotechnology, Agronomy and Society and Environment, 17(1), 76–86.

Beldring, S., Engen-Skaugen, T., Førland, E. J., & Roald, L. A. (2008). Climate change impacts on hydrological processes in Norway based on two methods for transferring regional climate model results to meteorological station sites. Tellus A: Dynamic Meteorology and

Oceanography, 60(3), 439–450. https://doi.org/10.1111/j.1600-0870.2007.00306.x

Bergström, S., Carlsson, B., Gardelin, M., Lindström, G., Petterson, A., & Rummukainen, M. (2001). Climate change impacts on runoff in Sweden - Assessments by global climate models, dynamical downscalling and hydrological modelling. Climate Research, 16(2), 101–112. https://doi.org/10.3354/cr016101

Beven, K., & Binley, A. (1992). The Future of Distributed Models: Model Calibration and Uncertainity Prediction. Hydrological Processes, 6, 279–298.

Biddanda, B. A., & Cotner, J. B. (2002). Love handles in aquatic ecosystems: The role of dissolved organic carbon drawdown, resuspended sediments, and terrigenous inputs in the carbon balance of Lake Michigan. Ecosystems, 5(5), 431–445. https://doi.org/10.1007/s10021-002-0163-z

Bintanja, R. (2018). The impact of Arctic warming on increased rainfall. Scientific Reports, 1–7. https://doi.org/10.1038/s41598-018-34450-3

Bintanja, R., & Andry, O. (2017). Towards a rain-dominated Arctic. Nature Climate Change, 7(4), 263–267. https://doi.org/10.1038/nclimate3240

Burd, K., Tank, S. E., Dion, N., Quinton, W. L., Spence, C., Tanentzap, A. J., & Olefeldt, D. (2018). Seasonal shifts in export of DOC and nutrients from burned and unburned peatland-rich catchments, Northwest Territories, Canada. Hydrology and Earth System Sciences, 22(8), 4455–4472. https://doi.org/10.5194/hess-22-4455-2018

Burn, D. H., & Mcbean, E. A. (1985). Modelling Water Quality in Uncertain Environment, 21(7), 934–940.

Camino-Serrano, M., Guenet, B., Luyssaert, S., Ciais, P., Bastrikov, V., De Vos, B., … Janssens, I. A. (2018). ORCHIDEE-SOM: Modeling soil organic carbon (SOC) and dissolved organic carbon (DOC) dynamics along vertical soil profiles in Europe. Geoscientific Model Development, 11(3), 937–957. https://doi.org/10.5194/gmd-11-937-2018

Chapman, P. J., Reynolds, B., & Wheater, H. S. (1995). The seasonal variation in soil water acid neutralizing capacity in peaty podzols in Mid-Wales. Water, Air, & Soil Pollution, 85(3), 1089–1094. https://doi.org/10.1007/BF00477126

Chapman, S. K., Hayes, M. A., Kelly, B., & Adam Langley, J. (2019). Exploring the oxygen sensitivity of wetland soil carbon mineralization. Biology Letters, 15(1), 11–15. https://doi.org/10.1098/rsbl.2018.0407

Chow, A. T., Tanji, K. K., & Gao, S. (2003). Production of dissolved organic carbon (DOC) and trihalomethane (THM) precursor from peat soils. Water Research, 37(18), 4475–4485. https://doi.org/10.1016/S0043-1354(03)00437-8

Ciais, P., Sabine, C., Bala, G., Bopp, L., Brovkin, V., Canadell, J., … P. Thornton. (2013). Carbon and other biogeochemic cycles. Climate Change 2013: The Physical Science Basis. Contribution of Working Group I to the Fifth Assessment Report of the Intergovernmental Panel on Climate Change [Stocker, T.F., D. Qin, G.-K. Plattner, M. Tignor, S.K. Allen, J. Boschung, A. Nauels, Y. Xia,. Cambridge University Press, Cambridge, United Kingdom and New York, NY, USA. https://doi.org/10.1017/CBO9781107415324.015

Clair, T. A., Dennis, I. F., Vet, R., & Laudon, H. (2008). Long-term trends in catchment organic carbon and nitrogen exports from three acidified catchments in Nova Scotia, Canada. Biogeochemistry, 87(1), 83–97. https://doi.org/10.1007/s10533-007-9170-7

Clair, T. A., Ehrman, J. M., & Higuchi, K. (1999). Changes in freshwater carbon exports from Canadian terrestrial basins to lakes and estuaries under a 2xCO2 atmospheric scenario. Global Biogeochemical Cycles, 13(4), 1091–1097. https://doi.org/10.1029/1999GB900055

Connon, R. F., Quinton, W. L., Craig, J. R., & Hayashi, M. (2014). Changing hydrologic connectivity due to permafrost thaw in the lower Liard River valley, NWT, Canada. Hydrological Processes, 28(14), 4163–4178. https://doi.org/10.1002/hyp.10206

Cott, P. A., Zajdlik, B. A., Palmer, M. J., & McPherson, M. D. (2016). Arsenic and mercury in lake whitefish and burbot near the abandoned Giant Mine on Great Slave Lake. Journal of Great Lakes Research, 42(2), 223–232. https://doi.org/10.1016/j.jglr.2015.11.004

Couture, R. M., Tominaga, K., Starrfelt, J., Moe, S. J., Kaste, Y., & Wright, R. F. (2014). Modelling phosphorus loading and algal blooms in a Nordic agricultural catchment-lake system under changing land-use and climate. Environmental Sciences: Processes and Impacts, 16(7), 1588–1599. https://doi.org/10.1039/c3em00630a

Creed, I. F., Beall, F. D., Clair, T. A., Dillon, P. J., & Hesslein, R. H. (2008). Predicting export of dissolved organic carbon from forested catchments in glaciated landscapes with shallow soils. Global Biogeochemical Cycles, 22(4). https://doi.org/10.1029/2008GB003294

Currie, W. S., & Aber, J. D. (1997). Modeling Leaching as a Decomposition Process in Humid Montane Forests. Ecological Society of America, 78(6), 1844–1860. Retrieved from https://www.jstor.org/stable/2266106

D. N. Moriasi, J. G. Arnold, M. W. Van Liew, R. L. Bingner, R. D. Harmel, & T. L. Veith. (2007). Model Evaluation Guidelines for Systematic Quantification of Accuracy in Watershed Simulations. American Society of Agricultural and Biological Engineers, 50(3), 885–900. https://doi.org/10.13031/2013.23153

Daniels, S. M., Agnew, C. T., Allott, T. E. H., & Evans, M. G. (2008). Water table variability and runoff generation in an eroded peatland, South Pennines, UK. Journal of Hydrology, 361(1–2), 214–226. https://doi.org/10.1016/j.jhydrol.2008.07.042

de Wit, H. A., Ledesma, J. L. J., & Futter, M. N. (2016). Aquatic DOC export from subarctic Atlantic blanket bog in Norway is controlled by seasalt deposition, temperature and precipitation. Biogeochemistry, 127(2–3), 305–321. https://doi.org/10.1007/s10533-016-0182-z

DeBeer, C. M., Wheater, H. S., Carey, S. K., & Chun, K. P. (2016). Recent climatic , cryospheric , and hydrological changes over the interior of western Canada : a review and synthesis. Hydrology and Earth System Sciences, 1573–1598. https://doi.org/10.5194/hess-20-1573-2016

Déry, S. J., Stadnyk, T. A., Macdonald, M. K., & Gauli-sharma, B. (2016). Recent trends and variability in river discharge across northern Canada, (2002), 4801–4818. https://doi.org/10.5194/hess-20-4801-2016

Dick, J. J., Tetzlaff, D., Birkel, C., & Soulsby, C. (2015). Modelling landscape controls on dissolved organic carbon sources and fluxes to streams. Biogeochemistry, 122(2–3), 361–374. https://doi.org/10.1007/s10533-014-0046-3

Dillon, P. J., & Molot, L. A. (1997). Dissolved organic and inorganic carbon mass balances in central Ontario lakes. Biogeochemistry, 36(1), 29–42. https://doi.org/10.1023/A:1005731828660

Douville, H., K. Raghavan, J. Renwick, R. P. Allan, P. A. Arias, M. Barlow, R. Cerezo-Mota, A. Cherchi, T. 43 Y. Gan, J. Gergis, D. Jiang, A. Khan, W. Pokam Mba, D. Rosenfeld, J. Tierney, O. Z. (2021). Water Cycle Changes. Cambridge University Press.

Eimers, M. C., Watmough, S. A., & Buttle, J. M. (2008). Long-term trends in dissolved organic carbon concentration: A cautionary note. Biogeochemistry, 87(1), 71–81. https://doi.org/10.1007/s10533-007-9168-1

Esterby, S. R. (1996). Review of methods for the detection and estimation of trends with emphasis on water quality applications. Hydrological Processes, 10(2), 127–149. https://doi.org/10.1002/(SICI)1099-1085(199602)10:2<127::AID-HYP354>3.0.CO;2-8

Evans, C. D., Monteith, D. T., & Cooper, D. M. (2005). Long-term increases in surface water dissolved organic carbon: Observations, possible causes and environmental impacts. Environmental Pollution, 137(1), 55–71. https://doi.org/10.1016/j.envpol.2004.12.031

Evans, Christopher D., Chapman, P. J., Clark, J. M., Monteith, D. T., & Cresser, M. S. (2006). Alternative explanations for rising dissolved organic carbon export from organic soils. Global Change Biology, 12(11), 2044–2053. https://doi.org/10.1111/j.1365-2486.2006.01241.x

Falk, M., Miller, M., & Kostuik, S. (1973). Biological effects of mining wastes in the northwest territories, (Technical Report CENT/T-73-10), 29.

Foy, N., Copland, L., Zdanowicz, C., Demuth, M., & Hopkinson, C. (2011). Recent volume and

area changes of Kaskawulsh Glacier, Yukon, Canada. Journal of Glaciology, 57(203), 515–525. https://doi.org/10.3189/002214311796905596

Freeman, C., Evans, C. D., Monteith, D. T., Reynolds, B., & Fenner, N. (2001). Export of organic carbon from peat soils. Nature, 412(6849), 785. https://doi.org/10.1038/35090628

Freeman, C., Fenner, N., Ostle, N. J., Kang, H., Dowrick, D. J., Reynolds, B., … Hudson, J. (2004). Export of dissolved organic carbon from peatlands under elevated carbon dioxide levels. Nature, 430(6996), 195–198. https://doi.org/10.1038/nature02707

Furgal, C., & Prowse, T. D. (2007). Northern Canada. In J. L. and E. B. D.S. Lemmen, F.J. Warren (Ed.), From Impacts to Adaptation: Canada in a Changing Climate (pp. 57–118). Government of Canada, Ottawa,ON.

Futter, M. N., Butterfield, D., Cosby, B. J., Dillon, P. J., Wade, A. J., & Whitehead, P. G. (2007). Modeling the mechanisms that control in-stream dissolved organic carbon dynamics in upland and forested catchments. Water Resources Research, 43(2), 1–16. https://doi.org/10.1029/2006WR004960

Futter, M. N., Erlandsson, M. A., Butterfield, D., Whitehead, P. G., Oni, S. K., & Wade, A. J. (2014). PERSiST: A flexible rainfall-runoff modelling toolkit for use with the INCA family of models. Hydrology and Earth System Sciences, 18(2), 855–873. https://doi.org/10.5194/hess-18-855-2014

Futter, M. N., Whitehead, P. G., Sarkar, S., Rodda, H., & Crossman, J. (2015). Rainfall runoff modelling of the Upper Ganga and Brahmaputra basins using PERSiST. Environmental Science: Processes and Impacts, 17(6), 1070–1081. https://doi.org/10.1039/c4em00613e

Futter, M N, Butterfield, D., Cosby, B. J., Dillon, P. J., Wade, A. J., & Whitehead, P. G. (2007). Modeling the mechanisms that control in-stream dissolved organic carbon dynamics in upland and forested catchments. Water Resources Research, 43, 1–16. https://doi.org/10.1029/2006WR004960

Futter, M N, Forsius, M., Holmberg, M., & Starr, M. (2009). A long-term simulation of the effects of acidic deposition and climate change on surface water dissolved organic carbon concentrations in a boreal catchment. Hydrology Research, 291–306.

Futter, Martyn N., & de Wit, H. A. (2008). Testing seasonal and long-term controls of streamwater DOC using empirical and process-based models. Science of the Total Environment, 407(1), 698–707. https://doi.org/10.1016/j.scitotenv.2008.10.002

Galloway, J. M., Sanei, H., Patterson, R. T., Mosstajiri, T., Hadlari, T., & Falck, H. (2012). Total arsenic concentrations of lake sediments near the City of Yellowknife , Northwest Territories. https://doi.org/10.4095/xxxxxx

Gbondo-Tugbawa, S. S., Driscol, C. T., Aber, J. D., & Likens, G. E. (2001). Evaluation of an

integrated biogeochemical model (PnET-BGC) at a northern hardwood forest ecosystem. Water Resources Research, 37(4), 1057–1070.

Ge, S., Yang, D., & Kane, D. L. (2013). Yukon river basin long-term (1977-2006) hydrologic and climatic analysis. Hydrological Processes, 27(17), 2475–2484. https://doi.org/10.1002/hyp.9282

Gillet, N., Flato, G., Zhang, X., Derksen, C., Bonsal, B., Greenan, B., … Gilbert, D. (2019). Canada's Changing Climate Report; Government of Canada. Retrieved from http://www.changingclimate.ca/CCCR2019

GNWT. (2008). NWT Climate Change Impacts and Adaptation Report. Retrieved from www.enr.gov.nt.ca/_live/documents/content/NWT_climate_change_impacts_and_adaptation_report.pdf

GNWT. (2017). Status and Trends of Water Chemistry and Flow of Tributaries into Great Slave Lake. NWT, Canada. https://doi.org/ENW.VENW03044-01

GNWT. (2019). Giant Mine Remediation Project Closure and Reclamation Plan. Retrieved from http://registry.mvlwb.ca/Documents/MV2007L8-0031/MV2007L8-0031 - DIAND-GIANT - GMRP Closure and Reclamation Plan (C and R Plan) - Apr1-19.pdf

Golder. (2013). 2011 Baker Creek Assessment Giant Mine, Yellowknife, NWT.

Golder. (2018). Giant Mine Remediation Project. Retrieved from https://www.aadnc-aandc.gc.ca/eng/1100100027364/1100100027365

Grant, F., Young, J. P. W., Harrison, P. A., Sykes, M. T., Skourtos, M., Rounsevell, M. D. A., … Watt, A. S. (2008). Ecosystem Services and Drivers of Biodiversity Change: Report of the RUBICODE electronic conference, April 2008. In Rubicode (pp. 1–94).

Gudasz, C., Bastviken, D., Steger, K., Premke, K., Sobek, S., & Tranvik, L. J. (2010). Temperature-controlled organic carbon mineralization in lake sediments. Nature, 466(7305), 478–481. https://doi.org/10.1038/nature09186

Hanson, P. C., Pollard, A. I., Bade, D. L., Predick, K., & Stephen R Carpenter, J. A. F. (2004). A model of carbon evasion and sedimentation in temperate lakes. Global Change Biology, 10, 1285–1298. https://doi.org/10.1111/j.1365-2486.2004.00805.x

Hoegh-Guldberg O., Jacob D., Taylor M., Bindi M., Brown S., Camilloni I., Diedhiou A., D. R. et al. (2018). Impacts of 1.5°C of global warming on natural and human systems. In: Global Warming of 1.5°C. An IPCC Special Report on the impacts of global warming of 1.5°C above pre-industrial levels and related global greenhouse gas emission pathways, in the context of strengthening the global response to the threat of climate cha.

Hood, E., McKnight, D. M., & Williams, M. W. (2003). Sources and chemical character of

dissolved organic carbon across an alpine/subalpine ecotone, Green Lakes Valley, Colorado Front Range, United States. Water Resources Research, 39(7). https://doi.org/10.1029/2002WR001738

Howell, D. (2014). Arsenic in Lakes Surrounding Yellowknife: Anthropogenic or Naturally Derived? Queen's University Kingston, Ontario.

Hudson, J. J., Keith, M., Dillon, P. J., & Somers, K. M. (2003). Long-term patterns in dissolved organic carbon in boreal lakes: the role of incident radiation, precipitation, air temperature, southern oscillation and acid deposition. Hydrology and Earth System Sciences Discussions, 7(3), 390–398. Retrieved from http://hal.archives-ouvertes.fr/hal-00304787

IPCC. (2014). Climate Change 2014 Synthesis Report Summary Chapter for Policymakers, AR5, 32.

IPCC. (2021). Summary for Policymakers. Cambridge University Press. https://doi.org/10.1260/095830507781076194

Jacques, J. M. S., & Sauchyn, D. J. (2009). Increasing winter baseflow and mean annual streamflow from possible permafrost thawing in the Northwest Territories, Canada. Geophysical Research Letters, 36(1). https://doi.org/10.1029/2008GL035822

Jamieson, H. E., Maitland, K. M., Oliver, J. T., & Palmer, M. J. (2017). Regional distribution of arsenic in near-surface soils in the Yellowknife area.

Jenicek, M., & Ledvinka, O. (2020). Importance of snowmelt contribution to seasonal runoff and summer low flows in Czechia. Hydrology and Earth System Sciences, 1–23. https://doi.org/10.5194/hess-2019-611

Kane, E. S., Veverica, T. J., Tfaily, M. M., Lilleskov, E. A., Meingast, K. M., Kolka, R. K., … Chimner, R. A. (2019). Reduction-Oxidation Potential and Dissolved Organic Matter Composition in Northern Peat Soil: Interactive Controls of Water Table Position and Plant Functional Groups. Journal of Geophysical Research: Biogeosciences, 124(11), 3600–3617. https://doi.org/10.1029/2019JG005339

Kaplan, L. A., & Bott, T. L. (1982). Diel fluctuations of DOC generated by algae in a piedmont stream. Limnology and Oceanography, 27(6), 1091–1100. https://doi.org/10.4319/lo.1982.27.6.1091

Koprivnjak, J.-F., & Moore, T. R. (2006). Sources, Sinks, and Fluxes of Dissolved Organic Carbon in Subarctic Fen Catchments. Arctic and Alpine Research, 24(3), 204. https://doi.org/10.2307/1551658

Kothawala, D., Kellerman, A., Catalan, N., & Tranvik, L. (2016). Controls on the dynamics of dissolved organic matter in boreal lakes. Geophysical Research Abstracts EGU General Assembly (Vol. 18).

Ledesma, J., & Futter, M. (2020). Precipitation , Evapotranspiration and Runoff Simulator for Solute Transport (PERSiST) Parameter description and Calibration strategy, (January), 1–30.

Ledesma, J. L. J., Köhler, S. J., & Futter, M. N. (2012). Long-term dynamics of dissolved organic carbon: Implications for drinking water supply. Science of the Total Environment, 432(November 2017), 1–11. https://doi.org/10.1016/j.scitotenv.2012.05.071

Lemmen, D.S., Warren, F.J., Lacroix, J., and Bush, E., editors. (2008). From Impacts to Adaptation: Canada in a Changing Climate 2007. Government of Canaada. Ottawa,ON. https://doi.org/10.2307/j.ctv172zm.4

Lin, Y., Campbell, A. N., Bhattacharyya, A., DiDonato, N., Thompson, A. M., Tfaily, M. M., … Pett-Ridge, J. (2021). Differential effects of redox conditions on the decomposition of litter and soil organic matter. Biogeochemistry, 154(1), 1–25. https://doi.org/10.1007/s10533-021-00790-y

Lotsari, E., Veijalainen, N., Alho, P., & Käyhkö, J. (2010). Impact of climate change on future discharges and flow characteristics of the tana river, sub-arctic northern fennoscandia. Geografiska Annaler, Series A: Physical Geography, 92(2), 263–284. https://doi.org/10.1111/j.1468-0459.2010.00394.x

Ma, Q., Jin, H., Yu, C., & Bense, V. F. (2019). Dissolved organic carbon in permafrost regions: A review. Science China Earth Sciences, 62(2), 349–364. https://doi.org/10.1007/s11430-018-9309-6

McClelland, J. W., Déry, S. J., Peterson, B. J., Holmes, R. M., & Wood, E. F. (2006). A pan-arctic evaluation of changes in river discharge during the latter half of the 20th century. Geophysical Research Letters, 33(6). https://doi.org/10.1029/2006GL025753

McDowell, W. H., & Likens, G. E. (1988). Origin , Composition , and Flux of Dissolved Organic Carbon in the Hubbard Brook Valley. Ecological Society of America, 58(3), 177–195.

McKnight, D. M., Aiken, G. R., Thorn, K. A., Bencala, K. E., Zellweger, G. W., & Feder, G. L. (1992). Sorption of Dissolved Organic Carbon by Hydrous Aluminum and Iron Oxides Occurring at the Confluence of Deer Creek with the Snake River, Summit County, Colorado. Environmental Science and Technology, 26(7), 1388–1396. https://doi.org/10.1021/es00031a017

Michalzik, B., Tipping, E., Mulder, J., Gallardo Lancho, J. F., Matzner, E., Bryant, C. L., … Vicente Esteban, M. A. (2003). Modelling the production and transport of dissolved organic carbon in forest soils. Biogeochemistry, 66(3), 241–264. https://doi.org/10.1023/B:BIOG.0000005329.68861.27

Monteith, D. T., Evans, C. D., Henrys, P. A., Simpson, G. L., & Malcolm, I. A. (2014). Trends in

the hydrochemistry of acid-sensitive surface waters in the UK 1988-2008. Ecological Indicators, 37(PART B), 287–303. https://doi.org/10.1016/j.ecolind.2012.08.013

Monteith, Donald T., Stoddard, J. L., Evans, C. D., De Wit, H. A., Forsius, M., Høgåsen, T., … Vesely, J. (2007). Dissolved organic carbon trends resulting from changes in atmospheric deposition chemistry. Nature, 450(7169), 537–540. https://doi.org/10.1038/nature06316

Moore, R. D., S.W.Fleming, Menounos, B., Wheate, R., Fountain, A., Stahl, K., … Jakob, M. (2009). Glacier change in western North America: influences on hydrology, geomorphic hazards and water quality. Hydrological Processes, 23, 42–61. https://doi.org/10.1002/hyp

Moore, T. R. (1989). Dynamics of dissolved organic carbon in forested and disturbed catchments, Westland, New Zealand: 1. Maimai. Water Resources Research, 25(6), 1321–1330. https://doi.org/10.1029/WR025i006p01321

Morse, P. D., Wolfe, S. A., Kokelj, S. V., & Gaanderse, A. J. R. (2015). The Occurrence and Thermal Disequilibrium State of Permafrost in Forest Ecotopes of the Great Slave Region, Northwest Territories, Canada. Permafrost and Periglacial Processes, 27(2), 145–162. https://doi.org/10.1002/ppp.1858

Mostofa, K. M. G., Liu, C. qiang, Feng, X., Yoshioka, T., Vione, D., Pan, X., & Wu, F. (2013). Complexation of Dissolved Organic Matter with Trace Metal Ions in Natural Waters. Environmental Science and Engineering. https://doi.org/10.1007/978-3-642-32223-5_9

Nasser, N. A. (2014). Arcellaceans (Testate Lobose Amoeba) as Proxies for Arsenic and Heavy Metal Contamination in the Baker Creek Watershed Region , Northwest Territories , Canada. Carleton University.

Nathan, S. (2018). Baker Creek Remediation. In Giant Mine Remediation Project. Edmonton.

Nistor, M. M, & Petcu, M. I. (2015). Quantitative analysis of glaciers changes from passage canal based on GIS and satellite images, South Alaska. Applied Ecology and Environmental Research, 13(2), 307–324. https://doi.org/10.15666/aeer/1302

Nistor, Mărgărit Mircea. (2017). Climate change impact on glaciers retreat in passage Canal Fjord, Alaska. Carpathian Journal of Earth and Environmental Sciences, 12(1), 259–267.

Noacco, V., Duffy, C. J., Wagener, T., Worrall, F., Fasiolo, M., & Howden, N. J. K. (2019). Drivers of interannual and intra-annual variability of dissolved organic carbon concentration in the River Thames between 1884 and 2013. Hydrological Processes, 33(6), 994–1012. https://doi.org/10.1002/hyp.13379

Olivie-Lauquet, G., Gruau, G., Dia, A., Riou, C., Jaffrezic, A., & Henin, O. (2001). Release of trace elements in wetlands: Role of seasonal variability. Water Research, 35(4), 943–952. https://doi.org/10.1016/S0043-1354(00)00328-6

Oni, S. K., Futter, M. N., Bishop, K., Köhler, S. J., Ottosson-Löfvenius, M., & Laudon, H. (2012). Long term patterns in dissolved organic carbon, major elements and trace metals in boreal headwater catchments: trends, mechanisms and heterogeneity. Biogeosciences Discussions, 9(12), 19121–19163. https://doi.org/10.5194/bgd-9-19121-2012

Oni, S. K., Futter, M. N., Molot, L. A., & Dillon, P. J. (2012). Modelling the long term impact of climate change on the carbon budget of lake simcoe, ontario using INCA-C. Science of the Total Environment, 414, 387–403. https://doi.org/10.1016/j.scitotenv.2011.10.025

Oni, Stephen K., Futter, M. N., & Dillon, P. J. (2011). Landscape-scale control of carbon budget of Lake Simcoe: A process-based modelling approach. Journal of Great Lakes Research, 37(SUPPL. 3), 160–165. https://doi.org/10.1016/j.jglr.2010.05.003

Oni, Stephen K., Futter, M. N., Teutschbein, C., & Laudon, H. (2014). Cross-scale ensemble projections of dissolved organic carbon dynamics in boreal forest streams. Climate Dynamics, 42(9–10), 2305–2321. https://doi.org/10.1007/s00382-014-2124-6

Oni, Stephen K, Futter, M. N., Molot, L. A., & Dillon, P. J. (2014). Adjacent catchments with similar patterns of land use and climate have markedly different dissolved organic carbon concentration and runoff dynamics, 1449(January 2013), 1436–1449. https://doi.org/10.1002/hyp.9681

Overland, J. E., Wang, M., Walsh, J. E., & Stroeve, J. C. (2013). Future Arctic climate changes: Adaptation and mitigation time scales. Earth's Future, (2), 68–74. https://doi.org/10.1002/2013EF000162

Palmer, M. J., Chételat, J., Richardson, M., Jamieson, H. E., & Galloway, J. M. (2019). Seasonal variation of arsenic and antimony in surface waters of small subarctic lakes impacted by legacy mining pollution near Yellowknife, NT, Canada. Science of the Total Environment, 684, 326–339. https://doi.org/10.1016/j.scitotenv.2019.05.258

Petrone, K. C., Jones, J. B., Hinzman, L. D., & Boone, R. D. (2006). Seasonal export of carbon, nitrogen, and major solutes from Alaskan catchments with discontinuous permafrost. Journal of Geophysical Research: Biogeosciences, 111(2), 1–13. https://doi.org/10.1029/2005JG000055

Phillips, R. W., Spence, C., & Pomeroy, J. W. (2011). Connectivity and runoff dynamics in heterogeneous basins. Hydrological Processes, 25(19), 3061–3075. https://doi.org/10.1002/hyp.8123

Quéré, C., Andrew, R., Friedlingstein, P., Sitch, S., Hauck, J., Pongratz, J., … Zheng, B. (2018). Global Carbon Budget 2018. Earth System Science Data, 10(4), 2141–2194. https://doi.org/10.5194/essd-10-2141-2018

Rautio, M., & Korhola, A. (2002). Effects of ultraviolet radiation and dissolved organic carbon on

the survival of subarctic zooplankton. Polar Biology, 25(6), 460–468. https://doi.org/10.1007/s00300-002-0366-y

Ravichandran, M. (2004). Interactions between mercury and dissolved organic matter - A review. Chemosphere, 55(3), 319–331. https://doi.org/10.1016/j.chemosphere.2003.11.011

Robert B. Ambrose, Tim A. Wool, John P. Connolly, R. W. S. (1988). WASP4, A Hydrodynamic and water quality modeling_Manual. Washington: United States Environmental Protection.

Roiha, T., Peura, S., Cusson, M., & Rautio, M. (2016). Allochthonous carbon is a major regulator to bacterial growth and community composition in subarctic freshwaters. Scientific Reports (Vol. 6). Nature Publishing Group. https://doi.org/10.1038/srep34456

Rood, S. B., Kaluthota, S., Philipsen, L. J., Rood, N. J., & Zanewich, K. P. (2017). Increasing discharge from the Mackenzie River system to the Arctic Ocean, 160(August 2016), 150–160. https://doi.org/10.1002/hyp.10986

Salmonsson, T. (2013). Assessing the impacts of climate change on runoff along a climatic gradient of Sweden using PERSiST, (December).

Santín, C., & Doerr, S. H. (2016). Fire effects on soils: The human dimension. Philosophical Transactions of the Royal Society B: Biological Sciences, 371(1696), 28–34. https://doi.org/10.1098/rstb.2015.0171

Schadel, C., Bader, M. K. F., Schuur, E. A. G., Biasi, C., Bracho, R., Capek, P., … Wickland, K. P. (2016). Potential carbon emissions dominated by carbon dioxide from thawed permafrost soils. Nature Climate Change, 6(10), 950–953. https://doi.org/10.1038/nclimate3054

Schuur, E. A. G., Abbott, B. W., Bowden, W. B., Brovkin, V., Camill, P., Canadell, J. G., … Zimov, S. A. (2013). Expert assessment of vulnerability of permafrost carbon to climate change. Climatic Change, 119(2), 359–374. https://doi.org/10.1007/s10584-013-0730-7

Schuur, E. A. G., McGuire, A. D., Romanovsky, V., Schädel, C., & Mack, M. (2018). Arctic and boreal carbon, Chapter 11. Second State of the Carbon Cycle Report (SOCCR2): A Sustained Assessment Report.

Shannon, S., Smith, R., Wiltshire, A., Payne, T., Huss, M., Betts, R., … Harrison, S. (2019). Global glacier volume projections under high-end climate change scenarios. Cryosphere, 13(1), 325–350. https://doi.org/10.5194/tc-13-325-2019

Sinsabaugh, R. L. (2010). Phenol oxidase, peroxidase and organic matter dynamics of soil. Soil Biology and Biochemistry, 42(3), 391–404. https://doi.org/10.1016/j.soilbio.2009.10.014

Song, F., Leung, L. R., Lu, J., & Dong, L. (2018). Seasonally dependent responses of subtropical highs and tropical rainfall to anthropogenic warming. Nature Climate Change, 8(9), 787–792. https://doi.org/10.1038/s41558-018-0244-4

Spence, C., Guan, X. J., Phillips, R., Hedstrom, N., Granger, R., & Reid, B. (2010). Storage dynamics and streamflow in a catchment with a variable contributing area. Hydrological Processes, 24(16), 2209–2221. https://doi.org/10.1002/hyp.7492

Spence, C., Kokelj, S. V., Kokelj, S. A., McCluskie, M., & Hedstrom, N. (2015). Evidence of a change in water chemistry in Canada's subarctic associated with enhanced winter streamflow. Journal of Geophysical Research: Biogeosciences, 120(2), 113–127. https://doi.org/10.1002/2014JG002809

Spence, Christopher. (2006). Hydrological processes and streamflow in a lake dominated watercourse. Hydrological Processes, (2006), 3665–3681. https://doi.org/10.1002/hyp

Spence, Christopher, & Hedstrom, N. (2018). Hydrometeorological data from Baker Creek Research Watershed, Northwest Territories, Canada. Earth System Science Data, 10(4), 1753–1767. https://doi.org/10.5194/essd-10-1753-2018

Spence, Christopher, Hedstrom, N., Tank, S. E., Quinton, W. L., Olefeldt, D., Goodman, S., & Dion, N. (2020). Hydrological resilience to forest fire in the subarctic Canadian shield. Hydrological Processes, 34(25), 4940–4958. https://doi.org/10.1002/hyp.13915

Spence, Christopher, Kokelj, S. A., Kokelj, S. V., & Hedstrom, N. (2013). The process of winter streamflow generation in a subarctic Precambrian Shield catchment. Hydrological Processes, 28(14), 4179–4190. https://doi.org/10.1002/hyp.10119

Spence, Christopher, Kokelj, S. V., & Ehsanzadeh, E. (2011). Precipitation trends contribute to streamflow regime shifts in northern Canada. IAHS-AISH Publication, 346(July), 3–8.

Spence, Christopher, & Woo, M. K. (2003). Hydrology of subarctic Canadian shield: Soil-filled valleys. Journal of Hydrology, 279(1–4), 151–166. https://doi.org/10.1016/S0022-1694(03)00175-6

Stagl, J., Mayr, E., Koch, H., & Hattermann, F. F. (2014). Managing Protected Areas in Central and Eastern Europe Under Climate Change, 58(May 2016). https://doi.org/10.1007/978-94-007-7960-0

Streeter, H. W., & Phelps, E. B. (1958). A Study of the Pollution and Natural Purfication of the Ohio River. Retrieved from http://dspace.udel.edu:8080/dspace/handle/19716/1590

Striegl, R. G., Aiken, G. R., Dornblaser, M. M., Raymond, P. A., & Wickland, K. P. (2005). A decrease in discharge-normalized DOC export by the Yukon River during summer through autumn. Geophysical Research Letters, 32(21), 1–4. https://doi.org/10.1029/2005GL024413

Talebbeydokhti Nasser, Shokoufeh Pourshahabi, G. Reza Rakhshandehroo, Mohammad Reza Nikoo, A. M. (2017). Review of Reservoir Water Quality Monitoring and Modelling.

Tarnocai, C., Canadell, J. G., Schuur, E. A. G., Kuhry, P., Mazhitova, G., & Zimov, S. (2009).

Soil organic carbon pools in the northern circumpolar permafrost region. Global Biogeochemical Cycles, 23(2), 1–11. https://doi.org/10.1029/2008GB003327

Tim, U. S., & Jolly, R. (1994). Evaluating agricultural nonpoint-source pollution using integrated geographic information systems and hydrologic/water quality model. Journal of Environmental Quality, 23(1), 25–35. https://doi.org/10.2134/jeq1994.00472425002300010006x

Tipping, E. and H., & Anne, M. (1988). A model of solid-solution interactions in acid organic soils, based on the complexation properties of humic substances. Journal of Soil Science, 39(4), 505–519. https://doi.org/10.1111/j.1365-2389.1988.tb01235.x

Tranvik, L. J., & Jansson, M. (2002). Clean air slots amid atmospheric pollution. Nature, 415(6874), 861–862. https://doi.org/10.1038/415861a

Tsakiris, G, & Alexakis, D. (2014). Water quality models : An overview Water quality models : An overview, (March).

Tsakiris, George, Spiliotis, M., Paritsis, S., & Alexakis, D. (2009). Assessing the water potential of karstic saline springs by applying a fuzzy approach: The case of Almyros (Heraklion, Crete). Desalination, 237(1–3), 54–64. https://doi.org/10.1016/j.desal.2007.12.022

USEPA. (1998). Water Quality Models. World Bank Group. Retrieved from http://water.epa.gov/scitech/datait/models/index.cfm

Vihma, T., Screen, J., Tjernström, M., Newton, B., Zhang, X., Popova, V., … Prowse, T. (2016). The atmospheric role in the Arctic water cycle: A review on processes, past and future changes, and their impacts. Journal of Geophysical Research G: Biogeosciences, 121(3), 586–620. https://doi.org/10.1002/2015JG003132

Wade, A. J., Durand, P., Beaujouan, V., Wessel, W. W., Raat, K. J., Whitehead, P. G., … Lepisto, A. (2002). A nitrogen model for European catchments : INCA , new model structure and equations. Hydrology and Earth System Sciences, 6(3), 559–582.

Walvoord, M. A., & Striegl, R. G. (2007). Increased groundwater to stream discharge from permafrost thawing in the Yukon River basin : Potential impacts on lateral export of carbon and nitrogen, 34. https://doi.org/10.1029/2007GL030216

Wang, Q., Li, S., Jia, P., Qi, C., & Ding, F. (2013). A Review of Surface Water Quality Models. The Scientific World Journal, 2013, 7. Retrieved from http://dx.doi.org/10.1155/2013/231768

Weiman, S. (2015). Microbes Help To Drive Global Carbon Cycling and Climate Change. Microbe Magazine, 10(6), 233–238. https://doi.org/10.1128/microbe.10.233.1

Whitehead, P. G., Wilson E.J., B. D. (1998). A semi-distributed Integrated Nitrogen Model for

multiple source assessment in Catchments (INCA). Swindon, UK: Aquatic Environments Research Centre, Department of Geography.

WHO. (2011). Guidelines for Drinking-water Quality. https://doi.org/10.1007/springerreference_30502

Wit, H. A. de, Monteith, D. T., & Stoddard, J. L. (2016). Climatic and chemical drivers of trends in DOC in northern surface waters in Europa and North America, 18(2007), 16886.

World Meteorological Organization. (2017). WMO Greenhouse Gas Bulletin, (13), 1–4.

Worrall, F., & Burt, T. P. (2007). Flux of dissolved organic carbon from U.K. rivers. Global Biogeochemical Cycles, 21(1), 1–14. https://doi.org/10.1029/2006GB002709

Wrye, L. A. (2008). Distinguishing between natural and anthropogenic sources of arsenic in soils from the Giant mine, Northwest Territories and the North Brookfield mine, Nova Scotia, 241. Retrieved from http://qspace.library.queensu.ca/handle/1974/1547

Xu, J., Morris, P. J., Liu, J., Ledesma, J. L. J., & Holden, J. (2020). Increased Dissolved Organic Carbon Concentrations in Peat-Fed UK Water Supplies Under Future Climate and Sulfate Deposition Scenarios. Water Resources Research, 56(1), 1–19. https://doi.org/10.1029/2019WR025592

Yang, Y., He, Z., Wang, Y., Fan, J., Liang, Z., & Stoffella, P. J. (2013). Dissolved organic matter in relation to nutrients (N and P) and heavy metals in surface runoff water as affected by temporal variation and land uses - A case study from Indian River Area, south Florida, USA. Agricultural Water Management, 118, 38–49. https://doi.org/10.1016/j.agwat.2012.12.001